Time-Varying Autoregressive Model Based Signal Processing with Applications to Interference Rejection in Spread Spectrum Communications

by

Peijun Shan

Dissertation submitted to the faculty of the
Virginia Polytechnic Institute and State University
in partial fulfillment of the requirements for the degree of

DOCTOR OF PHILOSOPHY
in
Electrical Engineering

APPROVED:

_____
Dr. A. A. (Louis) Beex, Chairman

_____ _____
Dr. Hugh F. VanLandingham Dr. Brian D. Woerner

_____ _____
Dr. Theodore S. Rappaport Dr. Helen J. Crawford

July 1999
Blacksburg, Virginia

Keywords: Time-Varying Filtering, TVAR, Interference, Spread Spectrum, FM

Time-Varying Autoregressive Model Based Signal Processing with Applications to Interference Rejection in Spread Spectrum Communications

by

Peijun Shan
A. A. (Louis) Beex, Chairman

Electrical Engineering

(ABSTRACT)

The objective of this research is to develop time-varying signal processing methods for rapidly varying non-stationary signals based on time-varying autoregressive (TVAR) modeling, and to apply such methods to frequency-modulated (FM) interference rejection in direct-sequence spread spectrum (DSSS) communications. For fast varying non-stationary signal processing, such as the task to reject an FM interference that could chirp over the entire DSSS bandwidth in a symbol interval, an explicit description of the variation is necessary to form a time-varying filter. This is realized using the TVAR model, which is an autoregressive model whose coefficients are time-varying with the variation modeled as a linear combination of a set of known functions of time. In DSSS communications, when the strength of an interference - which could be a hostile jammer or overlaid communication signal - possibly exceeds the inherent spread spectrum processing gain, interference rejection is necessary to secure a usable bit-error-rate.

The contributions of this research include: a) revealed the advantageous performance of TVAR model based instantaneous frequency estimation (TVAR-IF), which is expected to change the prevailing opinion that regards TVAR-IF as a poor estimator; b) proposed a time-varying Prony method to improve TVAR-IF at low SNR; c) proposed to use TVAR-IF for time-varying FIR notch filter based FM jammer suppression in DSSS communications; d) developed TVAR model based time-varying optimum filters, including the TVAR based Kalman filter (TVAR-KF) and the TVAR based Wiener filter (TVAR-WF); e) developed a TVAR-WF based formulation of FM interference soft-cancellation in DSSS communications; and f) proposed a TVAR based linear prediction error (TVAR-LPE) filter for soft-cancellation of FM interference in DSSS communications.

For the interference rejection problem, our TVAR-IF controlled notch filter yields high processing gain close to that using the known IF and much higher than that using the WVD based IF estimate. Furthermore, unlike the IF based notch filter approaches, the proposed soft-cancellation methods utilize the full spectral information captured by the TVAR model. Our soft-cancellation approaches, including TVAR-WF and TVAR-LPE, maintain at least the DSSS system performance expected when no filtering is used, even under estimated conditions. The latter is in contrast to the notch filter based approaches, which may cause deterioration of overall system performance at low jammer-to-signal ratios.

Acknowledgments

Foremost, I wish to express my deepest gratitude to my advisor, Dr. A. A. (Louis) Beex, for being an excellent professor guiding me through the journey. Without his advice, insight, encouragement, patience and support, this work would be impossible. I am grateful to his generous sacrifice in time and financial support.

I extend my sincere thanks to Dr. Brian D. Woerner, Dr. Hugh F. VanLandingham, Dr. Theodore S. Rappaport and Dr. Helen J. Crawford for spending their time serving on my advisory committee. It is Dr. Woerner who introduced me to the field of spread spectrum communications and DSSS receivers.

My gratitude also goes to Dr. Karl H. Pribram and Dr. Joe S. King, both at the Center for Brain Research and Information Sciences at Radford University, for their years of support.

My special appreciation goes to my wife, my parents, my parents-in-law, my brother, my brother-in-law, and my daughters. It is their sacrifice, encouragement, support, understanding and compassion, one way or another, that makes this work possible and meaningful.

"The Times, They Are A-Changin'."

by **Bob Dylan** (1941-)

"All is flux, nothing is stationary."

"Change alone is unchanging."

by **Heraclitus** (c. 535–c. 475 B.C.)

Contents

Chapter 1

INTRODUCTION AND LITERATURE REVIEW

This research explores and develops parametric model based time-varying signal processing methods, including time-varying Wiener filtering (TVWF) and instantaneous frequency (IF) estimation, as well as their applications to interference suppression for spread spectrum (SS) communications. In this chapter we review the related works in the literature.

1.1 Time-Varying Filtering

Before addressing the time-varying Wiener filtering problem, we first review the studies on time-varying filtering. Time-frequency analysis has been one of the most active research areas in the signal processing community over the past two decades. Besides a large amount of work on time-frequency analysis, there has also been substantial research effort on time-frequency based signal processing, i.e. processing signals in the time-frequency plane, usually using the information obtained from time-frequency analysis. In time-frequency filtering problems, both the desired signal and the contaminating noise may be nonstationary and, in general, can not be separated by either

temporal windowing or conventional time-invariant frequency-selective filtering, and therefore filtering in the joint time-frequency domain is necessitated.

The earlier methods of time-frequency filtering were based on signal synthesis [1-3]. These methods operated in a procedure consisting of three steps: 1) "transform" the original observed signal to some form of time-frequency representation (TFR) [32], linear or nonlinear, such as the short-time Fourier transform (STFT), Wigner-Ville Distribution (WVD), or some other Cohen class of TFR [4]; 2) mask the TFR of the observed signal to retain the desired signal component(s) and excise the unwanted component(s); and 3) synthesize the filtered signal from the masked TFR. In 1986, Boudreaux-Bartels and Parks [1] first proposed the time-frequency filter based on WVD synthesis. Since the masked TFR may not be a valid TFR, approximation and optimization were often needed in the final step of signal synthesis. This type of filtering operation was highly non-linear and usually very demanding computationally. In addition, the performance of the WVD synthesis based filtering procedure was shown to be potentially poor [5, 2]. Linear TFRs, such as the STFT [6-8], the Gabor Transform [9], and the Wavelet Transform [10], were also used for time-frequency filtering in a similar way. A major drawback of these linear TFR based filters was the limitation of the time-frequency resolution inherited with these TFRs.

In the early 1990's, the studies on time-frequency filtering shifted from signal synthesis to time-frequency projection filters [11-15]. A time-frequency projection filter is an orthogonal projection operator of a linear signal space. The filter design was accomplished by constructing an optimal linear signal space corresponding to the time-frequency pass-region [12, 13]. A more general linear time-varying filter design method

based on Weyl Correspondence (WC) was investigated [14, 15]. It was illustrated that the WC based filter performed better than the signal synthesis methods [15].

In the mid 1990's, time-frequency strip filters [16-18], including fractional Fourier domain filters [18], were proposed for the special cases where the pass-regions in the time-frequency plane are in strip shapes. A strip filter first rotates the signal in the time-frequency plane to make the strip-shaped pass-region perpendicular to the time axis, then windows the rotated signal such that the desired signal is retained and the unwanted components are suppressed, and finally reverses the rotation to obtain the filtered signal. Conventional time-domain windowing and linear time-invariant (LTV) filtering can be viewed as special cases of strip filtering with rotation angles of 0 and 90 degrees respectively.

1.2 Time-Varying Wiener Filtering

The time-varying filtering methods mentioned above are generally pass-stop type of operations in the time-frequency plane, under the assumption that the desired signal and the undesired component(s) have disjoint time-frequency supports. In stationary cases, this corresponds to the classical pass-stop filtering, such as low/high/band pass filters and notch filters. Of major interest in this research are the more general cases where the signal and noise have overlapping time-frequency supports and both may have broad instantaneous bandwidths. We aim at achieving optimal or nearly optimal estimation of the desired signal based on the least mean square error criterion and refer to this problem as one of time-varying Wiener filtering (TVWF). This is the signal

estimation problem corresponding to the stationary case where optimal filters, referred to as Wiener Filters (WF) [19], are designed based on the mean-square error criterion.

To solve for the impulse response of the optimal filter from the autocorrelation functions of the signal and noise requires solving an integral equation known as the Wiener-Hopf equation [19], which, for stationary processes, reduces to a deconvolution problem. For wide-sense stationary processes, the optimal filter can be easily formulated in the frequency domain [19, 37]. For nonstationary cases, this problem, referred to as nonstationary Wiener filtering or time-varying Wiener filtering (TVWF), has been addressed by a few researchers from different points of view [20-23].

The earliest effort in TVWF was due to Abdrabbo and Priestley [20] in 1969, although it was not much noticed by the signal processing community then. The filtering was based on Priestley's evolutionary spectrum theory [24]. In 1995, Kirchauer, Hlawatsch and Kozek [21] proposed a time-frequency formulation of nonstationary Wiener filters. This work extended the spectral representation of stationary Wiener filters to the nonstationary case based on the Wigner-Ville Distribution (WVD) and the Weyl Symbol (WS) of linear operators. At the same time, Beex and Xie [22] proposed a time-varying Wiener filtering method based on their Multi-resolution Parametric Spectral Estimator (MPSE) [25, 26]. This method used sliding data windows and assumed local stationarity inside each sliding temporal window. It exhibited significant signal to noise ratio (SNR) gain for moderately slowly time-varying signals. More recently, Khan and Chaparro [23] further studied non-stationary Wiener filtering based on evolutionary spectral theory. They considered two cases of uncorrelation between the signal and the noise: disjoint supports of the generating kernels of the signal and noise, and orthogonal

innovation processes of the signal and noise. For the latter case, their solution coincided with that of Abdrabbo and Priestley [20].

In the present study, a new method for TVWF design is proposed [27] and will be investigated further. It is based on time-varying AR (TVAR) modeling [28, 29], i.e. modeling the signal and noise as auto-regressive processes with time-varying coefficients which are further modeled as combinations of a set of known functions of time.

1.3 Instantaneous Frequency Estimation

Time-frequency analysis is an extension of stationary spectral analysis. Time-varying filtering, or alternatively, time-frequency filtering, is an extension of the time-invariant filtering problem. In the same way, instantaneous frequency (IF) estimation can be viewed as an extension of stationary sinusoidal frequency estimation [30]. While these stationary problems have been studied extensively, there is still much unsolved for their nonstationary extensions. An extensive review on instantaneous frequency estimation techniques was contributed by Boashash [31] in 1992. According to this review and the references therein, the “primitive” methods such as phase difference estimators and zero-crossing IF estimators are conceptually and computationally simple, but they perform poorly for noisy signals. The Phase Locked Loops (PLL), which can be easily built and are widely used in communications systems, are a form of adaptive IF estimation. The PLL is relatively noise resistant, but is unable to track a wide ranging or rapidly varying frequency. Other adaptive IF estimation algorithms were developed, such as those based on Kalman filtering theory and those combining stationary auto-regressive (AR) modeling and adaptive filtering algorithms. The Kalman filtering based method can be

viewed as an extension of the PLL. All the PLL, Kalman filtering, and adaptive filtering based IF estimation methods are essentially IF tracking processes and therefore unable to respond to very rapidly varying frequencies.

An important class of IF estimation methods is based on TFR or time-frequency distributions (TFD). Any appropriate TFD, such as the spectrogram and WVD, can be applied to IF estimation. The IF is estimated through either peak detection or first-moment estimation of TFDs. For lower SNR, Boashash suggested an iterative procedure of combining time-frequency filtering and moment estimation to improve IF estimation [3]. Among these, WVD peak based IF estimation was reported to be optimal for linear frequency modulated (FM) signals with high to moderate SNR [33] and hence was recommended [31]. The present research [34] revealed that the optimality of the WVD based method requires the following conditions simultaneously: 1) a linear FM signal, 2) the time instances of the estimated IF are far from the data ends, 3) generous zero-padding or frequency interpolation, and 4) high SNR. Violation of any one of these conditions can lead to a performance ceiling for the WVD based method [34].

The TFD based IF estimators are non-parametric in the sense that there is no parametric modeling applied to the observation data, although by modeling the IF laws one can improve the TFD based estimators [35]. An extensively studied class of parametric IF estimation methods is based on polynomial phase modeling, i.e., modeling the signal as a complex exponential function with phase in the form of a finite order polynomial function of time. The polynomial coefficients for the phase can be estimated by solving a non-linear regression problem somehow or by a multi-dimensional search which leads to ML estimates [31].

The last IF estimation method to be introduced here is the IF estimation based on time-varying AR (TVAR) modeling, proposed by Sharman and Friedlander in 1984 [36]. Since being proposed, this method has been considered a poor estimator [31, 36] and, as a result, there has not been much further study of this method reported in the literature. As part of this research, we again study this approach. Our preliminary work has shown that the TVAR based method, though not optimal in any case, is robust and performs satisfactorily in various situations [34].

1.4 Time-Varying Interference Suppression for Direct Sequence Spread Spectrum (DSSS) Communications

A spread spectrum communication system uses a transmission bandwidth that is purposely made wider than the necessary information bandwidth of the signal. The spectrum spreading is typically accomplished with techniques such as direct sequence (DS), frequency hopping (FH), or a hybrid of DS and FH. The advantages of the spread spectrum techniques include low probability of signal interception, protection against interference and hostile jamming, resistance to multipath fading, and efficiency of frequency reuse. Based on the direct sequence spread spectrum (DSSS) technique the prevailing code-division multiple access (CDMA) systems were proposed and built. In the present study, we focus on the nonstationary interference suppression problem for DSSS communications.

The benefit of the immunity to noise and interference of a DSSS system is referred to as “processing gain.” However, excessive noise and/or interference beyond the protection of the processing gain still jeopardize the system. While an adequate signal

to noise ratio (SNR) can be assured by proper link budget design, it is impractical to predict or avoid excessive interference from uncooperative sources. Interference in a DSSS system can be classified into the following categories: 1) multiple access interference (MAI) in CDMA from other users' signals, 2) hostile jamming, and 3) co-channel interference from other sources, including other communications systems. MAI is usually mitigated through power control and multiuser detection techniques, which have been actively studied in recent years [42, 43 and the references therein]. This research focuses on suppression techniques for time-varying interference from jammer or overlaid communication systems, such as the FM signal from an AMPS system overlaid with a CDMA system.

In a direct sequence CDMA system, MAI has the same spectral characteristic as the signal of the desired user. Therefore, in general, MAI can not be mitigated through temporal filtering. Instead, the cancellation of MAI exploits either 1) the cross-correlation among the spreading codes of all users in a cell, which results in decorrelating multiuser receivers, 2) temporary decisions of all the users, which results in multi-stage interference cancellation multiuser receivers, or 3) spatial information from antenna arrays. In contrast, non-MAI interference usually has spectral characteristics different from the desired spread spectrum signal, and therefore temporal signal processing can help to improve the system performance.

In 1986, Milstein and Iltis [44] reviewed the earlier studies on interference rejection in spread spectrum communications, including least-squares estimation techniques, Fourier frequency domain processing, and adaptive spatial filtering. In the reviewed works it was assumed that the interference was stationary or slowly time-

varying and, therefore, traditional LTI filters were applied for the stationary cases and the adaptive algorithms were effective in tracking the changes. Later, the discrete wavelet transform (DWT) was applied to reject pulse jamming or interference with burst characteristics [45], in a similar way as the Fourier transform domain method for tone jamming or stationary narrow-band interference [46].

In recent years, time-frequency distributions are being applied to handle rapidly varying nonstationary interference in DSSS communications [47-50]. Amin and his colleagues [47, 48] studied interference excision using a time-varying notch filter with the null placed at the instantaneous frequency (IF) of the interference, where the IF was estimated from time-frequency distributions (TFD). The study suggested using the length-5 symmetric zero-phase transversal filter with the second order zero placed at the IF of the interference on the unit circle. The authors [49] also studied interference cancellation using the time-frequency synthesis technique mentioned in Section 1.1 as a method for time-varying filtering. With the assumption of constant modulus interference, the interference is synthesized in two steps: first the interference is synthesized by masking the time-frequency distribution of the received signal, and then the estimation is improved by projecting the synthesized signal onto a circle representing the space of the constant modulus jammer. The final jammer estimate was subtracted from the received signal and, by doing so, system performance was improved significantly. Bultan and Akansu [50] applied chirplet decomposition [51] to detect and excise the interference that was localized in the time-frequency plane. This technique used the iterative algorithm of matching pursuits [52] to extract the interference from the received signal. In all the

above time-frequency methods the interference was assumed to have narrow instantaneous bandwidth, as typical for FM signals.

1.5 Introduction to the Time-Varying Autoregressive (TVAR) Model

In this section we review the time-varying autoregressive (TVAR) model, which will be used throughout the following chapters. The idea of modeling a nonstationary time series with time-dependent parameters was first proposed by Rao [41] in 1970 and was studied by Liporace [61] soon after. It was not used for signal processing problems until Hall, Oppenheim and Willsky [28] and Grenier [29] investigated modeling and time-varying spectral estimation of speech signals with this type of model. Soon thereafter, in 1984, Sharman and Friedlander [36] proposed the idea of using time-varying AR (TVAR) modeling for instantaneous frequency estimation.

A discrete-time time-varying autoregressive (TVAR) process $x(t)$ of order p is expressed as

$$x(t) = -\sum_{i=1}^{p} a_i(t)x(t-i) + e(t) \tag{1-1}$$

where $e(t)$ is a stationary white noise process with zero mean and variance σ_e^2, and the TVAR coefficients $\{ a_i(t),\ i = 1,2,\cdots, p \}$ are modeled by linear combinations of a set of basis time functions $\{ u_k(t),\ k = 0,1,\cdots, q \}$:

$$a_i(t) = \sum_{k=0}^{q} a_{i\,k} u_k(t) \tag{1-2}$$

where $\{ u_k(t), k = 0,1,\cdots, q \}$ can be any appropriate set of basis functions. If $\{ u_k(t) \}$ are

chosen as powers of time, then $\{a_i(t)\}$ are polynomial functions of time t. If $u_k(t)$ are trigonometric functions, then (1-2) is a finite order Fourier series expansion. In any case, the TVAR model is described completely by the set of parameters $\{a_{ik}, i=1,2,\cdots,p; k=0,1,\cdots,q; \sigma^2\}$.

The estimation of $\{a_{ik}\}$ aims at minimizing the total squared prediction error in predicting the sequence $x(t)$:

$$E=\sum_t \left| x(t)+\sum_{i=1}^{p}\sum_{k=0}^{q} a_{ik}u_k(t)x(t-i)\right|^2 \tag{1-3}$$

If we define the generalized covariance function as

$$c_{kl}(i,j)=\frac{1}{N-p}\sum_{t=p}^{N-1} u_k(t)\,u_l(t)\,x(t-i)\,x(t-j) \tag{1-4}$$

then the solution $\{a_{ik},\ i=1,2,\cdots p,\ k=1,2,\cdots q\}$ that minimizes (1-3) can be solved for from the generalized covariance equations:

$$\sum_{i=1}^{p}\sum_{k=0}^{q} a_{ik}c_{kl}(i,j)=-c_{0l}(0,j),\ \ 1\le j\le p, 0\le l\le q \tag{1-5a}$$

This is a system of $p(q+1)$ linear equations that can be expressed in matrix form as

$$\mathbf{CA}=-\mathbf{D} \tag{1-5b}$$

where **A** is the coefficient vector, of $p(q+1)$ elements, which can be expressed as:

$$\mathbf{A}=\begin{bmatrix}\mathbf{a}_0\\ \mathbf{a}_1\\ \vdots\\ \mathbf{a}_q\end{bmatrix} \tag{1-6}$$

with

$$\mathbf{a}_k = \begin{bmatrix} a_{1k} \\ a_{2k} \\ \vdots \\ a_{pk} \end{bmatrix}, \; k = 0,1,\cdots,q\,, \tag{1-7}$$

and **C** is the extended covariance matrix of size $p(q+1)$ by $p(q+1)$:

$$\mathbf{C} = \begin{bmatrix} \mathbf{c}_{00} & \mathbf{c}_{01} & \cdots & \mathbf{c}_{0q} \\ \mathbf{c}_{10} & \mathbf{c}_{11} & \cdots & \mathbf{c}_{1q} \\ \vdots & \vdots & \ddots & \vdots \\ \mathbf{c}_{q0} & \mathbf{c}_{q1} & \cdots & \mathbf{c}_{qq} \end{bmatrix} \tag{1-8}$$

with

$$\mathbf{c}_{kl} = \begin{bmatrix} c_{kl}(1,1) & c_{kl}(1,2) & \cdots & c_{kl}(1,p) \\ c_{kl}(2,1) & c_{kl}(2,2) & \cdots & c_{kl}(2,p) \\ \vdots & \vdots & \ddots & \vdots \\ c_{kl}(p,1) & c_{kl}(p,2) & \cdots & c_{kl}(p,p) \end{bmatrix}, \; 1 \le k \le q,\, 0 \le l \le q\,, \tag{1-9}$$

and

$$\mathbf{D} = \begin{bmatrix} \mathbf{d}_0 \\ \mathbf{d}_1 \\ \vdots \\ \mathbf{d}_q \end{bmatrix} \tag{1-10}$$

with

$$\mathbf{d}_k = \begin{bmatrix} c_{0k}(0,1) \\ c_{0k}(0,2) \\ \vdots \\ c_{0k}(0,p) \end{bmatrix}, \;\; k = 0,1,\cdots q\,. \tag{1-11}$$

For the special case of $q = 0$, the above system of equations reduces to the Yule-Walker Equations for the stationary AR model.

If we change the summation interval in (1-4) from [p, N –1] to $[-\infty, +\infty]$, or equivalently [0, N–1+ p], by assuming that the data can be extended by zeros outside the data record, the resulting equations (1-5) are the generalized *correlation* equations.

The matrices $\mathbf{c}_{kl} = \mathbf{c}_{lk}$ are $(p \times p)$ symmetric. Therefore, $\mathbf{C}$ is a $(q+1)\times(q+1)$ block symmetric matrix with ($p \times p$) symmetric blocks. $\mathbf{C}$ is not Toeplitz, and hence the Levinson algorithm [30] can not be applied directly. For the *correlation* method, the matrix $\mathbf{C}$ is symmetric and block-Toeplitz so that a modified version of the Levinson algorithm can be used to solve (1-5) fast [29]. For the *covariance* method, the symmetry structure can also be explored to solve (1-5) [29].

1.6 Research Motivations and Objectives

In this section, we define our research objectives and outline. Our general motivation is to develop non-stationary signal processing methods based on time-varying parametric modeling. This is different from the parametric non-stationary signal processing methods based on temporal windowing, where stationary modeling is applied inside each data window [26]. It is also different from another type of extensively studied and applied time-varying signal processing – adaptive signal processing [38], where training data is required so that it is not suitable for short data records and rapidly varying processes. Our research is aimed at a better ability to handle rapidly varying signals and short data records. We consider short data records due to the fact that in many applications it is either desirable to deal with a smaller number of samples or only short data records are available.

Parametric stationary signal processing has been studied extensively in the past decades. Due to its attractive properties, such as high resolution, low computational complexity and noise resistance, applications can be found in a variety of areas, such as speech processing, radar/sonar, biomedical engineering and neural science. As a matter of fact, in many practical situations, most signals are non-stationary in nature. It may be of advantage to exploit non-stationary or as they are alternatively referred to, time-varying signal processing methods. As seen in Sections 1.1 through 1.3, most of the existing time-varying signal processing approaches are nonparametric. Our objective is to develop signal processing methods which combine the advantages of being both time-varying and parametric. Specifically, we focus on time-varying Wiener filtering and instantaneous frequency estimation, as well as their potential applications in interference suppression for spread spectrum communications.

We expect that the parametric time-varying signal processing methods under development have many potential applications. The scenario of most interest to us in this research is the time-varying interference suppression problem in communications. We apply the TVAR based IF estimator to time-varying notch filtering for cancellation of interference with narrow instantaneous bandwidth. We also formulate a nearly optimal time-varying interference suppression filter based on the idea of the TVWF proposed in this study.

1.7 Research Outline

The outline of the present research is presented below. The research work is divided into five parts. In summary, in this research, we plan to develop a time-varying

signal processing method based on TVAR modeling, and to explore a TVAR based IF estimation method. After validating the performance of these methods, they are applied to improve the performance of DSSS communication systems by suppressing time-varying interference.

1.7.1 Instantaneous Frequency (IF) Estimation Based on TVAR Modeling

First, we will examine the performance of TVAR based IF estimation, especially for the case of short data records, and compare with WVD peak based IF estimation. The TVAR method is expected to provide robust performance in moderate to high SNR and under various conditions such as linear or non-linear IF laws, shorter or longer data records, and close to or far from the ends of data blocks.

Then we will improve the performance of the TVAR based IF estimation method for low SNR environments. A higher model order is used to let the extra poles capture a portion of the noise components and the signal poles are distinguished from the noise poles based on a "best subset" criterion, which is to be developed further for the time-varying case. This idea was proven effective in the stationary case [53], and is expected to be extendable to the time-varying case.

1.7.2 FM Interference Suppression for Direct Sequence Spread Spectrum Communications Using TVAR based IF Estimation

After examining the performance advantages of the TVAR based IF estimation, we apply it to notch filter based FM interference suppression in DSSS communications. We will examine the system BER performance improvements due to the interference

cancellation using the TVAR based IF estimation, compare it with using the exact IF (supposedly known) and the existing method that uses the Wigner-Ville distribution (WVD) based IF estimates.

1.7.3 Time-Varying Optimum Filtering Based on TVAR Modeling

In the second part of the research, we develop TVAR model based optimum filtering methods, including the TVAR based Kalman filter and TVAR based Wiener filters. These formulations directly relate the filter parameters to the model parameters and provide optimum or nearly-optimum time-varying filters. The modeling parameters are identified from a block of observation data with the aid of *a priori* information. We will examine the performance of the proposed TVAR based filters through simulations, with both exact (supposedly known) TVAR parameters and estimated parameters. The comparison will show that the non-causal TVAR based Wiener filter performs significantly better than the TVAR based Kalman filter, which is the optimal causal filter. It will also be revealed that the causal TVAR based Wiener filter performs almost the same as the Kalman filter, and, therefore, is a nearly-optimum causal filter.

1.7.4 FM Interference Cancellation Based on TVAR Wiener Filtering

The TVAR based Wiener filter will be applied to perform time-varying interference suppression filtering for DSSS communications. Unlike the notch filter based cancellation method which uses only the frequency information to form a deep notch, this method is aimed at minimum signal distortion and exploits the full spectral information. We will examine the system BER performance improvements due to

application of the proposed filter and compare it with the notch filter method with exact IF information used.

1.7.5 Time-Varying Whitening Filter Based on the TVAR Model for FM Interference Cancellation in DSSS Communications

Finally, we will propose a simple, yet effective time-varying FIR filter for FM interference suppression filtering in DSSS communications. It is aimed at the spectral flatness of the filter output and is formed as the TVAR based linear prediction error filter. We will examine the system BER performance improvements due to application of the proposed filter and compare it with other methods.

Chapter 2

INSTANTANEOUS FREQUENCY ESTIMATION BASED ON TVAR MODELING

In this chapter, we introduce the TVAR based instantaneous frequency (IF) estimation method, and examine its performance by comparing it with the WVD peak based method for IF estimation through simulations. This work leads us to make a conclusion about TVAR based IF estimation that is contrary to the prevailing conclusion in the literature. The major content of this chapter was published earlier [34].

2.1 Introduction

For an observed signal consisting of single or multiple time-varying frequency components, such as frequency modulated (FM) components in white noise, it is of primary interest to estimate the instantaneous frequency (IF) of each component. This problem arises, for example, in the fields of radar, wireless communications, and underwater acoustics [3].

Boashash [31] reviewed and compared various IF estimation algorithms in terms of statistical performance as well as computational complexity. The estimator based on the peaks of the Wigner-Ville Distribution (WVD), which is briefly introduced in Appendix A for ease of reference, was reported to provide superior statistical performance with reasonable complexity. In addition, WVD peak based IF estimation (WVD-IF) was shown to be optimal for linear FM signals with high to moderate SNR [33]. Therefore, in order to evaluate the performance of the TVAR based IF estimator, we choose the WVD peak based IF estimator to compare against and choose a linear FM signal with high to moderate SNR as one of the scenarios.

TVAR model based instantaneous frequency estimation (TVAR-IF) has been considered a poor estimator since being proposed in 1984 [31, 36]. Consequently, not much further investigation of this method was reported in the literature. Our work on this method leads us to conclude that, contrary to the prevailing opinion, TVAR based IF estimation performs well, and is especially suitable for those practical cases where only a short data record is available and a linear IF law can not be assumed. TVAR model based IF estimation is thus worthy of further research. We compare TVAR based IF estimation with the Wigner-Ville Distribution (WVD) peak based method, which reveals performance ceilings due to end-effects, frequency quantization error, and bias associated with the WVD based approach.

Our work reveals that the performance of the WVD based method deteriorates for three reasons: the end-effects, the frequency quantization error, and the bias for general nonlinear FM. As in the stationary case, we expect that a parametric model, such as an autoregressive model, may perform significantly better by exploiting *a priori* knowledge

about the signal. We confirm this by comparing the statistical performance of the TVAR based and the WVD based algorithms through simulations.

2.2 TVAR Based IF Estimation: Method and Examples

In the stationary case, it is well known that tones in white noise can be modeled approximately as an AR process, when SNR is high, and high-resolution frequency estimation can be achieved through such AR modeling [30]. We can extend this idea to the time-varying case to achieve IF estimation through TVAR modeling.

2.2.1 Method

For a signal consisting of *M* FM components in white noise with high to moderate SNR, we model the signal with a TVAR model, with order $p=M$ for complex exponential FM components and $p=2M$ for real signals. The time-varying transfer function [39] corresponding to the TVAR model can be expressed as

$$H(t,z)=\frac{1}{A(t,z)}=\frac{1}{1+\sum_{i=1}^{p}a_i(t)z^{-i}} \tag{2-1}$$

By rooting the denominator polynomial $A(t,z)=1+\sum_{i=1}^{p}a_i(t)z^{-i}$ formed by the TVAR coefficient estimates, at each time instant t, we can obtain the p poles as functions of time: $p_i(t), i=1,2,\cdots,p$. The trajectories of the poles associated with the FM components are on or close to the unit circle for moderate to high SNR. The rooting operation could be trivial for low order p. For example, $p_1(t)=-a_1(t)$ for $p=1$ and

$p_{1,2}(t) = [\,-a_1(t) \pm \sqrt{a_1(t)^2 - 4a_2(t)}\,]/2$ for $p = 2$. The instantaneous angles of the poles associated with the FM components can be used as estimates of the instantaneous frequencies $\hat{f}_i(t)$:

$$\hat{f}_i(t) = \arg\, p_i(t) \quad \text{for } |p_i(t)| \approx 1 \tag{2-2}$$

Our procedure for IF estimation based on the TVAR model thus consists of the following steps:

1. Choose the basis functions $u_k(t), k = 0,1,\cdots,q$, and the orders *q* and *p*.
2. Calculate the generalized covariance function according to (1-4), solve for $a_{i\,k}$ from equation (1-5), and construct the TVAR coefficients $a_i(t)$ by (1-2).
3. Root the time-varying poles $p_i(t), i = 1,2,\cdots p$ at each instant t.
4. Find the time-varying angles of the poles $p_i(t), i = 1,2,\cdots p$ as the IF estimates of the FM components.

In addition, if a model for the frequency variation $f_i(t)$ is available, such as a polynomial function, a more accurate estimate of $f_i(t)$ can be achieved by fitting $\hat{f}_i(n)$ to that known model.

The basis function set and the orders p and q should be selected using *a priori* knowledge of the signal. For a signal consisting of continuous FM components such as an echo from moving targets, it is appropriate to use powers of time as the basis function set. Other alternatives include trigonometric functions [29] and wavelets [40].

2.2.2 Example 1: A Chirp Signal

To illustrate the TVAR based IF estimation method, we present an example in detail, as shown in Figure 2-1. Here we consider a block of linear FM signal with 32 samples at unit sampling rate, which chirps in frequency from 0.1 to 0.41 Hz according to $f(t) = 0.1 + 0.01t,\ t = 0,1,\cdots,31$, as plotted in Figure 2-1(a). The signal is corrupted by additive white Gaussian noise at SNR=20dB. A complex-valued data record is generated, as shown by the solid lines in Figure 2-1(c), for the real part, and in Figure 2-1(d), for the imaginary part. The real part and the imaginary part of the noise sequence are generated independently. The FM signal is a complex exponential function with the specified IF law, a random initial phase, and unity amplitude. We model the data record with a TVAR model with $p = 1$ and $q = 3$, and use polynomials as the set of "basis functions" $u_k(t), k = 0,1,\cdots,q$ to represent the TVAR coefficients $a_i(t)$, specifically, $u_k(t) = (\frac{t-1}{32})^k$, $k = 0,1,2,3,\ t = 1,2,\cdots,31$ is used. The resulting generalized covariance equations are

$$\begin{bmatrix} 32.2609 & 15.2330 & 9.6954 & 6.9455 \\ 15.2330 & 9.6954 & 6.9455 & 5.3086 \\ 9.6954 & 6.9455 & 5.3086 & 4.2259 \\ 6.9455 & 5.3086 & 4.2259 & 3.4592 \end{bmatrix} \begin{bmatrix} a_{1,0} \\ a_{1,1} \\ a_{1,2} \\ a_{1,3} \end{bmatrix} = - \begin{bmatrix} -1.1108 + 27.2977\mathrm{i} \\ -4.9798 + 12.7511\mathrm{i} \\ -4.5459 + 7.7954\mathrm{i} \\ -3.8274 + 5.3764\mathrm{i} \end{bmatrix},$$

and the solution is

$$\begin{bmatrix} a_{1,0} \\ a_{1,1} \\ a_{1,2} \\ a_{1,3} \end{bmatrix} = \begin{bmatrix} -0.7256 - 0.5969\mathrm{i} \\ 0.6736 - 1.8260\mathrm{i} \\ 3.0021 + 2.2982\mathrm{i} \\ -2.1379 - 0.3611\mathrm{i} \end{bmatrix}.$$

The TVAR coefficients determined by $a_i(t) = \sum_{k=0}^{q} a_{ik} u_k(t)$ are shown in Figure 2-1 (b). The TVAR one-step prediction, $\hat{x}(t), t = 1,2,\cdots 31$, based on this parameter estimate is plotted against the data $x(t), t = 0,1,\cdots 31$, in Figure 2-1 (c) for the real part and in Figure 2-1 (d) for the imaginary part. For this example with $p = 1$, the one-step prediction is simply $\hat{x}(t) = -a_1(t)x(t-1)$, $t = 1,2,\cdots 31$. This waveform comparison shows successful prediction by the TVAR model. Further calculation shows that the averaged squared prediction error, $\frac{1}{31}\sum_{t=1}^{31}\left|x(t) - \hat{x}(t)\right|^2$, is 0.0178, which is larger than, but fairly close to (with 2.5dB difference) the noise power of 10^{-2} for 20dB SNR.

Now we find the time-varying pole $p_1(t) = -a_1(t)$, which is all we have for this case. The trajectory of this pole is shown in Figure 2-1 (e) by the 31 "+" marks, corresponding to $t = 1,2,\cdots 31$. We can see that the pole trajectory is close to the unit circle. The IF estimate is then obtained by evaluating the angle of the pole at each time instant. In Figure 2-1 (f), the IF estimate (*solid*), after dividing by 2π to convert from radians per second to Hz, is compared against the exact IF (*dashed*). The TVAR based procedure is thus shown to result in good IF estimation. The averaged squared error of IF estimation (MSE estimate) evaluated over all 31 time instants ($t = 1,2,\cdots 31$, since no estimate is available at $t = 0$) is $6.37\times 10^{-6} = -52$ dB, or the 1/MSE estimated from this example is 52 dB.

A time-frequency distribution (TFD), or time-varying power spectrum, is not needed for the TVAR bases IF estimation procedure, which uses pole location information from the TVAR model. However, it is informative to examine the TFD

evaluated from the TVAR model identification and compare it with the WVD in order to appreciate why TVAR based IF estimation can outperform WVD peak based IF estimation. The TVAR based TFD is given as Figure 2-1 (g), and the WVD as Figure 2-1 (h). The TVAR based TFD is calculated in the same way as for AR model based spectrum estimation in the stationary case [30], which is $P(t,z)=\frac{\sigma^2}{A(t,z)A^*(t,1/z^*)}$ evaluated on the unit circle $z=e^{j2\pi f}$. For the result shown, we have 33 frequency samples, from 0 to 0.5 Hz with interval 1/64Hz, for all the time samples except for $t=0$. The WVD is calculated based on a 32-point discrete Fourier transform (DFT) at each time instant, which gives a TFD for the same frequency samples except for $f=0.5$. We see that the peak of the TVAR based TFD is consistent with the IF estimate, which is based on pole angle, shown in Figure 2-1 (f).

If we estimate the IF by searching for the peak of a TFD, which is possible for a single component signal, then the IF estimate will be taken from the limited number of frequency samples at each time instant. This is the case for WVD peak based IF estimation, and we refer to the error due to this limitation as "frequency quantization error." To reduce the frequency quantization error for WVD peak based IF estimation, we increase the number of frequency samples by using a large size DFT on the zero-padded "instantaneous correlation" sequence. Some sort of frequency interpolation may be also possible.

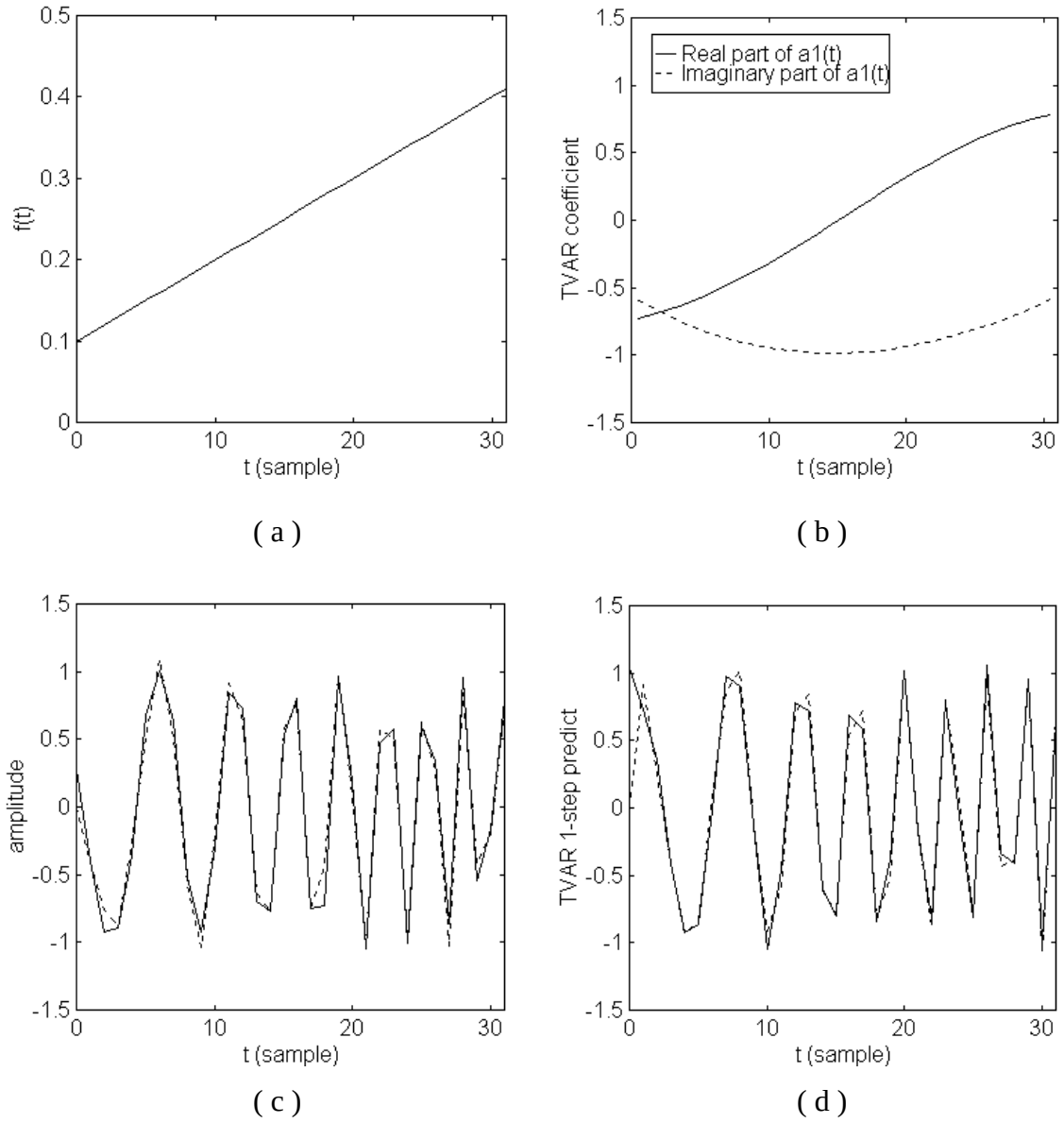

Figure 2-1. An example of TVAR based IF estimation from a complex-valued data record taken from an analytical linear FM signal in complex white noise, with $p = 1$ and $q = 3$ for the TVAR model (*continued on the next page*):

(a) the IF law used to generate the data,

(b) the estimated TVAR coefficient $a_1(t)$, $t = 1,2,\cdots,31$, in terms of its real (*solid*) and imaginary part (*dashed*),

(c) the real parts of the data (*solid*) and the TVAR 1-step prediction (*dashed*),

(d) the imaginary parts of the data (*solid*) and the TVAR 1-step prediction (*dashed*).

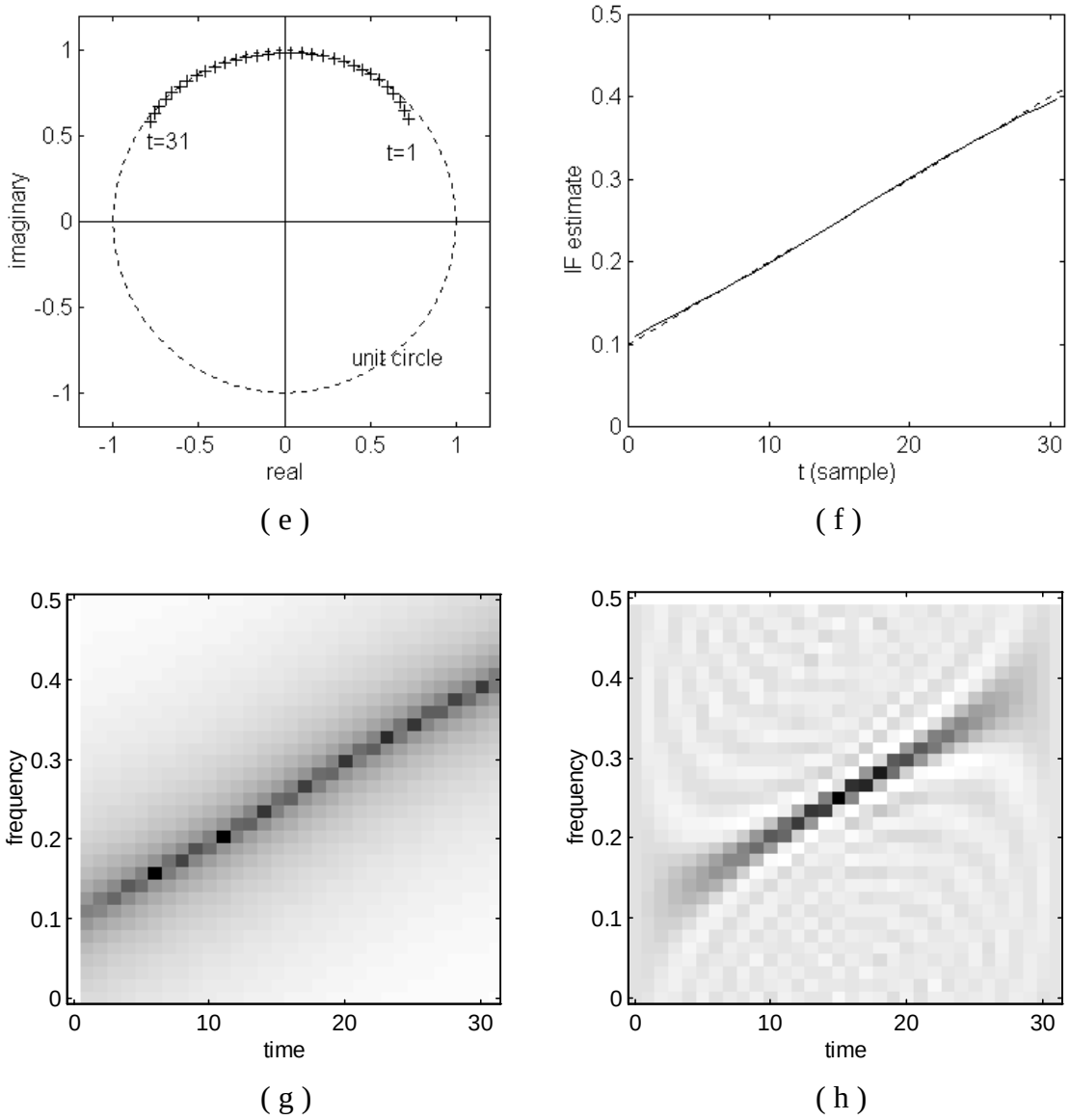

Figure 2-1. (*continued*) An example of TVAR based IF estimation, a complex-valued data record with an analytical linear FM signal in complex white noise, $p = 1$ and $q = 3$ for the TVAR model:
(e) the trajectory of the estimated time-varying pole of the TVAR model,
(f) IF estimate based on TVAR model (*solid*) vs. the exact IF (*dashed*),
(g) the time-varying spectrum evaluated from the TVAR model,
(h) the WVD of the data record.

In calculating the WVD estimate, a smaller and smaller number of data samples is available when estimating the instantaneous correlation function for a time instant near

the ends of the data record. Consequently, the peak of the WVD fades out towards the ends of the data record, as shown in Figure 2-1 (h). The latter will lead to very poor IF estimation near the ends of a data record. This limitation is referred to as "end effects" for the WVD peak based IF estimation.

Another drawback of TFD peak based IF estimation is that it requires calculating and storing the 2-dimensional distribution, the TFD, and 1-dimensional peak searching on the TFD. This could be a major implementation burden in terms of computing power and memory size. Another reason that we use the pole angle, rather than the location of the spectral (TFD) peak, derives from the analogy of TVAR based IF estimation to AR spectral estimation. For AR model based frequency (tone) estimation in the stationary case, pole angle based estimation was shown to lead to better performance than spectral peak based estimation [30].

2.2.3 Example 2: A Frequency-Hopping Signal

As another example, we demonstrate the TVAR based IF estimation approach on a record of a frequency-hopping signal. Here we consider a frequency-hopping signal with 32 samples at unit sampling rate. The IF hops from 0.1 to 0.3 Hz at $t = 20$, as plotted in Figure 2-2 (a). As in Example 1, the signal is corrupted by additive white Gaussian noise at SNR=20dB. A complex-valued data record is generated, as shown with solid lines in Figure 2-2 (c), for the real part, and in Figure 2-2 (d), for the imaginary part. We model the data record with a TVAR model with $p = 1$ and $q = 5$, and use polynomials as the set of "basis functions" $u_k(t), k = 0,1,\cdots,q$ to represent the TVAR coefficients $a_i(t)$. This is similar to Example 1 except for a difference in the polynomial

order. The estimated $a_1(t)$ is shown in Figure 2-2 (b). The TVAR one-step prediction is plotted against the data in Figure 2-2 (c) for the real part and in Figure 2-2 (d) for the imaginary part. We observe a close match between the data and the prediction.

Now we find the time-varying pole $p_1(t) = -a_1(t)$. The trajectory of the pole is shown in Figure 2-2 (e) by the "+" marks. The IF estimate is then obtained by evaluating the angle of the pole at each time instant. In Figure 2-2 (f), the IF estimate (*solid*) is compared against the exact IF (*dashed*). The TVAR model using the 5th order polynomial follows the frequency hopping successfully.

As in Example 1, we now examine the time-varying spectrum, evaluated from the identified TVAR model, and compare it with the WVD. The TVAR based TFD is given in Figure 2-2 (g), and the WVD in Figure 2-2 (h). The TVAR based TFD is consistent with the IF estimate. For the WVD, we can see the end-effects and the severe pseudo peaks due to cross-term interference.

2.3 Performance of TVAR Based IF Estimation

In this section, we evaluate the performance of the TVAR based IF estimation by comparing it through simulations with the WVD based IF estimation and the Cramer-Rao bound [31,62]. We first compare the TVAR based method with the WVD based method for a case of a linear FM signal since the WVD method had been shown to be optimal for such cases at high to moderate SNR. We then examine a more general case with a nonlinear IF law.

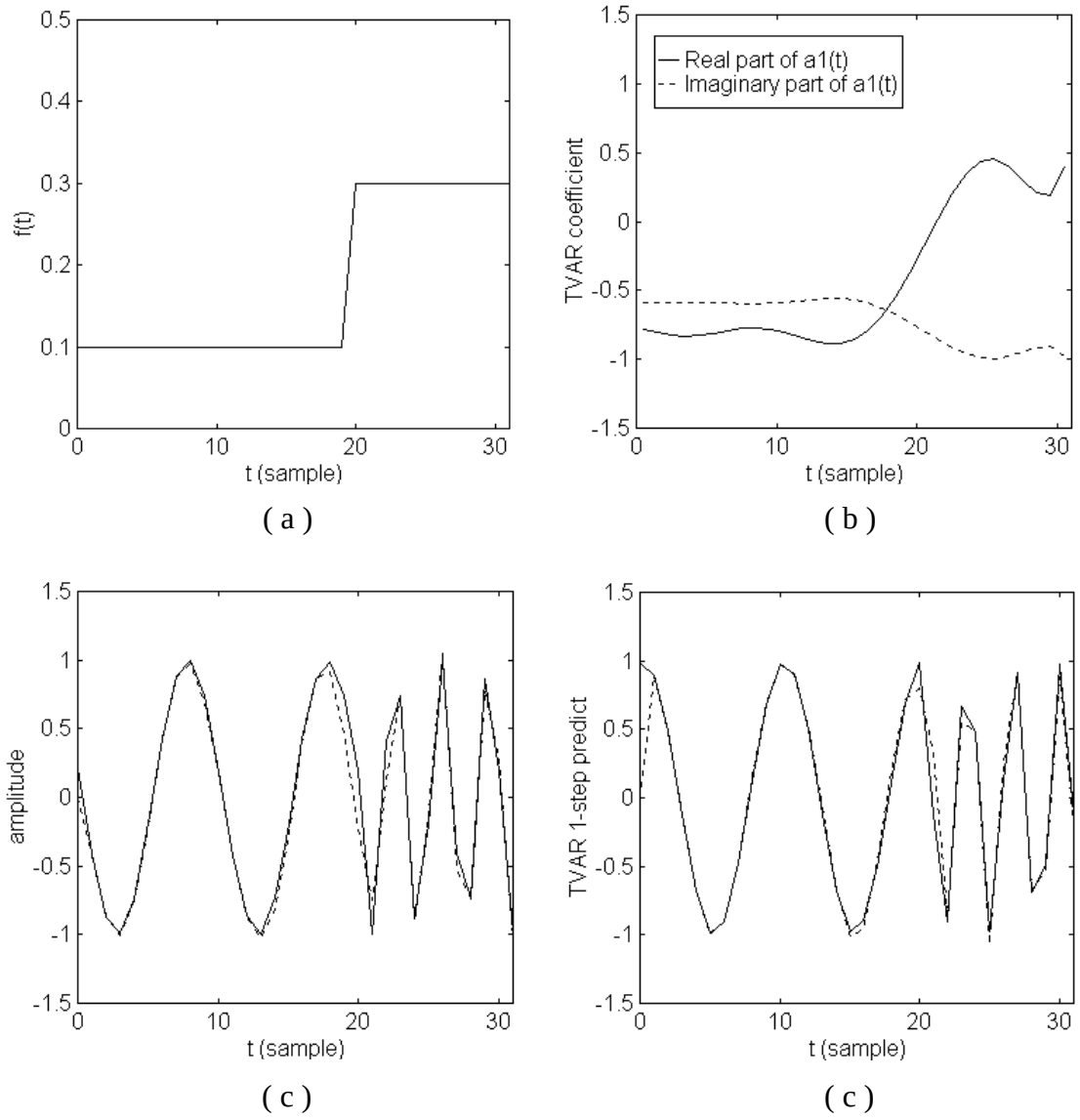

Figure 2-2. Example of TVAR based IF estimation, a complex-value data record with an analytical frequency-hopping signal in complex white noise, $p = 1$ and $q = 5$ for the TVAR model (*continued on the next page*):

(a) IF law used to generate the data,

(b) estimated TVAR coefficient $a_1(t), t = 1,2,\cdots,31$, ($a_i(0)$ is not available), real (*solid*) and imaginary part (*dashed*),

(c) real parts of data (*solid*) and TVAR 1-step prediction (*dashed*),

(d) imaginary parts of data (*solid*) and TVAR 1-step prediction (*dashed*).

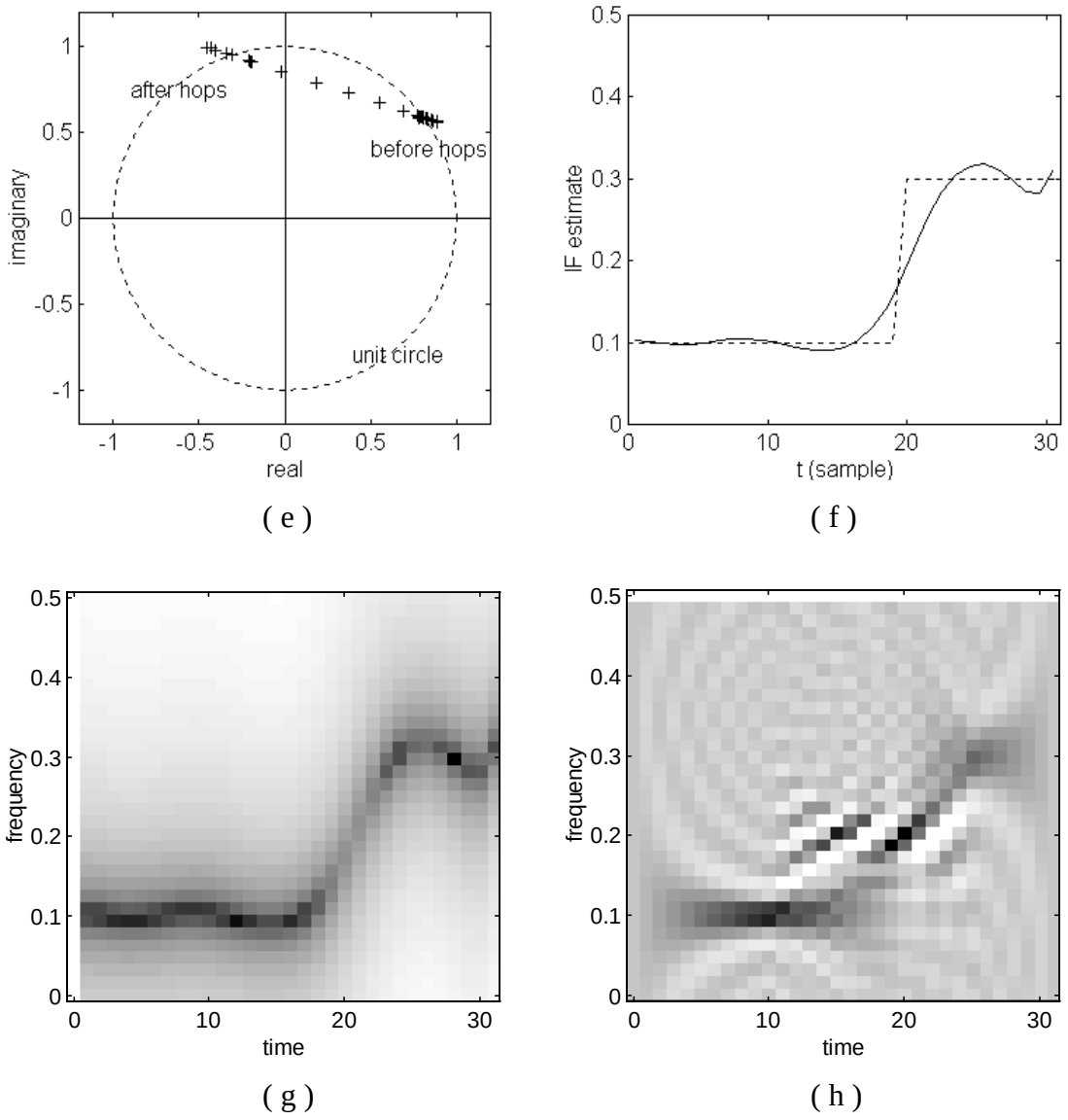

Figure 2-2. (c*ontinued*) An example of TVAR based IF estimation, a complex-value data record with an analytical frequency-hopping signal in complex white noise, $p = 1$ and $q = 5$ for the TVAR model:

(e) trajectory of the estimated time-varying pole of the TVAR model,

(f) IF estimate based on TVAR model (*solid*) vs. the exact IF (*dashed*),

(g) time-varying spectrum evaluated from the TVAR model,

(h) the WVD of the data record.

2.3.1 Experiment Setup and Implementation

In the simulation experiments, we consider a short data record of 32 samples. The data consists of an FM signal, linear or nonlinear, and additive white Gaussian noise. In generating the FM signal, the FM law is set as deterministic, while the initial phase is random (uniform over $[0,2\pi)$), and varies from trial to trial in the simulation.

We use complex-valued data representing an analytical FM signal in complex noise, rather than real-valued data. In practice, the complex-valued data could be analytic if it is obtained through Hilbert transformation from real-valued data. Nevertheless, here we consider the more general case where the signal part is analytic, while the noise part is not, and has double-sided non-symmetric spectrum. Using complex-valued data enables us to use a lower autoregressive order for the TVAR model, which implies simplicity in implementation. For the WVD based IF estimation method it is also necessary to use complex-valued data with an analytic signal component to avoid frequency aliasing of the signal component in the time-frequency plane.

In our implementation of the TVAR parameter estimation, the set of generalized covariance equations, of size $p(q+1)$, is solved simply using Gaussian elimination. While fast algorithms are available [29, 63, 64], these are beyond the topic of this research. To calculate the WVD for each data record of length 32, 32-point (without zero-padding) or, for example, 4096-point (with zero-padding) DFT's are performed for each time instant. The DFT at each time instant is performed on the "instantaneous auto-correlation" sequence, which computes the "instantaneous power distribution" for that time instant. In calculating the "instantaneous auto-correlation" sequence, zero values are assumed outside of the data record.

The IF estimation errors at each time instant are calculated by comparing the IF estimates with the exact IF value that was used to generate the data. The mean square error (MSE) of the IF estimation is estimated by averaging the squared IF errors across both time instants and simulation trials. Two ranges of time instants are used to evaluate the MSE of IF estimation: the 16 time instants near the time center of the data record, and the full time duration except the first p (the autoregressive order) instants, where the TVAR based IF estimates are not available. As a measure of IF estimation performance, the reciprocal of the estimated MSE, 1/MSE, is plotted versus SNR.

2.3.2 Linear FM Signal Scenarios

As shown in Figure 2-1, we use a linear FM signal with 32 samples at unit sampling rate, which chirps in frequency from 0.1 to 0.41 Hz according to $f(t) = 0.1 + 0.01t,\ t = 0,1,\cdots,31$, and is corrupted by additive white Gaussian noise. The signal is generated using the IF with unit amplitude and a random initial phase. The reason for choosing a linear FM signal is that the WVD peak based IF estimator is optimal for this type of signal at high to moderate SNR [31, 33]. The analytic signal in complex-valued noise is used. The model involved is a first-order autoregressive model (p=1) with the time-varying coefficient represented as a third-order polynomial function (q=3), denoted as TVAR(1,3). The generalized covariance method [28] is used to identify the TVAR parameters.

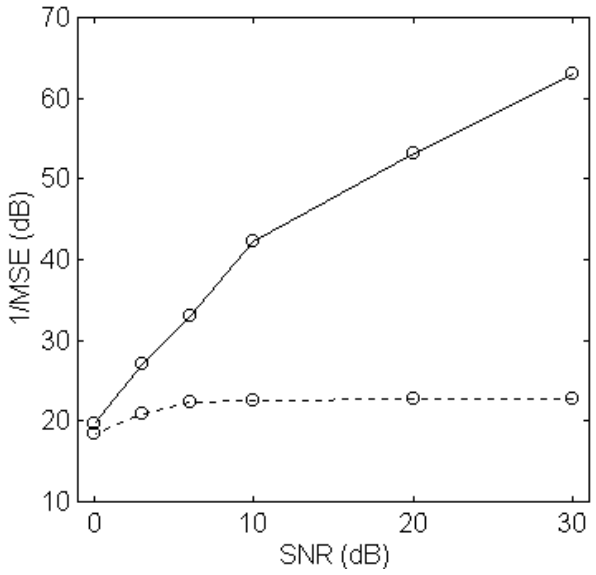

Figure 2-3. 1/MSE vs. SNR on the full time duration: TVAR-IF (*solid*) and WVD-IF (*dotted*).

In Figure 2-3, the reciprocal of the MSE is plotted against SNR, for both TVAR based and WVD peak based IF estimation. We ran 100 simulation trials for each SNR value and the MSE was calculated from the 100 IF estimates at samples t from 1 to 31. In this case, the TVAR based method outperforms the WVD based method and the end-effects of the WVD calculation produce a distinct performance ceiling for the WVD based IF estimates. The end-effects are due to the fact that, with finite-length data records, the number of data samples involved in calculating the discrete WVD is proportional to the distance from the closest end of the data record.

Next, we compare the two methods without the influence of the end-effects. The MSE of the IF estimates is evaluated for the time indices t=8 through 23, i.e. during the central half of the data record. The results are shown in Figure 2-4. While the TVAR based estimation did not change appreciably, the WVD based estimation performs

significantly better away from the ends of the data record. However, another performance ceiling materializes for WVD based IF estimation at SNR above 6dB. This ceiling is due to the frequency quantization error of the discrete WVD arising from the finite length of the data records. For 32-sample sequences, the time-frequency bins for the discrete WVD are of the size of 1 sample period in time by 0.5/32=1/64 Hz in frequency, if no zero-padding is applied.

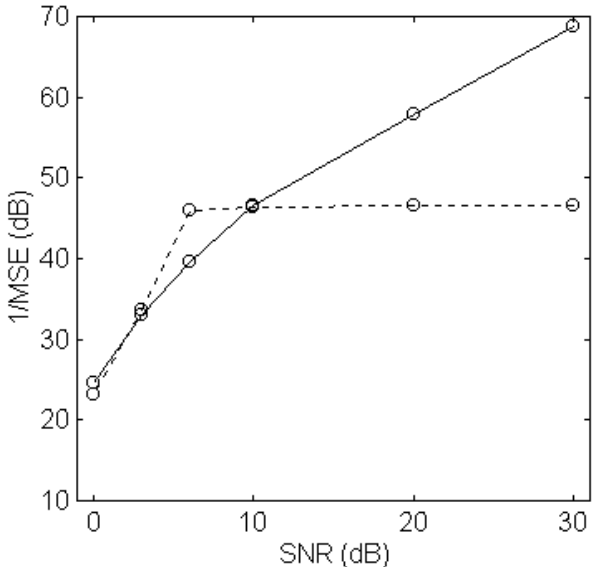

Figure 2-4. 1/MSE vs. SNR near the time center of the data record: TVAR-IF (*solid*) and WVD-IF peak (*dotted*).

When using WVD based IF estimation, for short records with moderate to high SNR, the associated frequency quantization error dominates the IF estimation error at the center of the data record, while the end-effects of the WVD calculation produce estimation errors that dominate the overall IF estimation performance. In comparison, TVAR based IF estimation is free of the frequency quantization error and its end-effects are slight. Here we chose the WVD peak based IF estimator to compare against, but our

conclusion may be generalized to other time-frequency distribution (TFD) peak or moment based IF estimators [31].

The results are consistent for various lengths of data records at high SNR. Figure 2-5 shows the simulation of 1/MSE versus number of samples *N* with SNR=20dB. For different *N*, we use similar linear FM signals with *N* samples at unit sampling rate, which chirp in frequency from 0.1 to 0.41~0.42 Hz according to $f(t) = 0.1 + 0.01\frac{32}{N}t$, $t = 0,1,\cdots,N-1$.

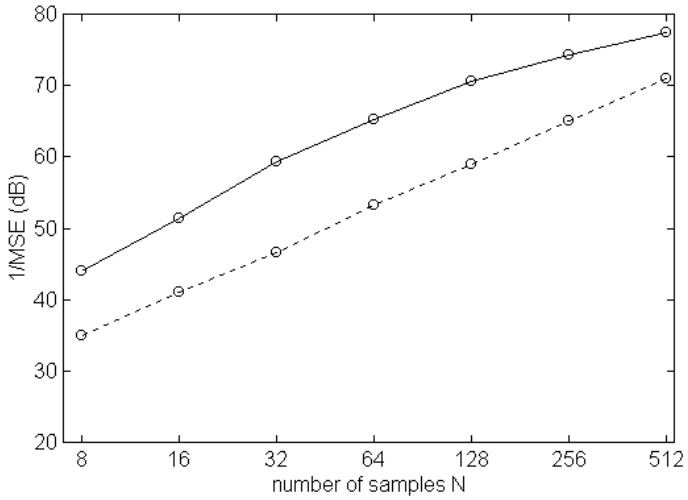

Figure 2-5. 1/MSE vs. number of samples *N* near the time center of the data record, SNR=20dB: TVAR-IF (*solid*) and WVD-IF (*dotted*).

To reduce the frequency quantization error, interpolation on the discrete WVD or zero-padding on the WVD kernel [33] or data is necessary. In this way the WVD based IF estimator may approach the optimal performance, i.e. the Cramer-Rao bound (CRB) for linear FM [31,61,62], at the center of the data record, as given by

$$\mathrm{var}[\hat{f}] \geq \frac{12}{(2\pi)^2 (A/\sigma^2) N(N^2-1)} \tag{2-3}$$

where N is the number of samples, A is the signal amplitude, and σ^2 is the noise variance. Figure 2-6 shows the simulation result for IF estimates at the center half of the data records (samples t=8~23) when zeros are padded so that a 4096-point DFT is used in calculating the WVD, rather than the 32-point DFT used earlier. At moderate to high SNR, the MSE of the TVAR based estimator is about 10dB higher than the Cramer-Rao bound.

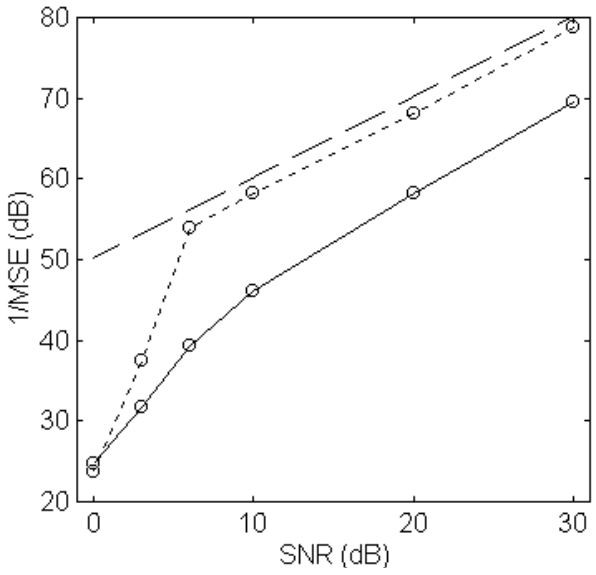

Figure 2-6. 1/MSE vs. SNR near the time center of the data record: TVAR-IF (*solid*), WVD-IF (*dotted*) with sufficient zero-padding, and the Cramer-Rao Bound (*dashed*).

2.3.3 Non-Linear FM Signal Scenarios

Now, we compare TVAR and WVD based IF estimators in the case of a nonlinear FM signal scenario. This simulation is the same as in the linear FM case except that here the desired IF law is $f(t) = 0.05 + 0.0004t^2$, $t = 0,1,\cdots,31$. Considering the higher order of the IF law, we increased the AR coefficient order to q=5. Zero-padding to 4096 points

is applied in the WVD method so that the effect of frequency quantization error is virtually removed. The 1/MSE results are plotted versus SNR in Figure 2-7, which represents IF estimation at the center half of the time record.

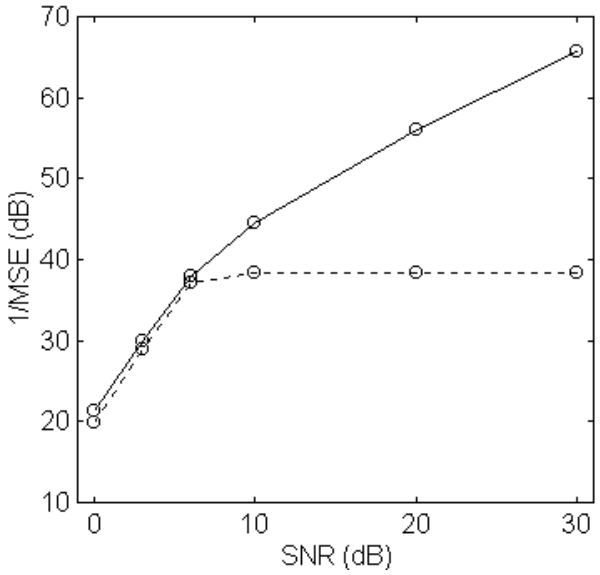

Figure 2-7. 1/MSE vs. SNR near the time center of the data record for a nonlinear FM signal: TVAR-IF (*solid*) with q=5, and WVD-IF peak (*dotted*) with zero-padding to 4096 points.

Comparing Figure 2-7 and Figure 2-6, the TVAR based method performs about the same as in the linear FM case while the WVD based method degrades noticeably. This means that the TVAR based method is significantly less sensitive to the nonlinearity of the IF law. The new performance ceiling of the WVD method in Figure 2-7 is due to the bias of the WVD based IF estimation. That is, when the IF law is not ideally linear, the peak of the WVD shifts away from the position of the actual instantaneous frequency.

Selecting a higher order q for TVAR based IF estimation, such as q=5 in Figure 2-7, reduces the AR coefficient fitting error which dominates the performance at high

SNR, but also accommodates more noise into the model which dominates the performance at low SNR. Figure 2-8 gives the performance of the TVAR-IF method when selecting the order q=3. Here the 1/MSE of the TVAR method increases slowly with SNR due to the AR coefficient fitting error, but it is about 4 dB higher at low SNR than when using q=5.

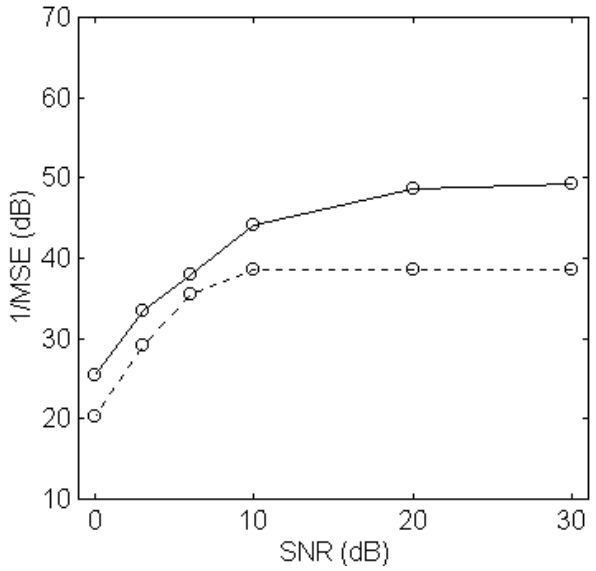

Figure 2-8. 1/MSE vs. SNR near the time center of data record for a nonlinear FM signal: TVAR-IF (*solid*) with q=3, and WVD-IF (*dotted*).

Figure 2-9 helps to observe and explain the performance degradation of the WVD based method for the nonlinear IF law. In Figure 2-9, we show the actual IF and 100 trials of IF estimation based on the WVD (with enough zero-padding) at each instant, for SNR=20 dB. Besides the end-effects, which produce significant IF estimation variance near the ends of the data record, we also see that the WVD based IF estimation is severely biased toward the inner side of the IF curve.

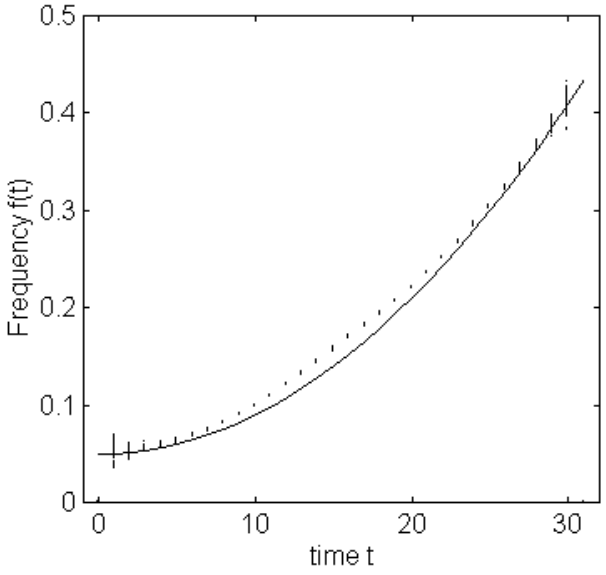

Figure 2-9. Exact IF (*solid line*) and WVD based 100 trials of estimates (*discrete points*) at each instant, for SNR=20 dB, using the WVD peak based IF estimator with zero-padding to length 4096.

In summary, the TVAR based IF estimator is a fairly good one, and especially advantageous for those practical cases where only a short data record is available and linear IF laws can not be assumed *a priori*. The optimality of the WVD based method requires the following simultaneous conditions: 1) a linear FM signal, 2) the time instances of the estimated IF are far from the ends of the data record, 3) generous zero-padding or frequency interpolation, and 4) high SNR. Violation of any of the conditions can make the WVD based method perform worse than the TVAR based method. The TVAR based method, though not optimal in any case, is more robust and performs satisfactorily in various situations. In addition, the benefit of the TVAR based method being cross-term free is highly desired for signals consisting of multiple closely spaced FM components.

2.4 Summary

In this chapter, we introduced the TVAR based IF estimation method with a detailed example, and then examined the performance of the TVAR based IF estimation method through simulations. The results suggested that it is worthwhile to further study this method. In the next chapter, we will propose a time-varying Prony method to improve the TVAR based method for noisy data and lower SNR. Convinced by the results in this chapter, we will apply the TVAR based IF estimation to communication interference cancellation in Chapter 4.

Chapter 3

A TIME-VARYING PRONY METHOD FOR IF ESTIMATION AT LOW SNR

In this chapter, we propose a time-varying Prony method to improve the TVAR based IF estimation performance at low SNR. The benefit of the method is evidenced through simulations. Part of the work in this chapter was published earlier [65].

3.1 Introduction

Instantaneous frequency (IF) estimation for frequency modulated (FM) signals in white noise is a classical problem. The available methods range from the classical zero-crossing counting and phase-lock-loop (PLL) to recently developed time-frequency distribution (TFD) based methods [31]. In high signal-to-noise ratio (SNR) environments, many methods yield accurate IF estimates and even reach the Cramer-Rao bound in some situations, whereas most of these methods deteriorate dramatically when SNR falls below some threshold [31].

Time-varying autoregressive (TVAR) model based IF estimation had been considered poor since being proposed in 1984 by Sharman and Friedlander [36,31]. Shan and Beex [34], as reported in Chapter 2, have recently shown that the TVAR method is fairly good, and especially advantageous for those practical cases where short data records are used or linear IF law can not be assumed *a priori*. This is further evidenced by the improved system performance provided by the TVAR based method when applied to interference cancellation in spread spectrum communications [57].

On the other hand, our results in Chapter 2 also revealed that, similar to other IF estimation methods [31], the reciprocal of MSE of the TVAR based IF estimation falls faster after the SNR falls below some value. In this chapter, we focus on improving the TVAR-IF method for low SNR environments.

In stationary cases, sinusoids in white noise can be approximately modeled as an AR process, and the frequencies can be estimated from the model. This AR model based frequency estimation method is referred to as the Prony method [30, 53]. At low SNR, the eigen-structure of the data correlation matrix can be exploited to improve frequency estimation precision significantly [30]. An alternative, less complicated, method to solve this problem was proposed by Kumaresan, Tufts, and Scharf [53]. The performance of this alternative approach was shown to be "close to that of the best available, more complicated, approaches which are based on maximum likelihood or on the use of eigenvector or singular value decompositions" [53].

We extend this less complicated low-SNR Prony method to time-varying cases to improve the TVAR based IF estimation at low SNR. First, the autoregressive order is set higher than that needed for pure signal components so that the extra poles capture part of

the noise. Then we choose "signal poles" based on a subset selection procedure. Simulations show significant improvement of the IF estimation, especially when SNR is low.

3.2 A Time-Varying Prony Method: Method and Example

3.2.1 Method

For a signal consisting of *M* FM components in white noise at low to moderate SNR, we model the signal with a TVAR model, with order $p>M$ for complex exponential FM components and $p>2M$ for real-valued signals. *M* is assumed known here. For the sake of presentation, in the rest of this section we assume to be using complex data, consisting of an analytic signal in complex noise.

As in the case of high SNR, the time-varying transfer function corresponding to the TVAR model can be expressed by (2-1). By rooting the denominator polynomial formed by the TVAR coefficient estimates at each time instant t, we obtain the *p* poles as functions of time: $p_i(t), i = 1,2,\cdots, p$. With order $p>M$ for the low SNR case, among the *p* pole trajectories, there are *M* signal pole trajectories and (*p*-*M*) noise pole trajectories. The trajectories associated with the FM components tend to be along the unit circle while the poles capturing the noise move wildly, mostly inside, but occasionally outside (especially near the ends of a data record) the unit circle.

The instantaneous angles of the pole trajectories associated with the FM components can be used as estimates of the instantaneous frequencies $f_i(t)$. The key problem here is to find, at each instant *t*, the best subset of the poles as the *M* signal poles.

Our objective is to find, at each moment, the best subset of size *M* out of the *p* poles so that the *M* trajectories formed from the subsets provides the least total squared prediction error over the entire data record. For data size *N*, we have $\binom{p}{M}^{N-p}$ potential combinations to choose from. Although we may use, for example, the Viterbi algorithm to solve this combinatorial optimization problem, it is desirable to have a less complicated way to find a subset of poles to improve the IF estimation for low SNR environments.

To meet this demand, we suggest a subset selection method that is based on the instantaneous squared prediction error. At time *t*, the autoregressive coefficients associated with a pole subset, denoted as ψ, of size *M*, are determined by

$$\sum_{i=0}^{M} a_i^{\psi}(t) z^{-i} = \prod_{m \in \psi} [1 - p_m(t) z^{-1}] \tag{3-1}$$

Then the squared prediction error at time *t* corresponding to the subset ψ is

$$\varepsilon^{\psi}(t) = \left| x(t) - \sum_{i=1}^{M} a_i^{\psi}(t) x(t-i) \right|^2 \tag{3-2}$$

At each time instant *t*, we choose the subset that gives the smallest $\varepsilon^{\psi}(t)$. We refer to this criterion as the instantaneous least squares (ILS) criterion.

At each time instant, there are $\binom{p}{M}$ possible subsets of size *M*. For small *M* and *p*, the desired subset can be easily determined by comparing all possible subsets. For cases of large *M* and *p*, the procedure of Hocking and Leslie [56] can be used to simplify the subset selection, as suggested by Kumaresan, Tufts, and Scharf for the stationary case [53]. In the latter procedure, the significance of each pole is evaluated in terms of the

prediction error increment after removing the pole from the entire set of *p* poles. All poles are sorted according to the significance measure, and from this ordering, a sub-best subset can be selected without exhausting all the possible combinations.

3.2.2 Example

Now we present an example to illustrate the proposed method. We use a noisy short data record with 32 samples at unity sampling rate. The data is complex-valued, and consists of a complex exponential function with time-varying frequency and additive complex Gaussian white noise. For the complex exponential signal part, we need one pole (M=1). For the proposed time-varying Prony method, to have an extra pole to capture some of the noise, we set the autoregressive order equal to two (p=2). The polynomial basis is used to represent the TVAR coefficients and the polynomial order is set, quite arbitrarily, equal to four (q=4). The proposed instantaneous least squares (ILS) criterion for subset selection is used to determine the signal pole at each time instant.

The example to be presented is for highly nonlinear FM at the low SNR of 3dB. The data is generated with a random initial phase and unity amplitude, and the IF varies between 0.1 and 0.4Hz (normalized to sampling rate) according to $f(t) = 0.1 + 0.3\sin(\frac{\pi t}{32})$, $t = 0,1,\cdots,31$. The real part and the imaginary part of the data sequence are plotted in Figure 3-1 (a). The proposed method, which uses autorgeressive order p=2 and the ILS criterion, is hereafter referred to as "TVAR(2)+ILS", for simplicity. The TVAR based IF estimation method for high SNR, studied in Chapter 2, which uses autoregressive order p=1 is referred to as "TVAR(1)." To demonstrate the

improvement of the proposed method we evaluate the performance of both methods and show them side by side.

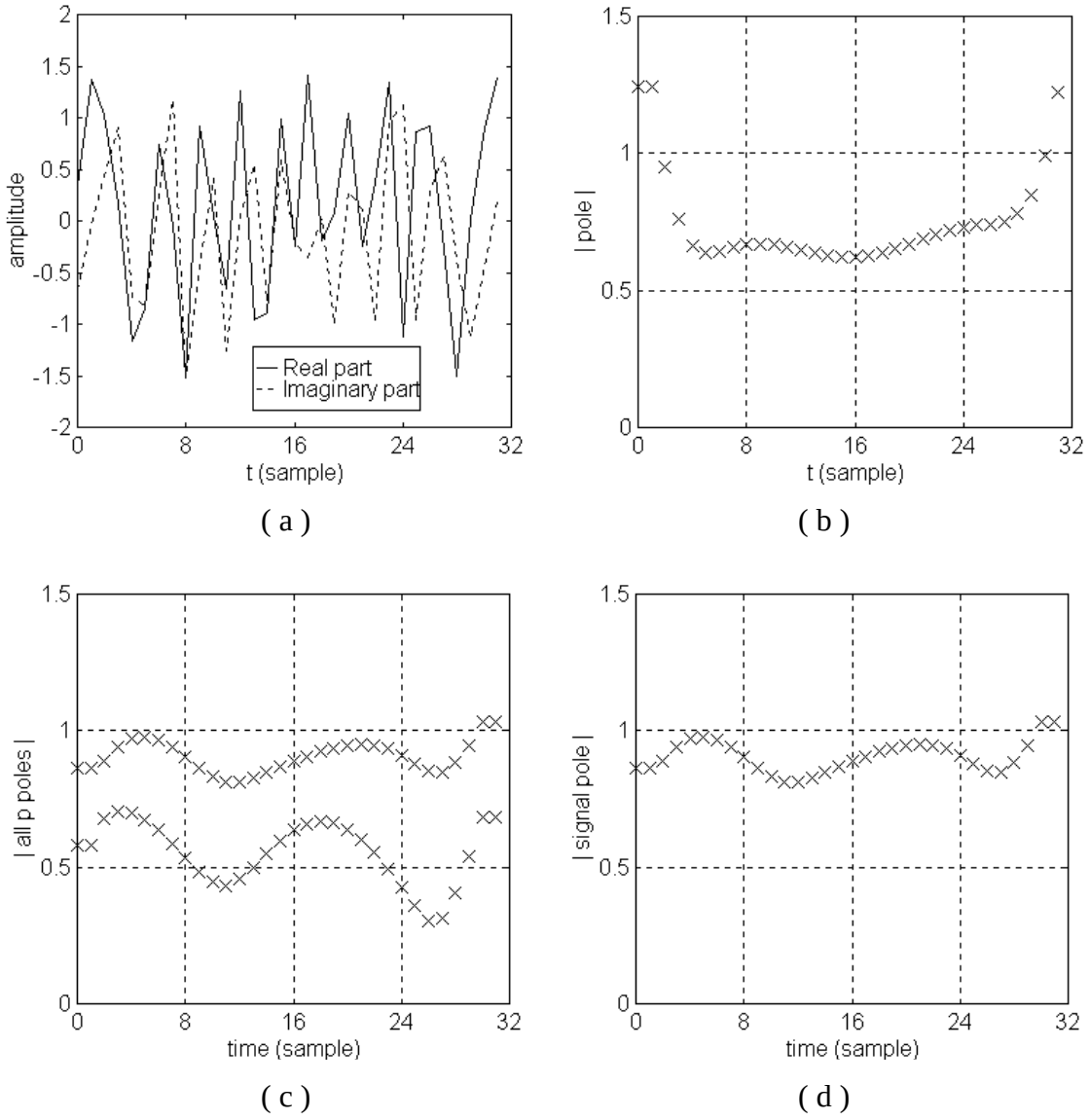

Figure 3-1. An example of IF estimation at low SNR for a highly non-linear FM at SNR=3dB (*continued on the next page*):
(a) real (*solid*) and imaginary part (*dashed*) of data,
(b) trajectory of pole radius for TVAR(1),
(c) trajectory of pole radii for TVAR(2),
(d) trajectory of signal pole radius as determined by TVAR(2) + ILS.

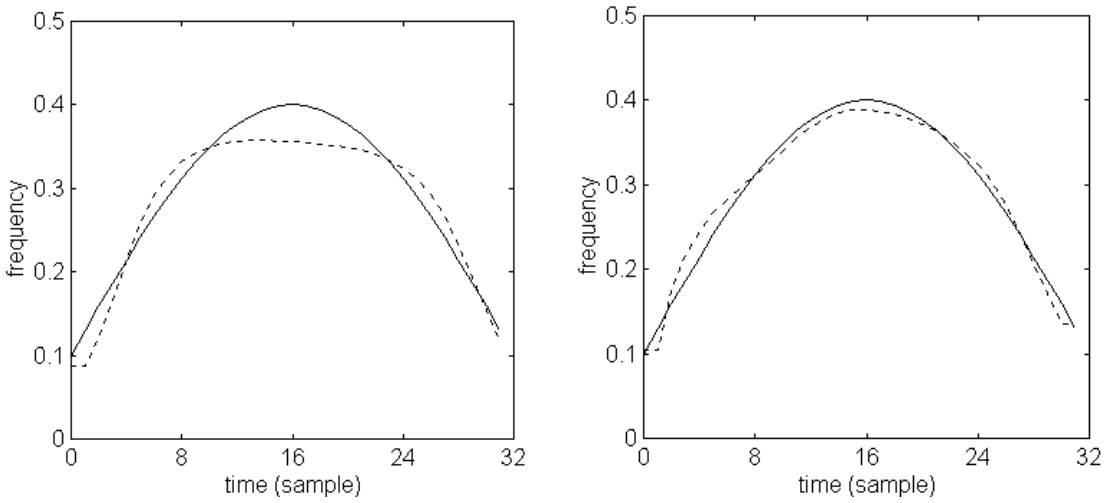

(e) (g)

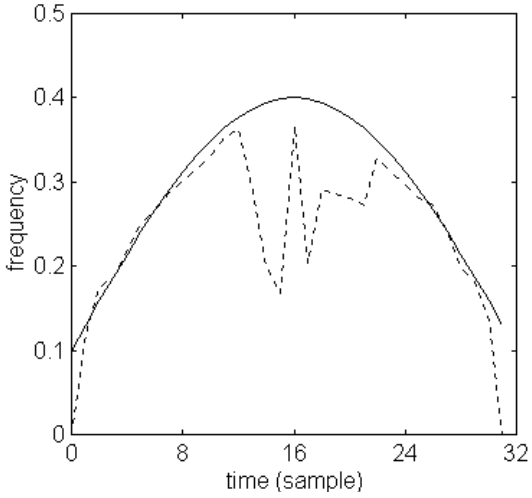

(g)

Figure 3-1. (*continued*) An example of IF estimation at low SNR, for a highly non-linear FM at SNR=3dB:
(e) TVAR(1), IF estimate (*dashed*) vs. the exact IF (*solid*),
(f) TVAR(2) + ILS, IF estimate (*dashed*) vs. the exact IF (*solid*),
(g) The WVD (zeros padded to 256 points) peak based IF estimate (*dashed*) vs. the exact IF (*solid*).

As expected, the TVAR based IF estimation without subset selection, TVAR(1), performs poorly in the low SNR case. The noise forces the pole trajectory away from the unit circle, as shown by Figure 3-1 (b), and the resulting IF estimate is poor, as given by

Figure 3-1 (e). By increasing the autoregressive order to 2, denoted as TVAR(2), we have 2 poles at each time instant (Figure 3-1 (c)). The proposed ILS criterion is used to make the decision on the signal pole subset. The subset selection result is shown in Figure 3-1 (d). The IF estimate, which is the angle of the selected signal pole, is given in Figure 3-1 (f). For the proposed TVAR+ILS method, an IF estimation improvement can be observed in this example. For comparison, the WVD based IF estimate is given in Figure 3-1 (g), and is poor in this case. More statistically significant comparisons of these methods will be presented in the following section.

3.3 Performance of the Time-Varying Prony Method

To observe the performance of the proposed IF estimator for noisy data, we compare it with two other methods: the TVAR based IF estimation for moderate to high SNR where $p=M$, as described in Chapter 2, and the WVD peak based IF estimator [31].

3.3.1 Case 1: Non-monotonic Nonlinear FM

First, we continue to consider the example shown in Figure 3-1, where the non-linear IF law $f(t) = 0.1 + 0.3\sin(\frac{\pi t}{32})$, $t = 0,1,\cdots,31$, was used. At each simulation trial, a new initial phase and complex noise process is generated independently from those in other trials. Figure 3-2 gives 20 trials of IF estimation for the three methods. Compared to the TVAR(1) based estimation, the proposed method apparently reduces the variance of the IF estimation, although we observe occasional outlying IF estimates due to wrong subset selection, which amount to about 6/(20 trials $\times$ 16 points) $\cong$ 2% of all subset

selection decisions in the center half of the data record (*t* from 8 to 23). The WVD (zeros padded to 256 points) method shows both severe outlying errors due to noise and bias as a result of the nonlinearity of the IF law.

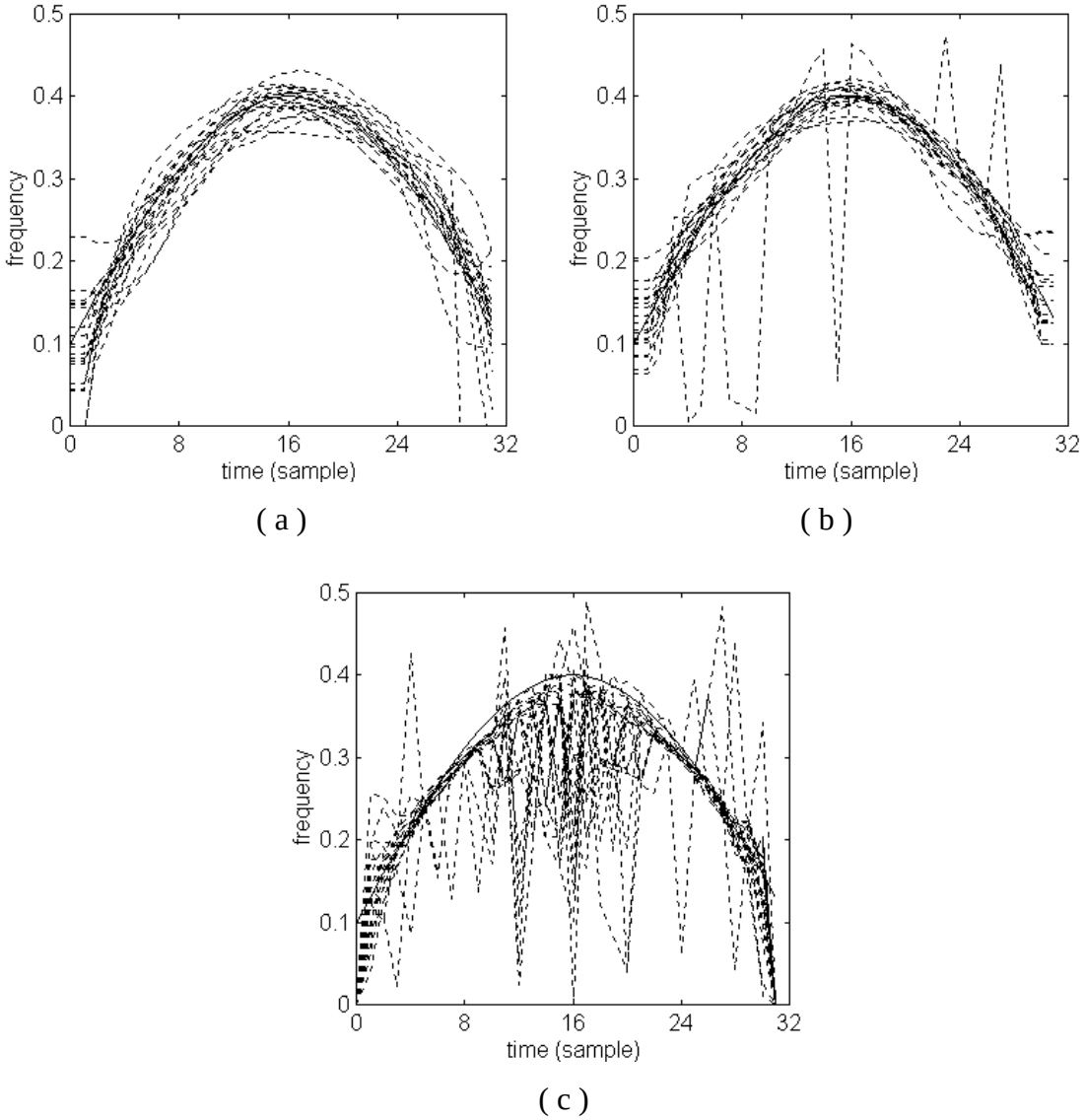

Figure 3-2. 20 trials of IF estimation (*dashed*) vs. the exact IF (*solid*), a highly non-linear FM at SNR=3dB:
(a) TVAR(1),
(b) TVAR(2) + ILS,
(c) The WVD peak based IF estimation.

To further examine the performance of the proposed method, we run 1000 simulation trials and the IF estimation errors in the center half of the data record (*t* from 8 to 23) are evaluated. The result is shown in Figure 3-3 in terms of the reciprocal of the mean squared error (MSE) of IF estimation, 1/MSE, versus SNR. Noticeable performance improvement is achieved for SNR below 3dB. In Figure 3-3, there is no noticeable improvement in 1/MSE at 3dB SNR, unlike what Figure 3-2 may suggest. This is due to the outlying errors with the proposed method. In spite of this, the improvement is significant for SNR near or below 0dB. The WVD method performs poorly even at higher SNR in this case due to its biased estimation, as evidenced in Figure 3-2.

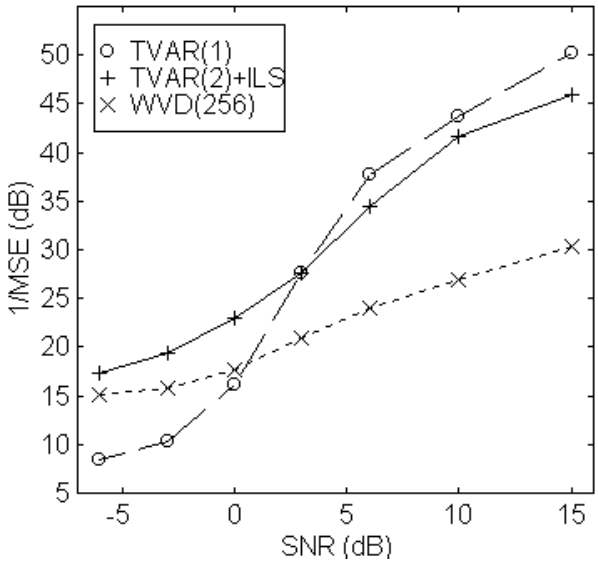

Figure 3-3. 1/MSE vs. SNR for IF estimation near the time center of the data record for a highly nonlinear FM signal.

3.3.2 Case 2: Monotonic Nonlinear FM

Now we consider another example of nonlinear FM, which chirps monotonically from frequency 0.05 to 0.4344 Hz (normalized to sampling rate) according to $f(t) = 0.05 + 0.004t^2, t = 0,1,\cdots,31$ and is corrupted by additive white Gaussian noise. The signal is generated using the described IF with unit amplitude and random initial phase. Zero-padding to 256 points is applied in the WVD method to reduce the frequency quantization error. For the proposed method, M=1, p=2, q=3 are used. We run 200 simulations and the IF estimation errors in the center half of the data record (t from 16 to 23) are evaluated. The result is shown in Figure 3-4 in terms of 1/MSE versus SNR. Noticeable performance improvement is achieved for SNR below 10dB. As mentioned earlier, the WVD method performs poorly due to its biased IF estimation at high SNR and due to noise at low SNR.

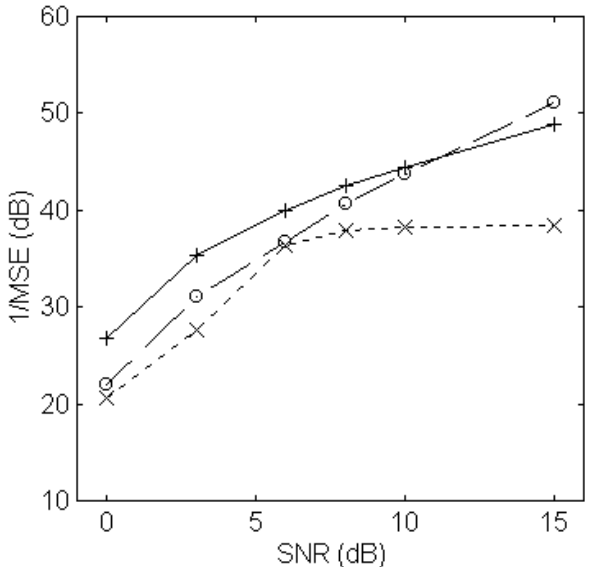

Figure 3-4. Case 2, 1/MSE vs. SNR for IF estimation near the time center of the data record for a nonlinear FM signal: the time-varying Prony method ("+", *solid*), the TVAR method for high SNR ("×", *dashed*), and the WVD method ("o", *dotted*).

3.3.3 Case 3: Linear FM

We now use 32 samples of a linear FM signal, which chirps from frequency 0.1 to about 0.4 Hz according to $f(t) = 0.1 + 0.01t, t = 0,1,\cdots,31$. Otherwise, the experiment is the same as in the nonlinear FM cases. The result is shown in Figure 3-5. Again, noticeable performance improvement is achieved for SNR below 10dB. The WVD method is potentially optimal for this case due to pure linearity of the FM law [31,34]. The optimality of the WVD method materializes when SNR is above 6dB. However, at lower SNR (below 3dB for this example), the proposed TVAR+ILS method provides the best estimation among the three methods.

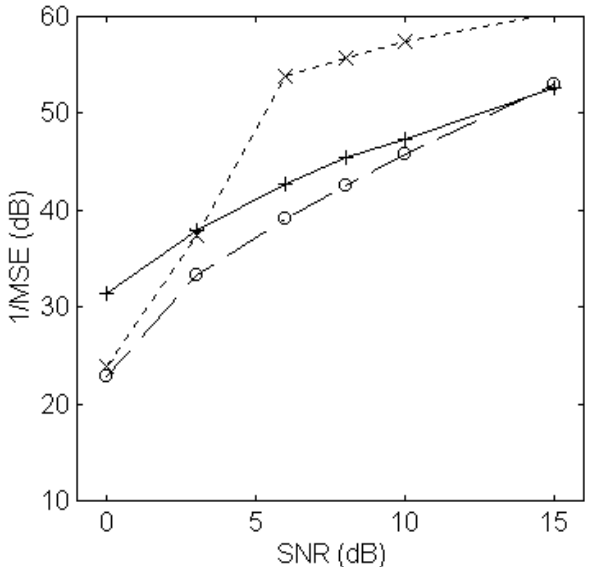

Figure 3-5. Case 3, 1/MSE vs. SNR for IF estimation near the time center of the data record for a linear FM signal: the time-varying Prony method ("+", *solid*), the TVAR method for high SNR ("×", *dashed*), and the WVD method ("o", *dotted*).

3.4 Summary

Most available instantaneous frequency estimation methods for FM signals in white noise deteriorate dramatically when SNR falls below some threshold. In this chapter, we proposed a time-varying Prony method for IF estimation from low SNR data. It is an extension of a frequency estimation method for stationary processes which was shown to be less complicated, yet close in performance to the best available approaches based on singular value decomposition or the principle of maximum likelihood. First, the time-varying autoregressive order is set higher than that needed for the pure signal components, so that the extra poles capture part of the noise. Then we choose “signal poles” based on a subset selection procedure. The performance improvement at low SNR over the TVAR method for high SNR is evidenced through simulation experiments. The proposed method also outperforms the “optimal” WVD method, when it loses optimality for low SNR scenarios.

Chapter 4

NOTCH FILTER BASED INTERFERENCE SUPPRESSION USING TVAR BASED IF ESTIMATION

In case of strong frequency modulated (FM) interference in a spread spectrum communication system, the interference can be effectively suppressed by applying a time-varying notch filter with its zero(s) placed at an instantaneous frequency (IF) estimate of the interference. As we mentioned in Chapter 1, the published studies use Wigner-Ville distribution (WVD) peak based IF estimation. In this chapter, we study the use of the time-varying autoregressive (TVAR) model based IF estimator of Chapter 2 in such a scenario. It is demonstrated that the TVAR-IF method provides improved performance compared to using the WVD based method. It is also shown that the TVAR method is capable of handling multiple component interference without separation into individual components. A major part of this work was published earlier [57].

4.1 Introduction

The problem of frequency modulated (FM) interference suppression in direct-sequence spread spectrum (DSSS) communications has been attracting many researchers recently [48-50,58]. Amin and his colleagues, Lach and Lindsey, studied methods using time-frequency distributions (TFD): time-varying notch filtering using an instantaneous frequency (IF) estimated from a TFD [48], time-frequency filtering through signal synthesis after masking of the TFD, specifically the Wigner-Ville distribution (WVD) [49], and a comparison of the two approaches [58]. Bultan and Akansu [50] used the iterative matching pursuit algorithm with a chirplet dictionary to detect and excise chirp-like interference. Wei, Harding, and Bovik [59] used an iterative time-frequency filtering algorithm based on masking of the Gabor transform followed by signal synthesis.

All the aforementioned filtering procedures are highly non-causal, and require data-block based time-frequency analysis before signal synthesis or linear filtering. For practical system implementation, the associated computation and memory requirements have to be controlled to an acceptable amount. This suggests that the entire filtering procedure be either implemented in a data-recursive form or perform well with short data blocks. Similar to stationary cases, an appropriate parametric method - with *a priori* information exploited - would perform better than those non-parametric methods that are based on TFDs, such as the WVD or other members of the Cohen class of time-frequency distributions. This is one of the reasons that we study FM interference suppression using parametric IF estimation. Another reason is that WVD based IF estimation is not appropriate for non-linear FM laws due to the associated bias problem, as shown in Chapter 2. In contrast, the parametric method we studied is not sensitive to non-linearity

of IF laws, is suitable for short data blocks, is free of frequency quantization and cross-terms, and produces lesser end effects [34].

We model the received signal consisting of an FM interference (single FM or multiple FM) thermal noise and DSSS signal with a time-varying autoregressive (TVAR) model. The IF of the interference is estimated from the model and then a notch filter is formed according to the IF estimate.

4.2 Notch filter Based FM Interference Suppression Using TVAR Based IF Estimation

At the receiver of a DSSS communications system, an interference suppression filter is applied before demodulation. We consider a received signal $r(t)$ composed of the DSSS signal $s(t)$, thermal noise $w(t)$, and interference $i(t)$:

$$r(t) = s(t) + w(t) + i(t) \tag{4-1}$$

Here the noise $w(t)$ is assumed stationary and white. The DSSS signal $s(t)$ is "slightly colored" in practice, which depends on the sampling rate (samples per chip) as well as the specific PN sequence. The FM interference $i(t)$ could be an intentional or unintentional jammer, such as a strong FM communication emitter. The components in (4-1) are assumed mutually independent.

In the stationary case, tones in white noise can be modeled as an AR process and the frequencies of the tones can be estimated from AR modeling. We can model the received signal $r(t)$ with a time-varying AR model, viewed as an FM in white noise process, if we treat the DSSS signal as approximately white. The IF of the FM

interference $i(t)$ is estimated as described in Chapter 2. Then $r(t)$ is fed into a time-varying filter $N(z,t)$ to suppress the interference. The filter $N(z,t)$ is a time-varying notch filter with its zeros placed at the IF estimate. A study of the design and performance issues of this filter can be found elsewhere [60]. The block diagram of the receiver (BPSK modulation assumed) with an IF based interference suppression filter is given in Figure 4-1.

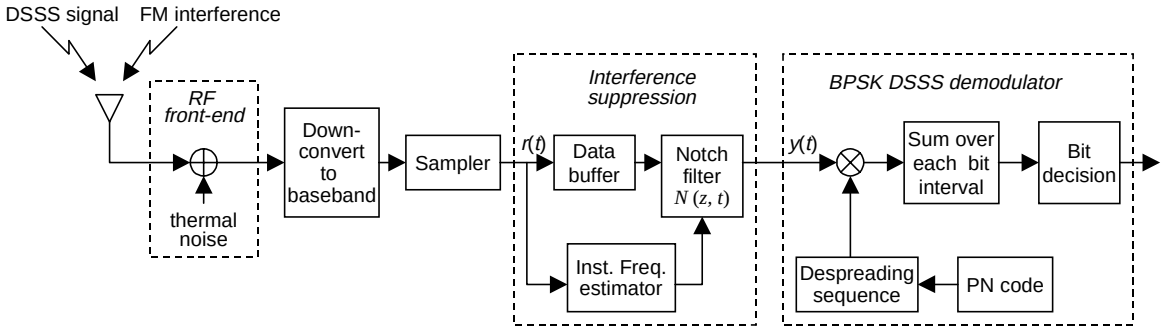

Figure 4-1. Block diagram of the DSSS receiver with IF estimation based FM interference suppression.

4.3 System Performance Improvement Due to Interference Rejection Using TVAR Based IF Estimation

In this section, we examine the system performance improvement due to the notch filter based interference rejection using the TVAR based IF estimation. We will compare the overall system performance with the notch filter controlled by the TVAR-IF, the WVD-IF, and exact IF information through simulation examples. After introducing the general experiment setting and implementation, we will present simulation cases. We start with linear FM interference since WVD based IF estimation was able to provide

optimal estimation in that case. Then a nonlinear FM interference case is considered. We also demonstrate that, unlike other methods, the TVAR method can handle multiple component interference well.

4.3.1 Experiment Setup and Implementation

To observe the performance of the TVAR based interference suppression method, we compare it with the notch filtering method using the WVD peak based IF estimation [48,58] and using the exact IF information. We consider a single-user code-on-pulse DSSS communication system with BPSK modulation and processing gain N=15 chips per bit. To focus on the effect of interference cancellation on BER performance, it is assumed that perfect phase and code synchronization exist, and that the channel is ideal (that is, multi-path effects are ignored). Since different PN codes may yield different signal spectra, to provide a result that is not dependent on a specific spreading PN code, we independently generate a random binary sequence as the PN code for each bit. The received signal is down-converted to baseband and over-sampled at the rate of 8 samples per chip. The interference suppression filtering procedure is then applied on data blocks. Each data block, of size 128 samples, consists of the current bit ($8\times15=120$ samples) and the last chip of the previous bit (8 samples). The extra 8 samples are included to cover the initial transient of the time-varying short (length-5) FIR filter. The length-5 FIR symmetric (zero-phase) time-varying double-zero notch filter was suggested by Amin [48, 60]. Bit decisions are made based on the current-bit portion of the filter output. The bit-error-rate (BER) is evaluated by estimating the mean and variance of the decision

statistic, which is assumed Gaussian. BERs estimated in this way were verified via long simulations, by counting error events.

Both real-valued and complex-valued data can be used for TVAR based IF estimation. Since we already demonstrated experiments with complex-valued data in Chapters 2 and 3, in this section, a real-valued signal is used in the modeling, filtering, and decision-making process. A length-5 symmetric (zero-phase) time-varying double-zero notch filter [48] is formed according to the TVAR IF estimate. With a given IF estimate $\hat{f}(t)$, the length-5 FIR time-varying notch filter is formed as

$$\begin{aligned} N(z,t) &= [z - 2\cos(2\pi\hat{f}(t)) + z^{-1}][z - 2\cos(2\pi\hat{f}(t)) + z^{-1}] \\ &= z^2 - 4\cos(2\pi\hat{f}(t))z^1 + 4\cos^2(2\pi\hat{f}(t)) - 4\cos(2\pi\hat{f}(t))z^{-1} + z^{-2} \end{aligned} \qquad (4\text{-}2)$$

which is implemented as a linear phase filter, i.e. $z^{-2}N(z,t)$, with a delay of 2 samples. To compensate for the delay, in the despreading stage, the PN sequence is synchronized to the delayed filter output. The magnitude responses of the length-5 FIR notch filter, at various notch frequencies $\hat{f}(t)$, are plotted in Figure 4-2. While the filter provides a deep notch at the designated frequency, the shape of the notch also varies as a function of the specified notch frequency.

To examine the performance of the proposed TVAR-IF based notch filtering method, we compare it with the notch filter using the exact (supposedly known) IF information. For this purpose, we substitute for the IF estimate $\hat{f}(t)$ in the filter (4-2) with the known IF information $f(t)$ that was used to generate the interference. With the substitution, we form exact IF based notch filter and evaluate the system performance using this filter.

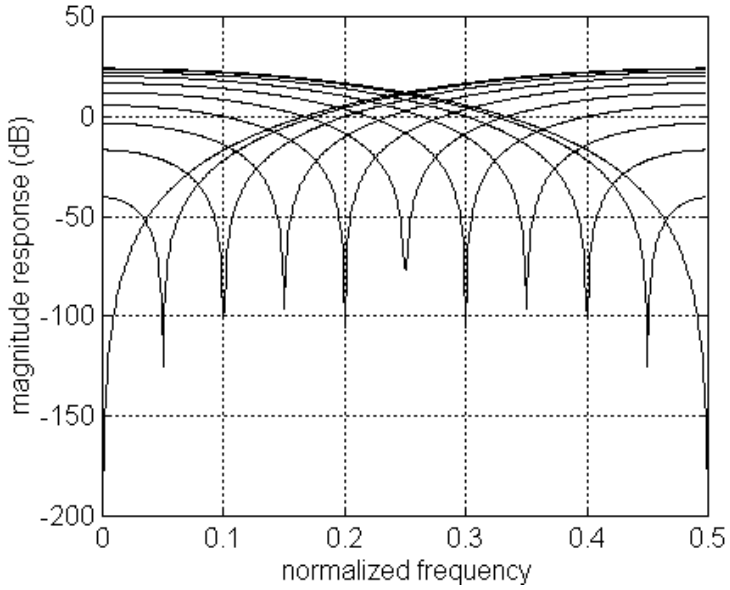

Figure 4-2. Magnitude response of the length-5 FIR notch filter with notch frequency at 0, 0.05, 0.1, 0.15, …, 0.5 Hz.

To compare the TVAR-IF based notch filtering method with the WVD-IF based notch filtering method, the WVD method is implemented in two versions: without zero-padding and with zero-padding.

4.3.2 Linear FM Interference

We first consider a system as depicted in Figure 4-1 with a jammer which chirps linearly from 0.1 to 0.4 Hz (normalized to unit sampling rate) according to $f(t) = 0.1 + 0.3t/127$, $t = 0,1,\cdots,127$, inside each data block. The model used is a second-order autoregressive model (p=2) with the time-varying coefficient represented as a fifth-order polynomial function (q=5). The BER vs. the jammer-to-signal ratio (JSR), defined as the power ratio before the interference rejection notch filter, is evaluated as the notch filter is controlled using the different IF estimates. These include the TVAR-IF method,

the WVD peak based IF estimates using a 128-point DFT (without zero-padding), denoted as WVD(128), the WVD peak based IF estimates using zero-padding to 512-points, denoted as WVD(512), notch filtering with the exact IF, and the plain receiver without filtering. Figure 4-3 shows a simulation result when the SNR is at E_b/N_0 =10dB (where E_b stands for the signal bit energy and N_0 is the single-sided noise power spectral density).

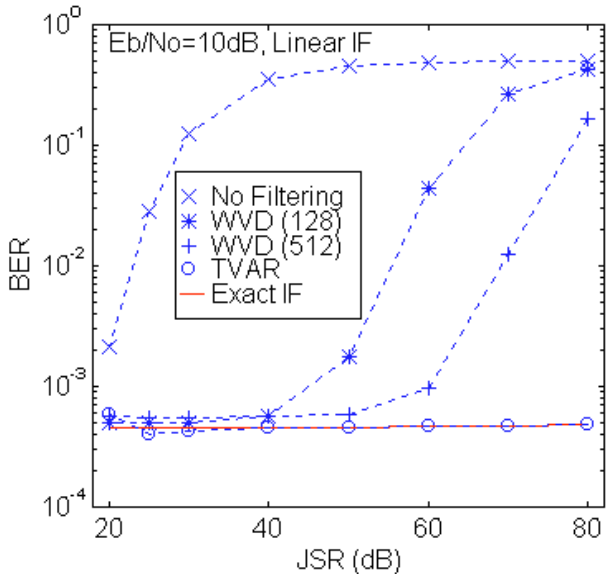

Figure 4-3. Linear IF law, BER vs. JSR for different IF estimates and exact IF.

For this case, it is observed from Figure 4-3 that the TVAR method significantly outperforms the WVD based method for high JSR. The residual interference after the WVD based filtering is substantial for JSR over 40dB. The WVD (without zero-padding) based filter reduces the apparent interference power by about 30dB. Zero-padding to 512 points, at a cost of computational effort, reduces the frequency quantization error and hence increases the filtering gain by another 15dB. By contrast, the BER curve of the

TVAR based method overlaps well with the one using the exact IF and the associated filtering gain appears to be nearly without limit. This is attributed to the high precision of the TVAR based IF estimates.

4.3.3 Non-Linear FM Interference

In the linear FM example, the BER performance when using the WVD method can be improved by reducing the IF quantization error via zero-padding. For a nonlinear FM jammer this may not be the case since the error of WVD based IF estimation may be dominated by the bias due to the non-linearity of the IF law. Consequently, the TVAR method is more advantageous for cases where FM interference linearity can not be assumed *a priori*.

We replace the linear FM jammer with a nonlinear FM law, which is $f(t) = 0.1 + 0.3\sin(\pi t/127)$, $t = 0,1,\cdots 127$, i.e., the instantaneous frequency starts from 0.1Hz at t=0, nonlinearly increases to 0.4Hz when t=64, and then nonlinearly decreases to 0.1 at the end of the block. We use the same orders p=2 and q=5 for the TVAR model, denoted as TVAR(2,5), and perform the same simulations as for the linear case. Figure 6-4 shows 10 trials of IF estimates using the TVAR method (*left column*) and using the WVD method with zero-padding to 512 points (*right column*) for E_b/N_0 =10dB and JSR = 20, 25, and 30 dB. It is obvious that, for this example at 20 and 25dB JSR, the WVD peak based IF estimation method suffers severely from cross-term interference, while the TVAR based method gives reliable IF estimates. At higher JSR, for example 30dB, the TVAR based estimation also exhibits smaller variance.

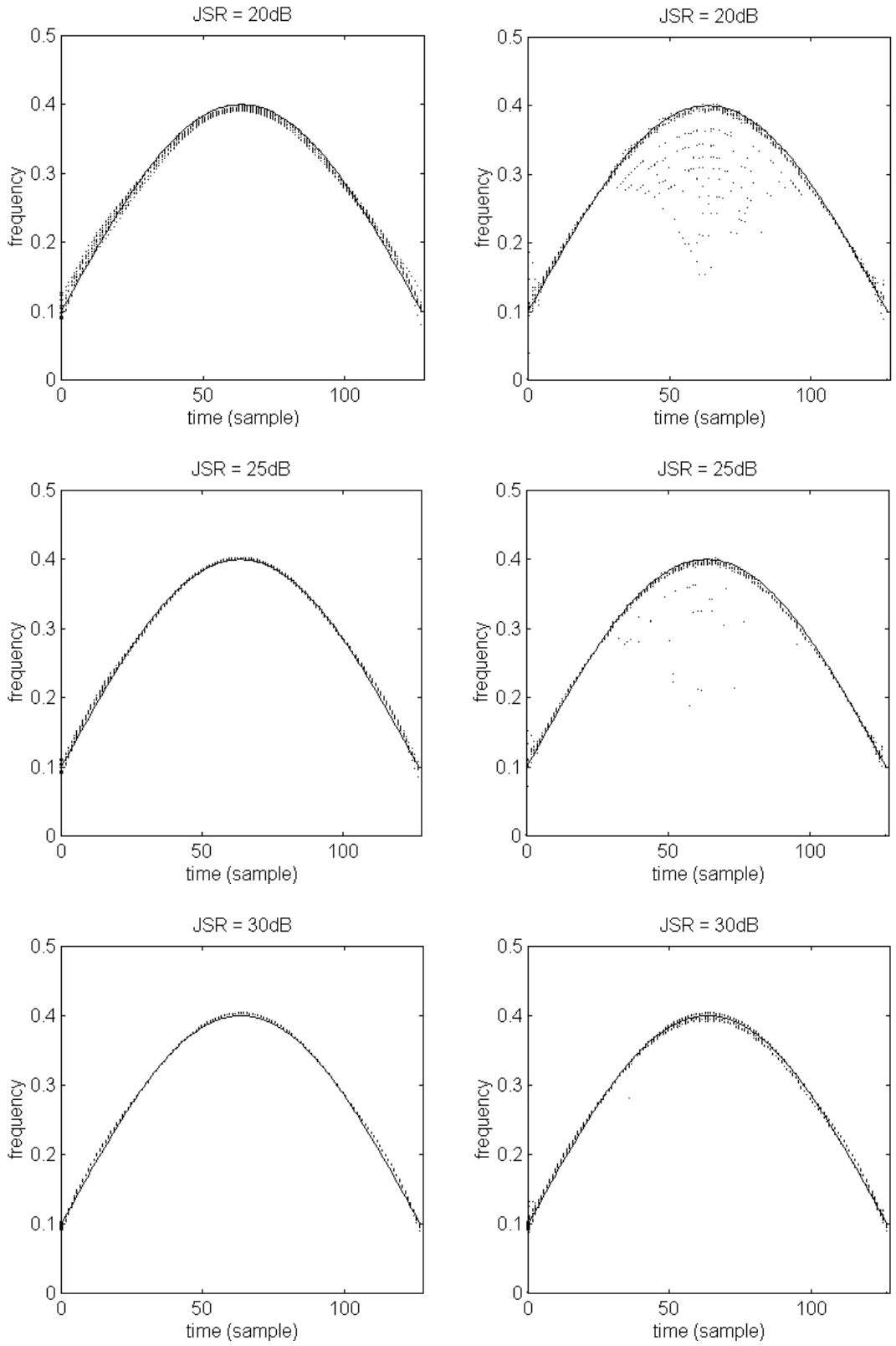

Figure 4-4. Real IF (*solid*) and 10 trials of IF estimates (*discrete*) with JSR=20, 25, and 30dB using TVAR(2,5) (*left*) vs. WVD(512) (*right*).

We simulate the BER system performance similar as in the linear FM case. The result is shown in Figure 4-5. The WVD based method, with or without zero-padding, can effectively reject the jammer up to about JSR=40dB while the TVAR method performs ideally for JSR up to nearly 70dB.

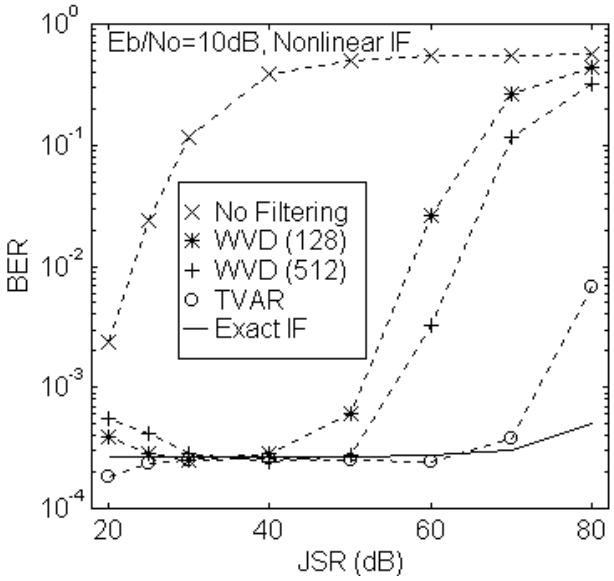

Figure 4-5. Simulated BER vs. JSR for the nonlinear FM case using different IF estimates and exact IF, p=2 and q=5 for the TVAR method.

Figure 4-6 shows a similar simulation result where the order q in the TVAR model is increased to 11. For this case, the higher order q is helpful in accommodating more detailed frequency variation, and hence leads to better system performance when JSR is high, at 80dB, where accurate IF estimation is more critical.

To offer an explanation of why the WVD based method fails for high JSR, while the TVAR method can successfully improve the system, Figure 4-7 shows the IF estimation errors, $f(t) - \hat{f}(t)$, for a simulation realization at JSR=80dB. The WVD based estimates are obviously biased toward the inner direction of the IF curve (positive

error). Further calculation shows that the summed squared error in the center half of the block, i.e., for $t = 33,34,\cdots 96$, is 4.0×10^{-3} for the 128-point WVD, 4.2×10^{-3} for the 512-point WVD, and 3.3×10^{-8} for the TVAR method, respectively.

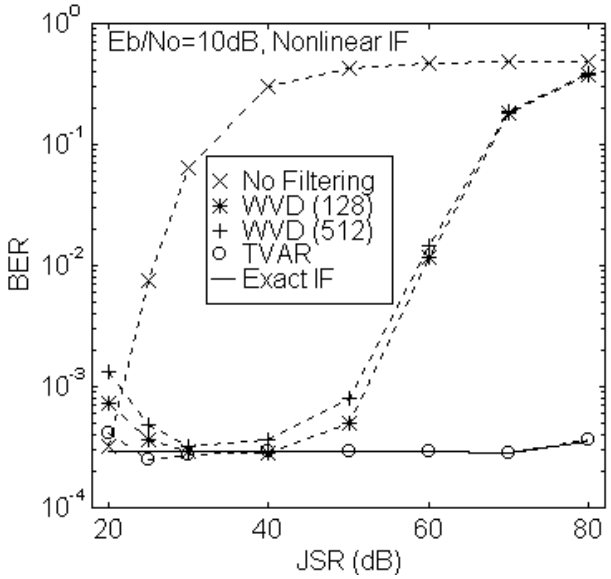

Figure 4-6. Simulated BER vs. JSR for the nonlinear FM case using different IF estimates and exact IF, *p*=2 and *q*=11 for the TVAR model.

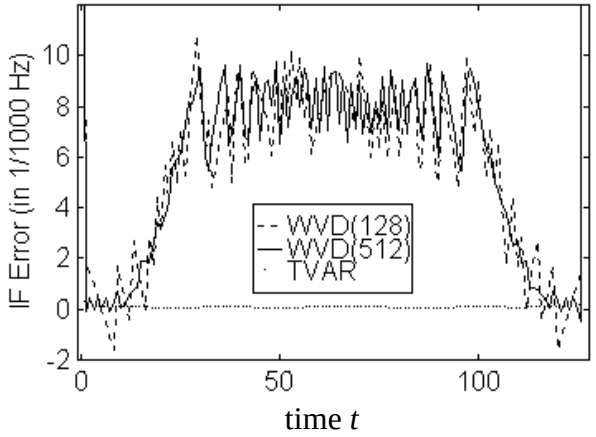

Figure 4-7. IF estimation error comparison for the nonlinear FM case with JSR=80dB, *p*=2 and *q*=11 for the TVAR model.

4.3.4 Multiple-FM Interference

One advantage of TVAR based IF estimation is that it can handle multiple-component signals without having to separate them first. For WVD or other TFD peak based IF estimation, a multiple component signal means multiple peaks and troublesome cross-term interference. However, for the TVAR model based method, only a higher autoregressive order p is needed to accommodate multiple FM components. Here the number of FM components is assumed known.

For the interference cancellation problem we considered, by forming a time-varying multiple-notch filter, the multiple-component interference can be rejected directly from the received data. This is impossible with the WVD based method due to the cross term interference in the WVD distribution and the mono-component assumption of TFD peak based IF estimation. In contrast, the TVAR based method only needs a higher auto-regressive order to handle multiple FM components overlapping in both time and frequency. In this experiment, we demonstrate the capacity of TVAR based IF estimation combined with multiple-notch filters to reject strong interference composed of two FM components. Since the WVD method is not suitable for the multiple interference case due to its mono-peak assumption, it is not compared with for this example.

The multiple-notch time-varying filter is formulated by simply cascading the mono-notch filter given in (4-2) with each stage corresponding to an individual frequency. For the case with the number of FM components M=2, the filter used consists of 2 stages of order-4 (length-5) FIR time-varying real-coefficient filters, and therefore the overall filter order is 8 (length-9). All 8 zeros are on the unit circle, with each double complex conjugate pair (a set of 4 zeros) corresponding to a TVAR based IF estimate.

Similar as in the single FM case, to compensate for the 4-sample delay associated with this linear phase filter, the PN code sequence is synchronized to the delayed filter output at the de-spreading stage.

We consider two (2) FM components with the same power, and refer to the JSR as the power ratio of each individual FM component to the desired communication signal. The same as in the previous cases, the received signal also comes with channel noise at E_b/N_0 =10dB. The TVAR model with orders p=4 and q=5 is used to estimate the two instantaneous frequencies from real-valued data. Figure 8 shows an example of notch filtering based dual-FM rejection using TVAR model based IF estimation. In this example, there is no frequency crossover between the two IF laws during the data block interval. We can see from Figure 8(a) that the TVAR method successfully estimates the frequencies of the two FM components without separating them. The TVAR based method is compared against the plain receiver without a filter and a receiver using the same FIR time-varying notch filter structure using exact FM information. The WVD based method is not included since it is not suitable for such a dual-FM case. As shown in Figure 8(b), for this case, the TVAR-IF based filter yields approximately the same flat BER performance as using the known IF information.

Next, we examine a case where the two IF laws cross during the data block interval. In such a case, the variance of the TVAR based IF estimates increases near the point of crossing and the correspondence between the IF estimates and the real IF laws may switch at the point of crossing. Figure 9 show the results of IF estimation and BER performance simulation. For this case, the TVAR based method still provides the same BER performance improvement as using the exact IF information at moderate JSR level.

As shown in Figure 9(b), at high JSR, the BER performance of the TVAR-IF method deteriorates faster than notch filtering using the known IF.

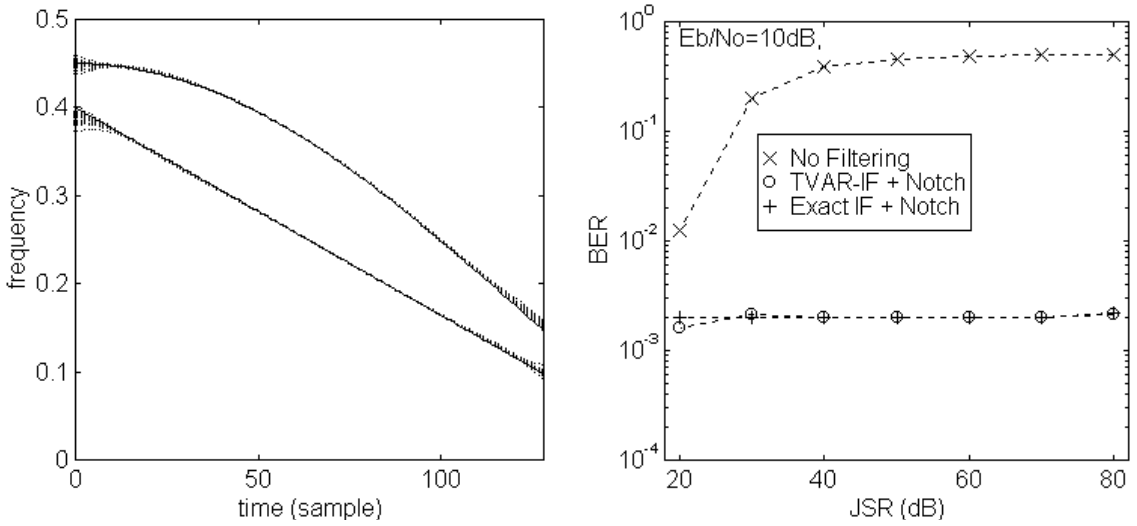

(a) (b)

Figure 4-8. Example of dual-FM rejection without frequency crossing:
(a) real IF (*solid*) vs. 20 trials of IF estimates (*discrete*) at JSR=40dB,
(b) simulated BER vs. JSR, compared with using known IF information.

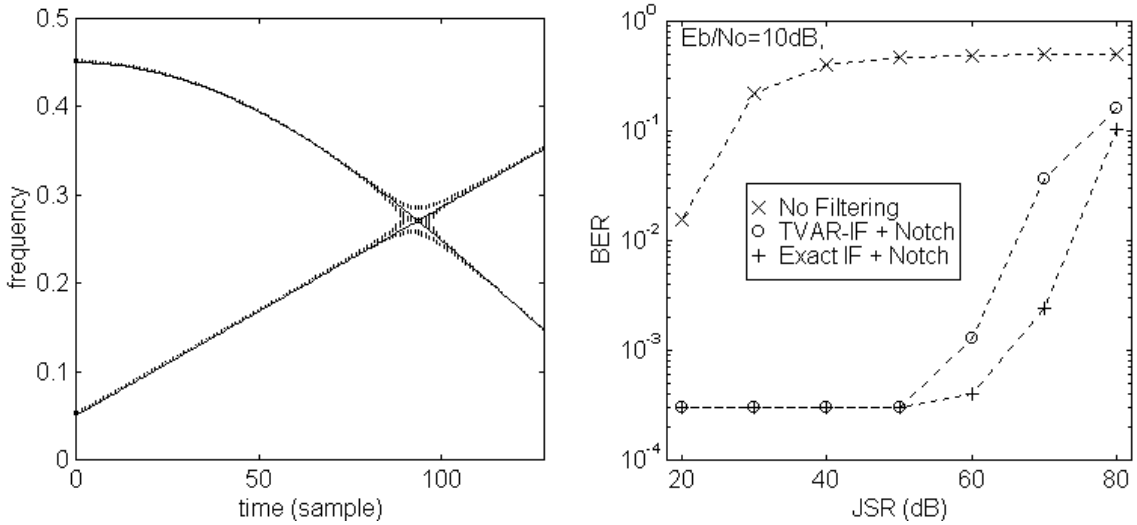

(a) (b)

Figure 4-9. Example of dual-FM rejection with a frequency crossover:
(a) real IF (*solid*) vs. 20 trials of IF estimates (*discrete*) at JSR=40dB,
(b) simulated BER vs. JSR, compared with using known IF information.

Finally, to intuitively illustrate how the time-varying notch filter based interference rejection - using TVAR based IF estimation - reduced the system bit error rate, we offer the set of waveforms in Figure 4-10. This set of waveforms corresponds to one of the simulation trials shown in Figure 4-8, i.e., with dual FM jammers at JSR=30dB. All the waveforms shown have 128 samples, corresponding to 16 chips sampled at the rate of 8 samples per chip. As mentioned earlier, the first chip (8 samples) of each data block of 128 samples overlaps with the last chip of the last data block and serves to accommodate the transient of the FIR notch filter. The other 15 chips (120 samples) correspond to an information bit spread by the PN code of length 15. Ideal synchronization is assumed.

Figure 4-10 (a) shows the transmitted waveform $s(t)$ which is a chip of −1 (from the last bit) followed by a information bit +1 spread by PN code [+1, −1, −1, +1, +1, +1, +1, −1, +1, +1, −1, −1, −1, −1, −1]. Figure 4-10 (b) shows the interference-free version of the received signal: $s(t)+w(t)$, the sum of the DSSS signal $s(t)$ and white Gaussian noise $w(t)$. With the amplitude of $s(t)$ normalized to unity, the "amplitude", or standard deviation of the noise sequence is set by E_b/N_0 to $\sqrt{\frac{NL}{2E_b/N_0}}$ where N is the "processing gain", number of chips per bit, and L is the over-sampling ratio, number of samples per chip. For the shown case, the noise standard deviation is $\sqrt{\frac{NL}{2E_b/N_0}} = \sqrt{\frac{15\times 8}{2\times 10^{\frac{10dB}{10}}}}$ = 2.45. Figure 4-10 (c) gives a realization of the interference $i(t)$, and (d) gives the resulting received signal $r(t)=s(t)+w(t)+i(t)$. The latter look

very close since the interference is much stronger than the signal and the noise. This interference sequence consists of two FM components as shown in Figure 4-8. The initial phases of the FM's are random variables. As shown in Figure 4-9, the BER performance of a conventional DSSS receiver fed with this received signal is unacceptably low (on the order of 10^{-1}).

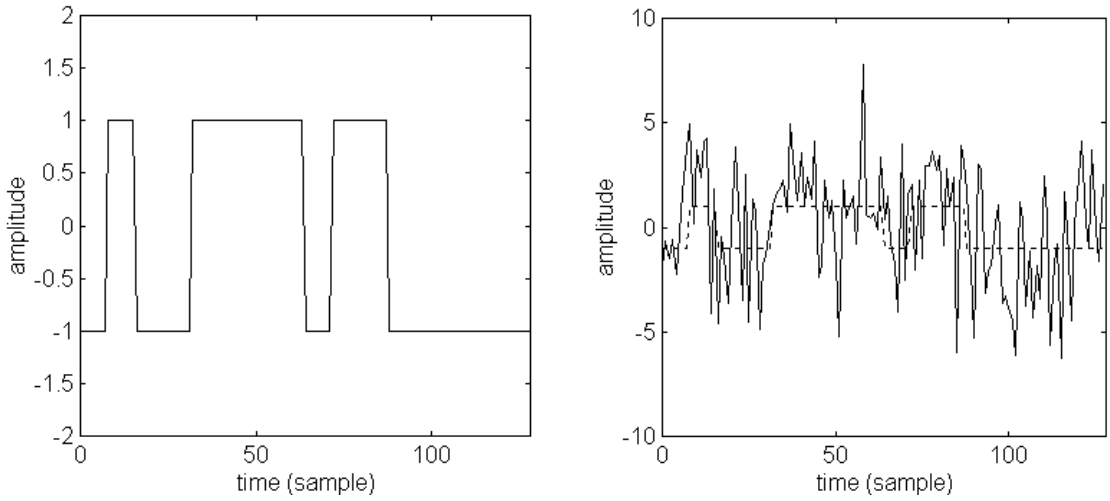

(a) (b)

Figure 4-10. A set of waveforms to illustrate notch filter based interference rejection using TVAR based IF estimation (*continued on the next page*):
(a) the transmitted DSSS signal,
(b) the DSSS signal plus channel noise,

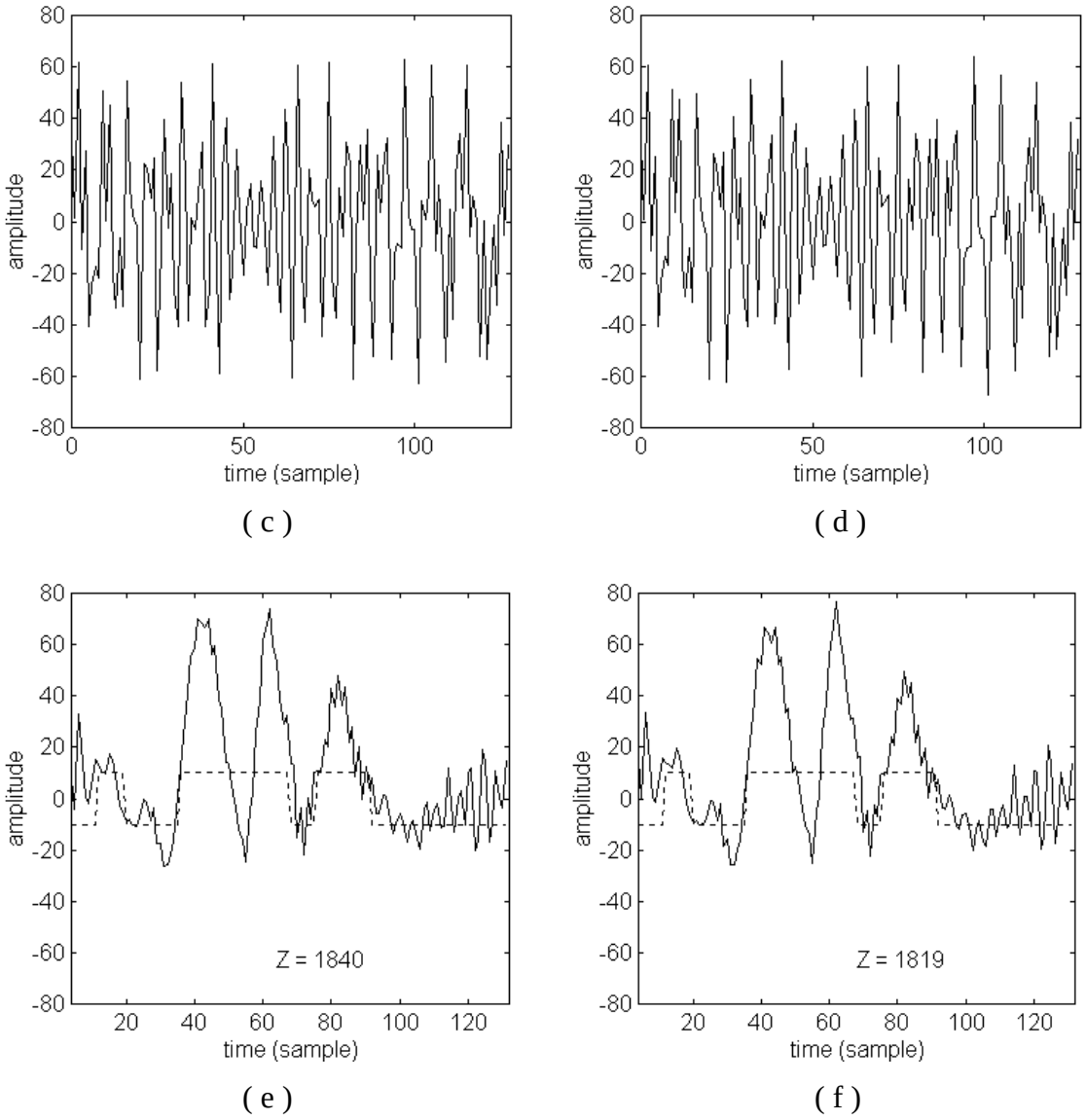

Figure 4-10. (*continued*) A set of waveforms to illustrate notch filter based interference rejection using TVAR based IF estimation:
(c) the dual-FM interference,
(d) the received signal,
(e) filter output using exact IF information,
(f) filter output using TVAR based IF estimation.

Now we apply the time-varying notch filter to reject the interference from the received signal. Using the exact IFs, the filter output is plotted in Figure 4-10 (e) with the synchronized despreading sequence shown against in dashed line. We see that the filter

output matches the despreading sequence quite well, which leads to a useful bit error rate, on the order of 10^{-4}, as shown in Figure 4-9. The decision statistic, i.e. the inner product between the filter output and the despreading sequence (120 samples) $Z = 1840$. The filter output using the TVAR based IF estimates is plotted in Figure 4-10 (f). The filter output waveform and the resulting decision statistics $Z = 1819$ are very close to using the exact IF's. Consequently, the BER performance of the TVAR method is close to that resulting from the using of exact IF information.

4.4 Summary and Discussion

We applied TVAR based IF estimation to notch filtering based interference suppression for DSSS communications. This method provides superior performance compared to using WVD peak based IF estimation. This conclusion may also apply to other time-frequency distributions that can be viewed as smoothed versions of the WVD. We use a parametric model rather than a 2-D distribution. This also leads to much less computational cost, and thus it is more suitable for real time implementation. In addition, the TVAR method is able to handle multi-component interference without first separating the components.

Chapter 5

TIME-VARYING OPTIMUM FILTERING

5.1 Introduction

From this chapter on, we will study time-varying optimum – minimum mean-square error - filtering. In this chapter, we present the basic optimum filtering methods, including the time-varying Wiener filter (TVWF) and the Kalman filter (KF). These methods, though theoretically perfect, usually can not be used directly for practical time-varying filtering since they require too much information. The TVWF requires time-varying statistical information about the desired signal and measurement noise. The Kalman filter requires a state-space description for the physical system that generates the signal and the statistical information about the input to the system and the measurement noise. In many practical cases, what we have is only a block of data and some limited *a priori* information. However, these optimal methods are essential for developing some more practical time-varying filtering methods. In Chapter 6, we will use them as the theoretical foundation and performance benchmark to develop TVAR model based time-varying filtering methods, including the TVAR based Wiener filter (TVAR-WF) and the TVAR based Kalman filter (TVAR-KF).

It is worth pointing out the distinction between the time-varying filtering (TVF) problem studied in this work and the adaptive filtering (AF) problem and methods widely applied to adaptive echo-cancellation, adaptive beamforming, adaptive equalization, and other applications [38]. Simply put, the basic distinction lies in the speed of the time-variation of the environment. The adaptive algorithms are for slowly-varying scenarios where the algorithms can converge to a steady state, under either training or blind adaptation, and subsequently attempt to track the time-variation of the environment based on some sort of feedback. In these cases, an explicit description of the time-variation is not evoked. On the other hand, the time-varying filtering problem we consider is for fast-varying scenarios where the variation is faster than what an adaptive algorithm can converge to or track. The TVF problem considered is also for those scenarios where only a short data record is available and significant time-variation accrues inside the data record. In such cases, an explicit description of the time-variation can be used to perform time-varying filtering.

5.2 Wiener Filtering

5.2.1 General Time-Varying Wiener Filter

The continuous-time optimal (minimum mean-square error) linear time-varying filter was described by Van Trees [19]. The time-varying impulse response is determined, in the form of an integral equation, by the time-dependent correlation function of the input and the time-dependent cross-correlation function between the input and the desired output. The discrete time counterpart can be briefly formulated as follows.

We denote the impulse response of a linear discrete time time-varying filter as $h(t,\tau)$, representing the response at time t contributed by an impulse input at time $(t-\tau)$. An input sequence $x(t)$ is applied to the filter to estimate a desired signal $d(t)$. The estimate of $d(t)$, $\hat{d}(t)$, is then

$$\hat{d}(t) = \sum_{\tau=T_1}^{T_2} h(t,\tau)x(t-\tau) \tag{5-1}$$

For causal filtering, we have $T_1 = 0$. For an IIR causal filter, we have $T_1 = 0$ and $T_2 = \infty$, and for a FIR causal filter, we have $T_1 = 0$ and $T_2 = P$ where P is the order of the filter. The filtering error sequence is defined as

$$\varepsilon(t) = d(t) - \hat{d}(t) \tag{5-2}$$

Minimizing the mean square error evokes the principle of orthogonality:

$$E[x(t-k)\varepsilon^*(t)] = 0, \quad k \in [T_1, T_2] \tag{5-3}$$

or

$$E[x(t-k)\sum_{\tau=T_1}^{T_2} h^*(t,\tau)x^*(t-\tau)] = E[x(t-k)d^*(t)], \quad k \in [T_1, T_2]$$

which becomes

$$\sum_{\tau=T_1}^{T_2} h^*(t,\tau)E[x(t-k)x^*(t-\tau)] = E[x(t-k)d^*(t)], \quad k \in [T_1, T_2] \tag{5-4a}$$

or

$$\sum_{\tau=T_1}^{T_2} R_x(t-k,t-\tau)\, h^*(t,\tau) = R_{xd}(t-k,t), \quad k \in [T_1, T_2] \tag{5-4b}$$

where

$$R_x(l,i) = E[x(l)x^*(i)] \tag{5-5}$$

is the time-dependent auto-correlation function of the data, and

$$R_{xd}(l,i) = E[x(l)d^*(i)] \tag{5-6}$$

is the time-dependent cross-correlation function between the data and the desired signal. Equation (5-4) is referred to as the general time-varying Wiener-Hopf equation. The solution to this system of equations is the time-varying Wiener filter (TVWF). For practical applications, a critical problem is to estimate the correlation functions so that one can then solve for the filter from the equation.

For stationary cases, the time-varying Wiener-Hopf equation (5-4) reduces to the well-known form of the Wiener-Hopf equation describing the linear time-invariant (LTI) Wiener filter, which is usually expressed as

$$\sum_{\tau=-\infty}^{\infty} R_x(k-\tau)\, h^*(\tau) = R_{xd}(k), \quad k \in [-\infty, \infty] \tag{5-7}$$

5.2.2 FIR Wiener Filter

If the optimum filter to be solved for is restricted to be causal and have a finite-duration impulse response (FIR), the impulse response can be solved for directly by matrix methods, as explained below.

Denoting the order of the FIR filter as P, the filter operation is

$$\hat{d}(t) = \sum_{\tau=0}^{P} h(t,\tau)x(t-\tau) \tag{5-8}$$

and the Wiener-Hopf equation becomes

$$\sum_{\tau=0}^{P} R_x(t-k, t-\tau)\, h^*(t,\tau) = R_{xd}(t-k,t), \quad k = 0,1,\ldots,P \tag{5-9}$$

For each time instant *t*, this is a set of *P*+1 linear equations with *P*+1 FIR filter taps

$h(t,\tau), \tau = 0,1,...,P$ as unknowns. If the time-dependent correlation functions $R_x(l,i) = E[x(l)x^*(i)]$ and $R_{xd}(l,i) = E[x(l)d^*(i)]$ are known or successfully estimated, then at each time instant *t*, the FIR filter coefficients can be solved for from equation (5-9) with matrix methods.

Unfortunately, the correlation functions are rarely known in practice, especially for time-varying cases. For stationary processes and time-invariant filtering, ergodicity is usually assumed to estimate the correlation functions from data. For time-varying cases, the challenge is to estimate the correlation functions without assuming stationarity and ergodicity. Some sacrifice and assumption are usually resorted to. In a geophysical signal processing application case, Wang [68] applied temporal windows to the data and assumed "piecewise stationarity." That is, for the duration of each data window, the data was treated as a stationary and ergodic process, and the "local" correlation function was estimated accordingly. By sliding data windows, the time-varying correlation functions were estimated and used to form an approximated time-varying Wiener filter. While this treatment may approximate well if the time-variation is slow enough, it is not valid for fast-varying non-stationarities and short data records.

5.2.3 IIR Wiener Filter

Another way to form the optimal filter from the general Wiener-Hopf equation is to obtain the solution in the frequency-domain. This relies on transforming the Wiener-Hopf equation from the time-domain to the frequency-domain. This is possible under the assumption of stationarity.

The stationary non-causal IIR version of the Wiener-Hopf equation, as a special case of (5-7), is written as

$$\sum_{\tau=-\infty}^{\infty} R_x(k-\tau)\, h^*(\tau) = R_{xd}(k), \quad k \in (-\infty, \infty) \tag{5-10}$$

By taking the Z-transform on both sides of (5-10), the correlation functions $R_x(\tau)$ and $R_{xd}(\tau)$ are transformed to the power spectrum $P_x(z)$ and the cross-spectrum $P_{xd}(z)$, and the convolutional operation on the left side of (5-10) is transformed to simple multiplication, which yields

$$H(z) \cdot P_x(z) = P_{xd}(z) \tag{5-11}$$

and this leads to the non-causal IIR Wiener filter

$$H_{nc}(z) = \frac{P_{xd}(z)}{P_x(z)} \tag{5-12}$$

where the subscript "*nc*" is added to emphasize the filter being non-causal.

For the stationary case, the causal IIR filter was also derived. Wiener [69] originally solved the continuous-time version of this problem using spectral factorization. The discrete-time version was presented in detail, for example, by Therrien [37]. Since the derivation procedure involves several steps and is rather long, we give only the result here, which is

$$H_c(z) = \frac{1}{KC(z)}\left[\frac{P_{xd}(z)}{C^*(1/z^*)}\right]_+ \tag{5-13}$$

where the subscript "*c*" is added to emphasize that the filter is causal, K is a constant, $C(z)$ - with all poles and zeros inside the unit circle - represents the causal minimum phase factor in the spectral factorization

$$P_x(z) = KC(z) \cdot C^*(1/z^*) \tag{5-14}$$

and the notation $[\quad]_+$ refers to taking the causal part of the inverse Z-transform.

Implementation of the IIR Wiener filters (5-12) and (5-13) requires the power spectrum of the data and the cross-spectrum between the data and the desired signal, both in the closed form of rational polynomials in z or $e^{-j\omega}$. This means that spectral estimates, if not in closed rational form, can not be used to form the optimal filters. Parametric spectrum estimation based on AR or ARMA models yields spectral estimates in the desired form, and therefore can be used to form the optimal filters. Based on this idea and combined with temporal windowing, Beex and Xie [22] proposed a filtering method for slowly-varying non-stationary processes. In Chapter 6, we will propose TVAR model based Wiener filters for fast-varying processes.

5.3 Kalman Filtering

The Kalman filter is a recursive linear optimum filter described in terms of state-space concepts, rather than in terms of the filter impulse response or filter transfer function. Using the observed data set, the Kalman filter provides the least mean-square estimate of the state vector of the dynamical system, given enough knowledge about the system and the noise processes involved. As remarked earlier, for the time-varying filtering problem considered, where we have only a data record and limited knowledge about the data, the Kalman filter can not be used directly. However, the Kalman filter provides us with a theoretical framework and benchmark for developing other methods. A complete presentation of the Kalman filter can be found in many texts, such as Van

Trees [19], Haykin [38], and Mendel [70]. Here we briefly review the Kalman filter result, to prepare for the development of a TVAR based Kalman filter in the next chapter.

Consider a linear discrete-time dynamical system described by the signal-flow graph shown in Figure 5-1, or, equivalently, by the following state-space equations:

Process equation

$$\mathbf{x}(t+1) = \mathbf{F}(t+1,t)\mathbf{x}(t) + \mathbf{v}(t) \tag{5-15}$$

Measurement equation

$$\mathbf{y}(t) = \mathbf{C}(t)\mathbf{x}(t) + \mathbf{w}(t) \tag{5-16}$$

where t is the discrete-time index, $\mathbf{x}(t)$ is the M-by-1 state vector at time t, $\mathbf{F}(t+1,t)$ is the M-by-M state transition matrix from time t to $t+1$, the M-by-1 $\mathbf{v}(t)$ is the process noise, $\mathbf{y}(t)$ is the N-by-1 observation vector, $\mathbf{C}(t)$ is the N-by-M measurement matrix, and the N-by-1 vector $\mathbf{w}(t)$ is the measurement noise.

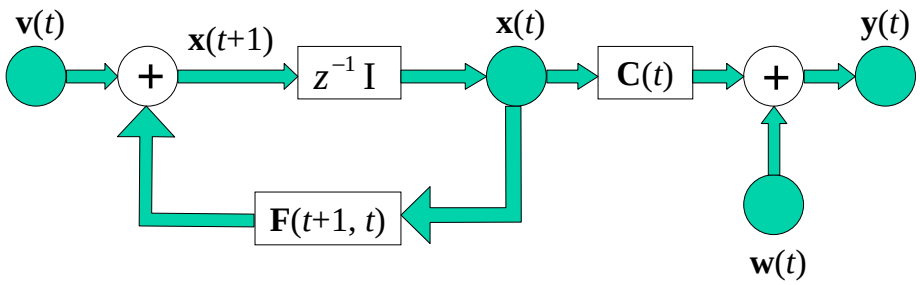

Figure 5-1. State-space signal-flow graph for a linear discrete-time dynamical system.

We assume that the process noise vector $\mathbf{v}(t)$ and the measurement noise vector $\mathbf{w}(t)$ are both zero-mean, white, and statistically independent, with the following correlation matrices:

$$E[\mathbf{v}(t)\mathbf{v}^H(k)] = \begin{cases} \mathbf{Q}_1(t), & t = k \\ \mathbf{0}, & t \neq k \end{cases} \tag{5-17}$$

$$E[\mathbf{w}(t)\mathbf{w}^H(k)] = \begin{cases} \mathbf{Q}_2(t), & t = k \\ \mathbf{0}, & t \neq k \end{cases} \tag{5-18}$$

$$E[\mathbf{v}(t)\mathbf{w}^H(k)] = \mathbf{0}, \quad \text{for all } t \text{ and } k \tag{5-19}$$

We assume that the observation data starts at time index $t = 0$. The Kalman filter can then be summarized as follows:

Input vector process

Observation = $\{\mathbf{y}(0), \mathbf{y}(1), \mathbf{y}(2), \ldots, \mathbf{y}(t)\}$

Known parameters

State transition matrix = $\mathbf{F}(t+1, t)$

Measurement matrix = $\mathbf{C}(t)$

Correlation matrix of the process noise vector = $\mathbf{Q}_1(t)$

Correlation matrix of the measurement noise vector = $\mathbf{Q}_2(t)$

Computation: $t = 0, 1, 2, \cdots$

Prediction equation:

$$\hat{\mathbf{x}}(t \mid t-1) = \mathbf{F}(t, t-1)\hat{\mathbf{x}}(t-1) \tag{5-20}$$

Innovation equation:

$$\mathbf{z}(t) = \mathbf{y}(t) - \mathbf{C}(t)\hat{\mathbf{x}}(t \mid t-1) \tag{5-21}$$

Filtering gain equation:

$$\mathbf{G}(t) = \mathbf{K}(t, t-1)\mathbf{C}^H(t)\left[\mathbf{C}(t)\mathbf{K}(t, t-1)\mathbf{C}^H(t) + \mathbf{Q}_2(t)\right]^{-1} \tag{5-22}$$

Filtering equation:

$$\hat{\mathbf{x}}(t) = \hat{\mathbf{x}}(t \mid t-1) + \mathbf{G}(t)\mathbf{z}(t) \tag{5-23}$$

Correlation matrix of the filtering error:

$$\mathbf{K}(t) = \mathbf{K}(t, t-1) - \mathbf{F}(t, t+1)\mathbf{G}(t)\mathbf{C}(t)\mathbf{K}(t, t-1) \tag{5-24}$$

Correlation matrix of the prediction error:

$$\mathbf{K}(t+1,t) = \mathbf{F}(t+1,t)\mathbf{K}(t)\mathbf{F}^{H}(t+1,t) + \mathbf{Q}_1(t) \tag{5-25}$$

where $\mathbf{F}(t,t+1) = \mathbf{F}(t+1,t)^{-1}$

Initial conditions:

$$\hat{\mathbf{x}}(-1) = E[\mathbf{x}(0)]$$

$$\mathbf{K}(-1) = E[(\mathbf{x}(0) - E[\mathbf{x}(0)]) \cdot (\mathbf{x}(0) - E[\mathbf{x}(0)])^{H}]$$

The Kalman filter summarized above is for estimating the state vector $\mathbf{x}(t)$. In the time-varying filter problem we consider, the filtering is for estimating the desired signal $d(t)$, embedded in the observed data $y(t) = d(t) + w(t)$ - here we assumed scalar (single-channel) output. The estimate of the desired signal can be obtained from the state vector estimate according to

$$\hat{d}(t) = \mathbf{C}(t)\hat{\mathbf{x}}(t) \tag{5-26}$$

5.4 Summary and Discussion

We reviewed the Wiener filter and the Kalman filter with the time-varying filtering problem in mind. The main obstacle in applying these optimum filters is the lack of information. As pointed out earlier, in many application scenarios, we have only observation data and do not have known state equations, time-dependent correlation functions, or power spectra. To solve this problem, in the next chapter, we will develop TVAR model based Kalman and Wiener filters.

Chapter 6

TIME-VARYING OPTIMUM FILTERING BASED ON TVAR MODELING

In this chapter, we develop the TVAR model based Kalman filter and TVAR model based Wiener filter. Their performance are compared using both known TVAR parameters and estimated TVAR parameters. The results show that the TVAR based causal Wiener filter is a nearly-optimal causal filter.

6.1 Introduction

In Chapter 3 we studied time-varying notch filtering using the TVAR based IF estimator for interference rejection in DSSS communications. Those “brute force” time-varying notch filters are controlled only by instantaneous frequency (IF) estimates, rather than formed according to some optimality criterion . In this chapter, we develop optimum time-varying filtering based on the TVAR model, including the TVAR based Kalman filter (TVAR-KF) and TVAR based Wiener filters (TVAR-WF). We model the observed data with a TVAR model, and use the general Kalman filter and Wiener filter, as presented in Chapter 5, to form filters using TVAR parameters.

We aim at optimal or nearly optimal recovery of a desired signal from a data record. The signal may be highly non-stationary, the additive contaminating noise may also be non-stationary, and the signal and noise may overlap in both time and frequency. From Chapter 5, we know that the optimum filter exists for such cases. The problem in implementing the optimum filter is the lack of required knowledge, such as the time-dependent correlation functions needed to solve for the Wiener filter in the time-domain.

In this chapter, we assume that the knowledge required to form the optimum filters given in Chapter 5 is not available. Instead, we assume that the observed data fits a TVAR model. Such data are widely found in engineering, such as speech signals and frequency modulated (FM) signals in noise. Based on this assumption, we can estimate the TVAR parameters from the data, and then use the parameter estimates to form an optimum or nearly-optimum filter.

The TVAR-KF is developed by setting up the state-space representation of the TVAR model. If the observed data is indeed generated from such a TVAR system, that is, there is no modeling error, and the exact TVAR parameters are used, which means they are free of estimation error, then the TVAR-KF is the optimal causal filter since it corresponds directly to the general KF. We also propose a time-varying Wiener filtering method based on TVAR modeling. By approximating the time-varying nature of the parameters with combinations of some known functions of time, the proposed TVAR based Wiener filter is able to handle rapidly varying processes. Both the ideal non-causal TVAR-WF and the causal TVAR-WF are formulated based on the TVAR model.

6.2 TVAR Kalman Filter

6.2.1 Method

Consider an observation $y(t)$, consisting of desired signal $d(t)$ and additive noise $w(t)$, which is assumed to be uncorrelated with the signal $d(t)$:

$$y(t) = d(t) + w(t) \tag{6-1}$$

We model the signal with a TVAR model, which is given by (1-1) and rewritten here as

$$d(t) = -\sum_{i=1}^{p} a_i(t) d(t-i) + e(t) \tag{6-2}$$

Now we want to find the state-space description equivalent of the TVAR model in (6-2). The state-space equations (5-15)-(5-16) are rewritten here as

$$\mathbf{d}(t+1) = \mathbf{F}(t+1,t)\mathbf{d}(t) + \mathbf{e}(t) \tag{6-3}$$

$$\mathbf{y}(t) = \mathbf{C}(t)\mathbf{d}(t) + \mathbf{w}(t) \tag{6-4}$$

It is straightforward to verify that a state-space description of the TVAR model is

$$\mathbf{d}(t) = [\, d(t-1), d(t-2), \cdots, d(t-p)]^T, \quad (p \times 1) \tag{6-5}$$

$$\mathbf{e}(t) = [e(t), 0, 0, \cdots, 0]^T, \quad (p \times 1) \tag{6-6}$$

$$\mathbf{y}(t) = [y(t)], \quad (1 \times 1) \tag{6-7}$$

$$\mathbf{w}(t) = [w(t)], \quad (1 \times 1) \tag{6-8}$$

$$\mathbf{F}(t+1,t) = \begin{bmatrix} -a_1(t) & -a_2(t) & \cdots & -a_{p-1}(t) & -a_p(t) \\ 1 & 0 & \cdots & 0 & 0 \\ 0 & 1 & & 0 & 0 \\ \vdots & & \ddots & & \vdots \\ 0 & 0 & & 1 & 0 \end{bmatrix}, \quad (p \times p) \tag{6-9}$$

$$\mathbf{C}(t) = [-a_1(t) \quad -a_2(t) \quad \cdots \quad -a_p(t)], \quad (1 \times p) \tag{6-10}$$

With TVAR parameters, Kalman filtering can be performed based on the state-space description of the TVAR model. We call this method the TVAR based Kalman filter (TVAR-KF).

6.2.2 Example

As an example of the application of the TVAR-KF, we apply the filter to a fast-varying signal in white Gaussian noise. A real-valued 200-sample data record starts as low-pass at $t = 0$ and ends as high-pass at $t = 199$. The data is generated as a fourth-order TVAR process plus white Gaussian noise at SNR = 0dB. The two complex-conjugate pole pairs coincide, and rotate in the *z*-plane over time according to

$$p_{1,2}(t) = p_{3,4}(t) = 0.5 \exp\left[\pm j2\pi(0.05 + \frac{3}{8}\frac{t}{200})\right], \quad t = 0,1,\cdots,199$$

The trajectories of the poles and the corresponding TVAR coefficients $a_i(t), i = 0,1,\cdots 4$, as functions of time, are shown in Figure 6-1.

The excitation process to the TVAR model is a zero-mean, unit-variance, white Gaussian process. The waveforms of a realization of the resulting TVAR process, which is the desired signal, and the noisy data are plotted together in Figure 6-2. Observe that the desired signal varies from low-pass to high-pass and wanes in the middle as the poles are getting farther apart when they meet the imaginary axis. Also note that the additive noise is stationary over the data record and dominates the observations in the middle of the data record.

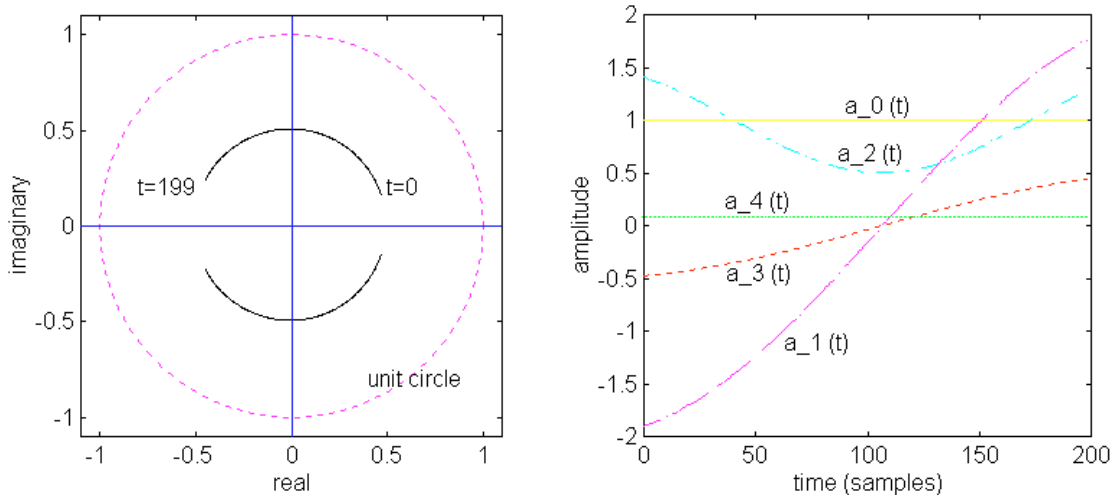

(a) (b)

Figure 6-1. A fast-varying fourth-order TVAR process that starts as low-pass and ends as high-pass: (a) pole trajectories in *z*-plane: (b) TVAR coefficients as functions of time.

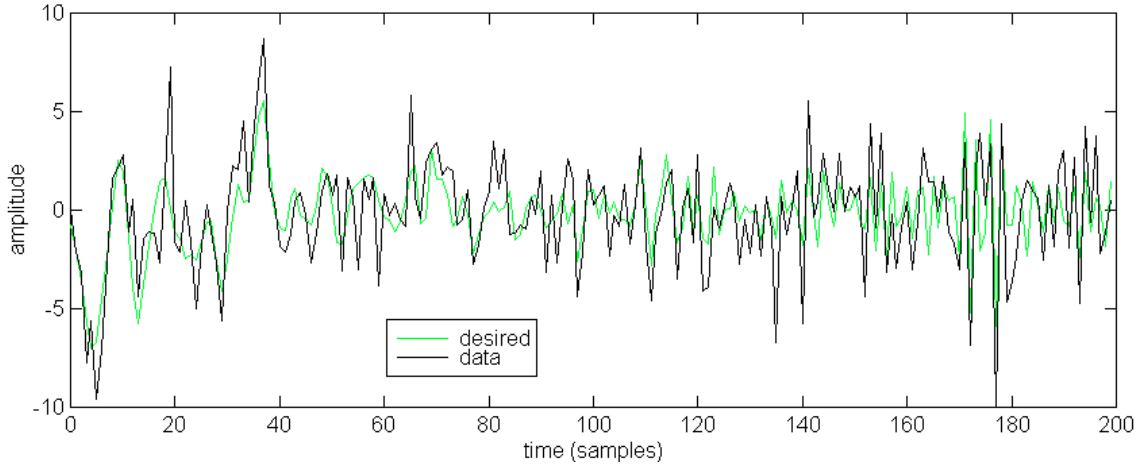

Figure 6-2. Waveforms of the data record and the desired signal, SNR=0dB.

Using the known TVAR parameters, that were used to generate the data, to form a TVAR-KF, boosts SNR from 0dB to 4.24dB, which is evaluated as the ratio of energies in the entire data record for the desired signal and the output error. The known TVAR-KF output is plotted in Figure 6-3 (a) against the desired signal.

Next we use the TVAR parameters estimated from the data record to form an estimated TVAR-KF. The resulting filtered output is compared with the desired signal in Figure 6-3 (b). The filter improves SNR from 0dB to 3.75dB, which is successful even though it produces about 0.5 dB less improvement than was obtained from using the exact parameters.

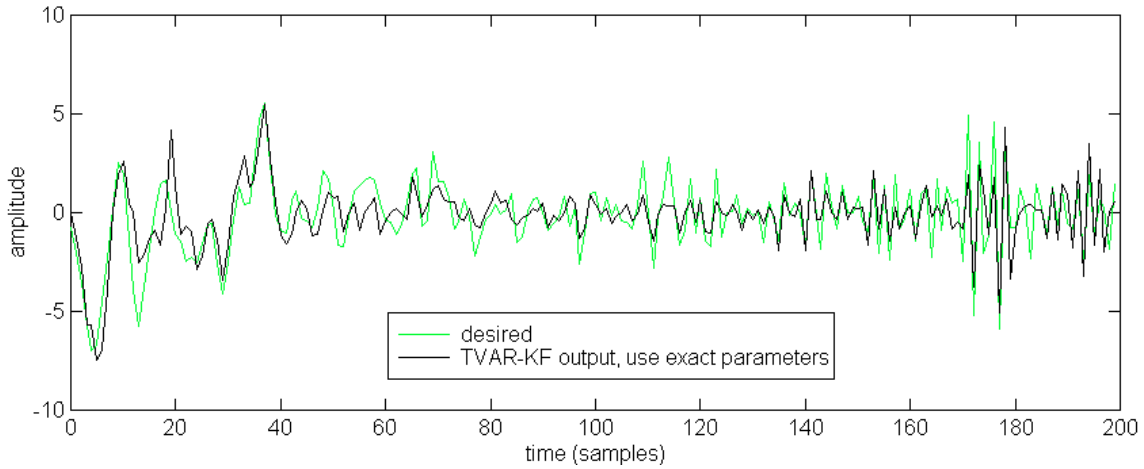

(a)

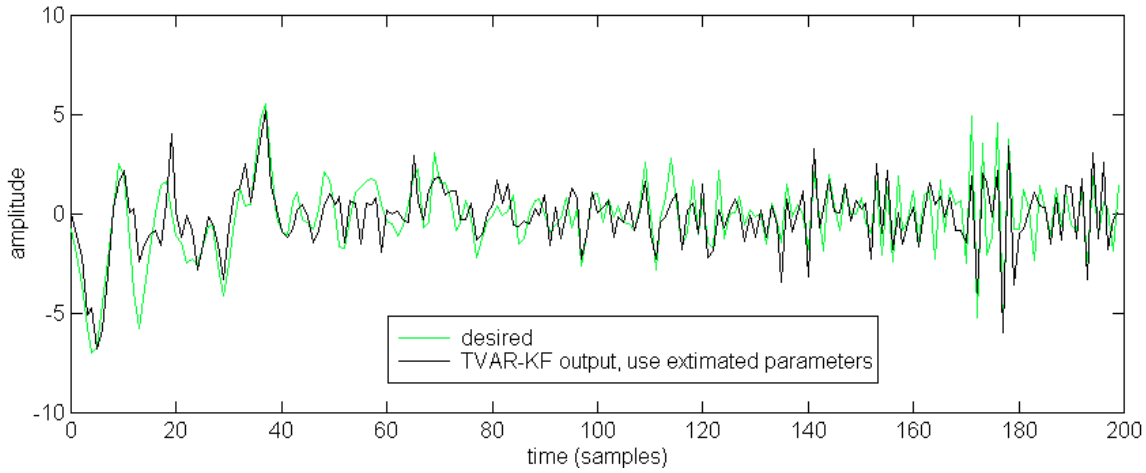

(b)

Figure 6-3. Output of TVAR-KF compared with desired signal:
(a) using known TVAR parameters, SNR=4.238dB,
(b) using estimated TVAR parameters, SNR=3.754dB.

6.3 TVAR Wiener Filter

In this section, we develop the TVAR model based Wiener filter, in both causal and non-causal versions, and then present an example in details. The performance of the proposed TVAR Wiener filter and the TVAR Kalman filter developed in Section 6.2 will be studied further through simulations in Section 6.4.

6.3.1 Method

Consider an observation $x(t)$, consisting of desired signal $d(t)$ and additive noise $w(t)$:

$$x(t) = d(t) + w(t) \tag{6-11}$$

Assuming that the noise $w(t)$ is uncorrelated with the signal $d(t)$, implies that the cross-spectrum between them is zero, i.e. $P_{wd}(z) = 0$. Consequently, the cross-spectrum between the data and the desired signal is

$$P_{xd}(z) = P_{dd}(z) + P_{wd}(z) = P_d(z) \tag{6-12}$$

and, similarly, the power spectrum of the data is

$$P_x(z) = P_d(z) + P_w(z) \tag{6-13}$$

Recall from Chapter 5 that minimizing the mean squared error (MSE) of estimating $d(t)$ from $x(t)$ leads to the Wiener filter [37]. Using (6-12) and (6-13), the IIR WF in the frequency domain is then expressed as

$$H(z) = \frac{P_{xd}(z)}{P_x(z)} = \frac{P_d(z)}{P_d(z) + P_w(z)} \tag{6-14}$$

which is the power spectrum ratio of the desired signal to the observed signal. This is the stationary Wiener filter, where second-order wide-sense stationarity was assumed in the derivation.

For time-varying cases, an optimal filter should be a time-varying system that minimizes the mean squared estimation error. When the time-varying nature is assumed to be relatively slow, adaptive algorithms [38] have been well established. Our interest is in those cases where the parameters of the desired signal and/or the observation noise varies so rapidly that adaptive filtering algorithms are not appropriate, and/or those cases where training data is not available.

For a non-stationary process, we form a time-varying filter $H(t,z)$ by concatenating the optimal filters at each time moment *t*, which can be expressed as

$$H(t,z) = \frac{P_{xd}(t,z)}{P_x(t,z)} = \frac{P_d(t,z)}{P_d(t,z) + P_w(t,z)} \tag{6-15}$$

where $P_d(t,z), P_w(t,z)$ and $P_x(t,z)$ are the time-dependent spectra or time-frequency power distributions. This time-varying filter is essentially the same as the time-frequency design of non-stationary Wiener filters theoretically derived via WVD and WS (Weyl Symbol) by Kirchauer, Hlawatsch, and Kozek [21], as mentioned in Chapter 1. We advocate the use of the TVAR model in the design of time-varying filters for the same reason that parametric methods are widely used for various problems in stationary cases, and also for the reason that we can form the causal Wiener filter by TVAR spectral factorization. Compared to the WVD, other attractive features of TVAR spectra include high spectral resolution, being cross-term free, and providing the ability to handle short data blocks.

The filter expressed in (6-15) is non-causal. Similar to the stationary case [37], based on the spectral factorization

$$P_x(t,z) = K(t)\ C(t,z)\ C^*(t,1/z^*) \tag{6-16}$$

yields the corresponding causal filter:

$$H_c(t,z) = \frac{1}{K(t)\ C(t,z)}\left[\frac{P_d(t,z)}{C^*(t,1/z^*)}\right]_+ \tag{6-17}$$

where $C(t,z)$, a rational form with monic numerator and denominator polynomials and all poles and zeros located inside the unit circle, represents the causal minimum-phase factor of $P_x(t,z)$, and the notation $[\ \ ]_+$ refers to the causal part of the inverse Z-transform.

If both signal and noise are modeled by a TVAR model, with TVAR coefficients denoted as $a_i(t), t = 0,1,\cdots p_d$, for the signal $d(t)$ and $b_i(t), t = 0,1,\cdots p_w$, for the noise $w(t)$, their respective TVAR based time-dependent power spectra are:

$$P_d(t,z) = \frac{\sigma_d^2}{A(t,z)A^*(t,1/z^*)} \tag{6-18a}$$

$$P_w(t,z) = \frac{\sigma_w^2}{B(t,z)B^*(t,1/z^*)} \tag{6-18b}$$

where σ_d^2 and σ_w^2 are the variances of the white excitation processes generating $d(t)$ and $w(t)$, respectively, and the polynomials are defined as follows

$$A(t,z) = \sum_{i=0}^{p_d} a_i(t)z^{-i}, \quad a_0 \equiv 1 \tag{6-19a}$$

$$B(t,z) = \sum_{i=0}^{p_w} b_i(t)z^{-i}, \quad b_0 \equiv 1 \tag{6-19b}$$

The TVAR power spectrum expression in (6-18) is a direct extension of the AR spectrum in the stationary case [30]. We also have shown that this expression can be derived from Priestley's evolutionary spectrum (ES) theory as a special case of the ES. A brief description of Priestley's evolutionary spectrum theory, its relation to this research, and how the ES leads to the TVAR spectrum in (6-18) is given at the end of this document as Appendix B.

Let $D(t,z)$ be the monic numerator polynomial of $C(t,z)$, i.e.

$$C(t,z)=\frac{D(t,z)}{A(t,z)B(t,z)} \tag{6-20}$$

Consequently, the ideal non-causal TVWF in (6-15) can now be expressed as

$$H_{nc}(t,z)=\left[\frac{B(t,z)}{\sqrt{K(t)}D(t,z)}\right]\left[\frac{B^{*}(t,1/z^{*})}{\sqrt{K(t)}\ D^{*}(t,1/z^{*})}\right] \tag{6-21}$$

Note two distinct factors in (6-21): the causal part in the first brackets, and the corresponding anti-causal part in the second brackets. Similarly, the causal TVWF in (6-17) is specified as

$$H_{c}(t,z)=\frac{A(t,z)B(t,z)}{K(t)\ D(t,z)}\left[\frac{B^{*}(t,1/z^{*})}{A(t,z)\ D^{*}(t,1/z^{*})}\right]_{+} \tag{6-22}$$

In many application cases, the additive measurement noise $w(t)$ in (6-13) can be treated as being white noise, such as receiver thermal noise in communications. In such cases $P_w(t,z)=\sigma_w^2$ and $B(t,z)\equiv B^{*}(t,1/z^{*})\equiv 1$, so that the filters in (6-21) and (6-22) are simplified accordingly.

The non-causal filter in (6-21) can be realized based on data blocks in two steps, similar to the MPSE based non-causal time-varying Wiener filter by Beex and Xie [22].

First the data block is filtered by the causal part, corresponding to the first bracketed term in (6-21), and then the anti-causal part is implemented by filtering the temporal output from the first step *backward* with the causal part of the transfer function.

In practice, with *a priori* information about the signal and the noise, $A(t,z)$ and $B(t,z)$ may be identified from the observations. Since the filter coefficients are directly related to the TVAR coefficients, the parameter estimation, filter coefficient calculation, and filtering operation can be implemented in a block-by-block fashion.

6.3.2 Example

We illustrate the performance of the proposed TVAR based IIR TVWFs through an example. The time-varying filters were implemented in the Direct Form I, with the coefficients updated for each sample. The implementation of the non-causal version is based on the entire data block filtered in the *forward-then-backward* way.

We use the same data as was used in the example for the TVAR-KF in Subsection 6.22, with the time-variation laws shown in Figure 6-1 and waveforms in Figure 6-2. First, we assume that the exact information on the TVAR parameters, used to generate the data, is known. Both the causal and non-causal versions of the TVAR-WF are formed using the exact TVAR parameters. Next we use the TVAR parameters estimated from the given data record to form the non-causal and causal TVAR-WFs.

In Figure 6-4, the magnitude responses of the non-causal TVAR-WFs using both the exact and the estimated TVAR parameters are shown in terms of gain contours (in decibels) on the time-frequency plane. These filters track the trajectory of the signal poles

shown in Figure 6-1: they both start as a low-pass response, vary to a band-pass, and end as a high-pass, even though their magnitude gain contours look different.

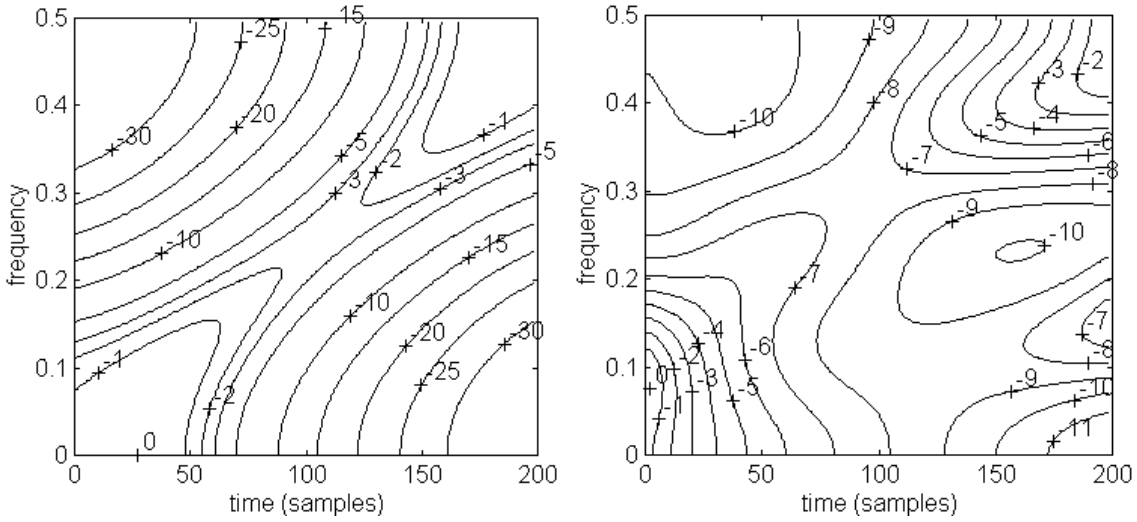

(a) (b)

Figure 6-4. The magnitude response (dB) contour plots of the ideal non-causal TVAR-WF:
(a) using the known TVAR parameters,
(b) using TVAR parameters estimated from the data record.

Applying the above filters to the data record, boosts the SNR from 0dB to 5.385dB and 4.249dB by using the known and estimated parameters respectively. The output waveforms are compared with the desired signal in Figure 6-5. Compared to the outputs of the TVAR-KF in Figure 6-2, for the same data and parameters, the non-causal TVAR-WF yields significantly higher filtering gains; about 1dB higher when using the known parameters and about 0.5dB higher when using estimated parameters. An explanation for the latter is that the TVAR-KF is causal while the ideal TVAR-WF is non-causal and hence may have much better performance.

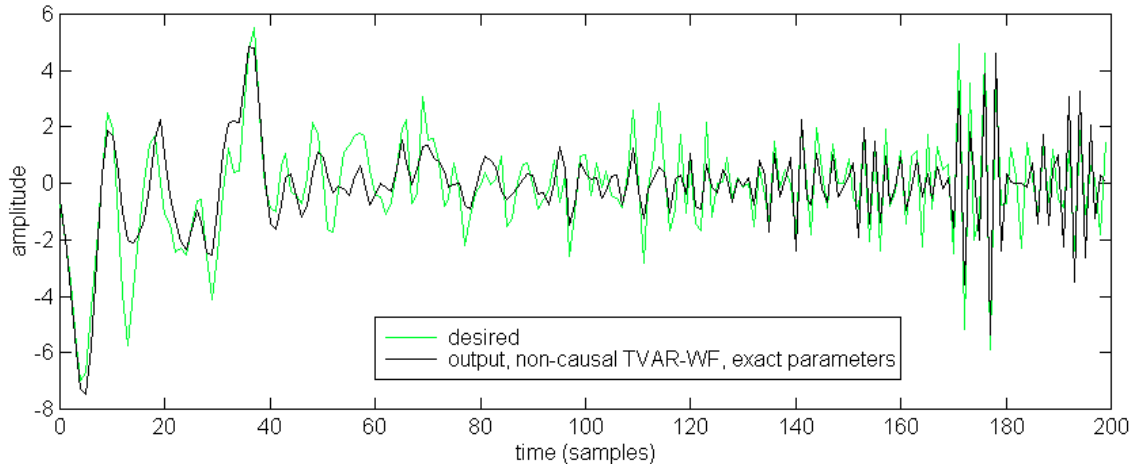

(a)

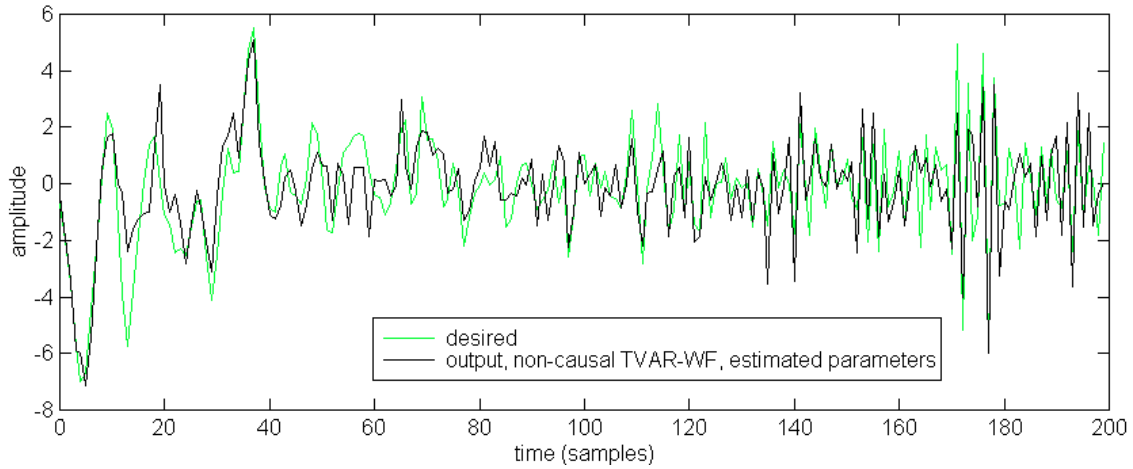

(b)

Figure 6-5. Output of the non-causal TVAR-WF compared with desired signal:
(a) using known TVAR parameters, SNR=5.385dB,
(b) using estimated TVAR parameters, SNR=4.249dB.

Now we examine the causal TVAR-WF. Similarly, the time-varying magnitude responses of the causal TVAR-WF are shown in Figure 6-6. Again, they start as a low-pass filter, become band-pass in the middle, and end as a high-pass filter. The output waveforms are shown in Figure 6-7. Using the known parameters, the causal TVAR-WF yields an SNR improvement of 4.204dB, which is very close to the 4.238dB provided by the (causal) TVAR-KF that uses the same information. Using the estimated parameters,

the causal TVAR-WF yields output SNR of 3.745dB, which is also very close to the output SNR of 3.754dB produced by the corresponding Kalman filter. This confirms that the proposed TVAR-WF is nearly optimal. We will further examine this issue through simulations in the next section.

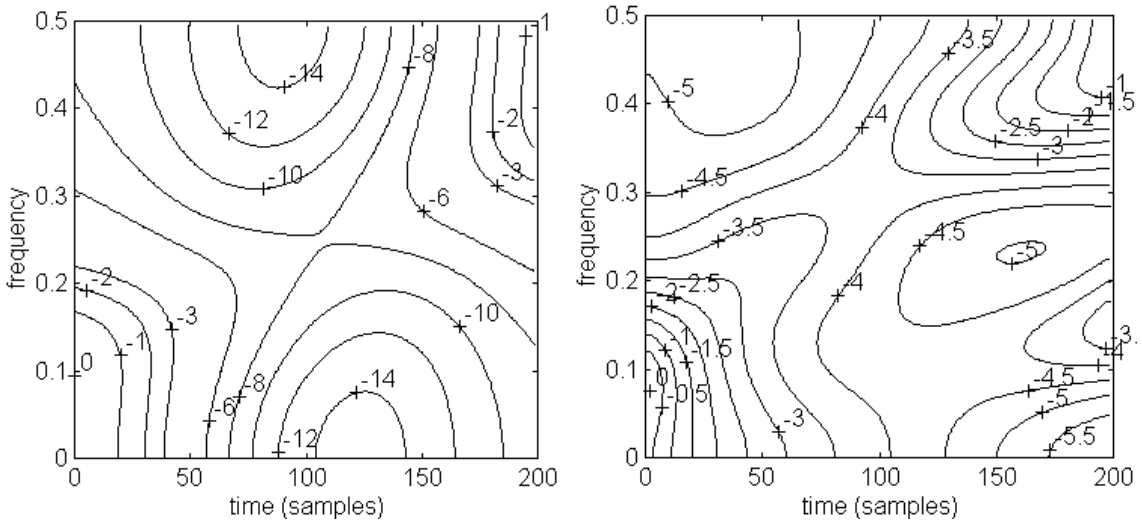

(a) (b)

Figure 6-6. The magnitude response (dB) contour plots of the ideal causal TVAR-WF:
(a) using the known TVAR parameters,
(b) using the TVAR parameters estimated from the data record.

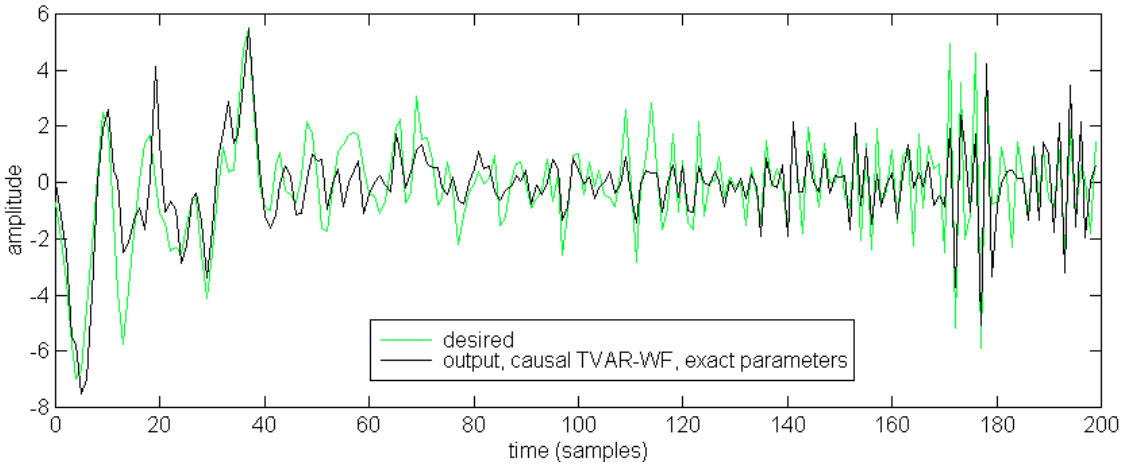

(a)

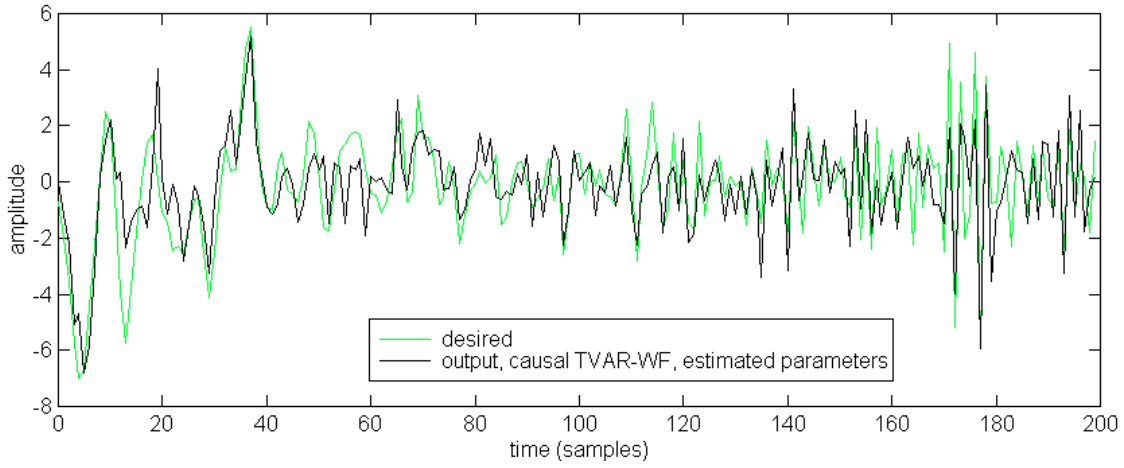

(b)

Figure 6-7. Output of causal TVAR-WF compared with desired signal:
(a) using known TVAR parameters, SNR=4.204dB,
(b) using estimated TVAR parameters, SNR=3.745dB.

6.4 Simulation Results for TVAR based Optimum Filters

We have developed the TVAR based optimum filters, including the TVAR-KF and the TVAR-WF, in both non-causal and causal versions. We also illustrated their SNR improvement capacity through an example. In this section, we further examine their performance through simulations. The results confirm that the proposed causal TVAR-

WF performs nearly as well as the Kalman filter that uses the same information, i.e., the TVAR-KF, implying that the causal TVAR-WF is a nearly-optimum causal filter.

In the simulations, the same pole trajectories and TVAR parameters are used as were used for the example in the preceding section, as shown in Figure 6-1. For each simulation trial, different realizations of both signal and noise are generated. The trials are repeated for various input SNR values. Figure 6-8 shows average filtering gain versus input SNR for different filters. The causal TVAR-WF performs almost identically as the TVAR-KF. As expected, the non-causal WF outperforms the causal filters significantly, for both cases, i.e. using known or estimated parameters. This is a major advantage for the non-causal filter. In some applications, causality is not too serious a concern when a limited processing delay is acceptable, such as in a communication system. In such scenarios, the non-causal TVAR-WF can be used.

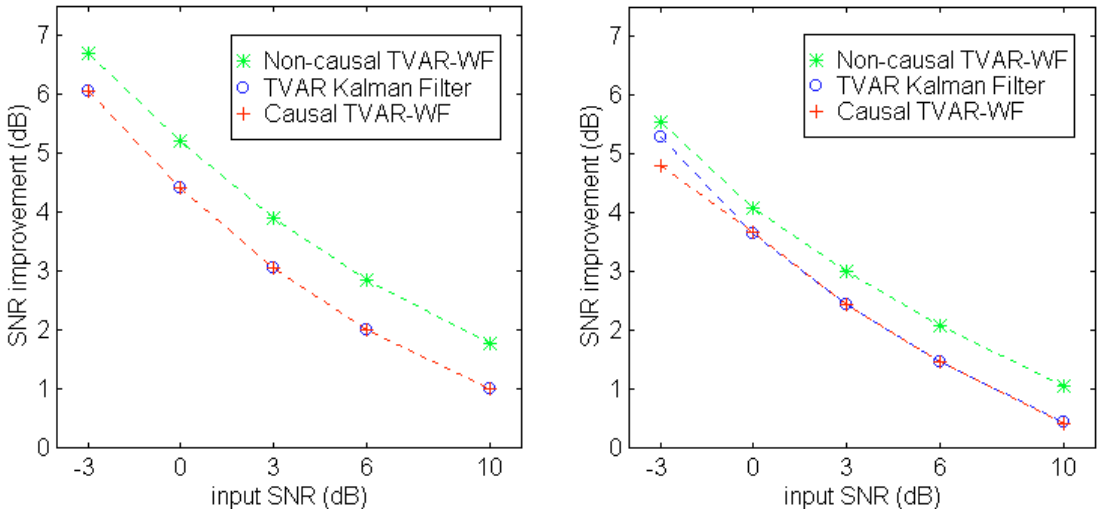

(a) (b)

Figure 6-8. Average SNR gain at various input SNR for the TVAR based filters:
(a) using known TVAR parameters,
(b) using estimated TVAR parameters.

We also observe the performance variation among different filters for the same data record and among different data realizations with the same statistical properties. Figure 6-10 shows output SNR values for different filters for each individual data record and their distributions among 25 trials at various input SNR levels. First, it is shown that the causal TVAR-WF performs consistently close to the optimal TVAR-KF for each given data record. This further confirms that the TVAR-WF is nearly-optimal. Second, parameter estimation error noticeably decreases the performance of these TVAR based filters. This means that the best performance that can be achieved in practice may be far below the theoretically potential optimum performance. Third, the performance varies significantly from data to data. Finally, nevertheless, the proposed TVAR based optimum filters, either using known or estimated parameters, always improve the SNR for a data block.

In the experiment, a wide band signal is used, with also wide instantaneous bandwidth (poles far inside the unit circle), in white (wideband) noise. This represents a tough case for the task of filtering. In such cases, a joint time-frequency cut-off filter is not appropriate, not to mention the conventional frequency-domain filter, and, consequently, an optimal or sub-optimal time-varying filter is necessary. For the cases of a signal with narrow instantaneous bandwidth in wideband noise, or vice versa, the filtering gain can be much higher (in terms of dB value) than shown in these examples, which is in the range of several decibels. The latter scenario will be shown in the next chapter, where the idea of the TVAR-WF is applied to FM interference rejection for DSSS communications. As seen in Chapter 4, in the latter problem we have a wideband communication signal and an interference with narrow instantaneous bandwidth.

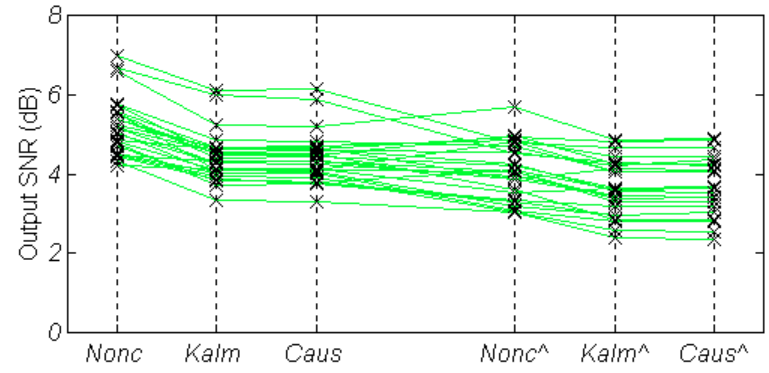

(a)

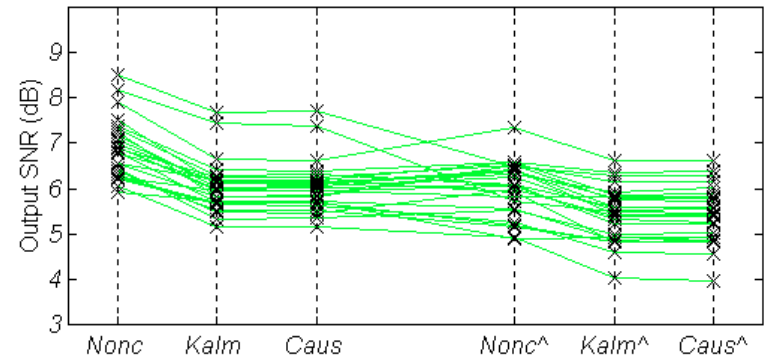

(b)

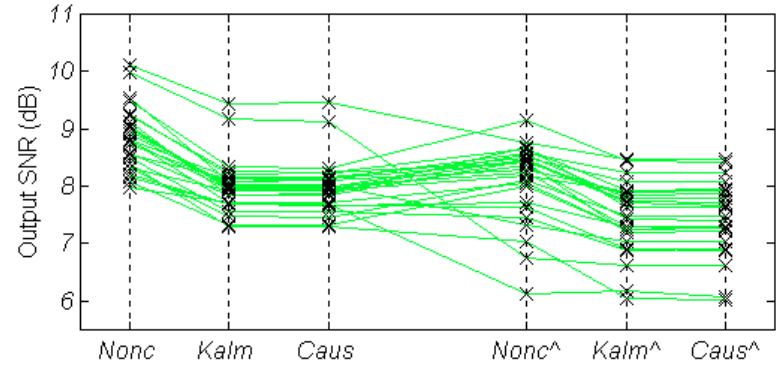

(c)

Figure 6-9. Output SNRs for different filters at each data record and their distribution among 25 trials,
Labels to denote types of filter:

Nonc, Kalm, Caus = Non-causal TVAR-WF, TVAR-KF, Causal TVAR-WF, using known TVAR parameters,

*Nonc^, Kalm^, Caus^* = Non-causal TVAR-WF, TVAR-KF, Causal TVAR-WF, using estimated parameters,

Input SNR: (a) 0dB, (b) 3dB, (c) 6dB.

6.5 Summary

In this chapter we developed TVAR based optimum filters, including the TVAR based Kalman filter and causal and non-causal Wiener filters. By modeling the data record with the TVAR model, the TVAR based filters were developed from the basic optimum filters presented in Chapter 5. We showed that the TVAR based time-varying extension of the stationary Wiener filter solution provided nearly optimal performance. Using TVAR parameters estimated from the data record yields significant filtering gain on average. However, individual realizations, while still producing non-negative filtering gain, can produce performance noticeably below the theoretically optimum gain due to parameter estimation errors.

Chapter 7

SOFT-CANCELLATION OF FM INTERFERENCE BASED ON OPTIMAL FILTERING

As an application of the TVAR based Wiener filter presented in Chapter 6, in this chapter, we develop a time-varying filter formulation for "soft-cancellation" of FM interference in DSSS communications. This filter uses full spectral information of the received data and is aimed at minimum signal distortion. Part of the results in this chapter were published earlier [67].

7.1 Introduction

Recently, time-frequency distributions (TFD) have been applied to suppress rapidly varying nonstationary interference in direct sequence spread spectrum (DSSS) communications [47-50,58]. Amin and his colleagues [47,48,60] studied interference excision using a time-varying notch filter with the null placed at the instantaneous frequency (IF) of the interference, where the IF was estimated from Wigner-Ville distributions (WVD). Other than invoking TFD's, in Chapter 4 we suggested using TVAR based IF estimation in the notch filter method to improve the IF estimation and

hence the system performance, especially for those practical situations where the frequency modulation can not be assumed to follow a linear law.

The FIR notch filter based interference suppression methods [48,57] are simple to implement once an IF estimate has been determined. However, this method suffers from a major limitation. That is, it uses only the IF information of the interference. The notch filter is formed regardless of the relative strength , instantaneous bandwidth, or other spectral characteristics of the interference. Such a notch filter significantly improves system performance for a strong mono-component tonal or FM interference by cutting the interference at the IF very deeply. However, when the interference becomes weak or absent, the brute force filter may significantly deteriorate system performance since it also distorts the signal. A threshold is thus needed to switch the notch filter on or off based on the received data energy or power [48]. To deal with this problem, Wang and Amin [66, 70] also suggested placing the filter zeros inside the unit circle with their radius determined by the relative interference power.

In this chapter, we attack these problems by exploiting the full spectral information about the interference, which is made possible with the TVAR model. Since the filter is not aimed at annihilating as much of the interference component as possible, we refer to our strategy as soft-cancellation. As earlier in Chapter 4, we model the received signal with a time-varying autoregressive model. However, here, instead of estimating the IF using the model, we use the model parameters to directly form a filter. We apply the time-varying Wiener filter that was developed in Chapter 6 to solve this problem. The TVAR-WF is tailored (as a result of its mean squared error criterion) to the received data with minimum signal distortion as the objective. In Chapter 6, we

developed the TVAR based optimum filters including the ideal non-causal TVAR-WF, the causal TVAR-WF, and the TVAR-KF. Among these, the non-causal TVAR-WF yields the best performance and the associated limited processing delay is tolerable in a communication system. Therefore, we will develop the interference rejecting filter based on the non-causal TVAR-WF.

7.2 A General Description of Interference Suppression Based on TVAR Modeling

In Figure 7-1, we give the system diagram of a DSSS receiver with interference suppression using time-varying filtering based on TVAR modeling. The TVAR parameters are identified from the received data and are used to form the time-varying filter. The filtering operation is performed before de-spreading in baseband. This method differs from the brute force notch filtering method, which may use a TVAR based IF estimate as studied in Chapter 4, in two respects. First, the filter $H(t,z)$ is formed directly from the TVAR parameters, without involving IF estimation. Second, the full spectral information carried by the set of TVAR parameters is used to form the cancellation filter. The objective that will be used here to form the filter $H(t,z)$ is minimum signal distortion, as presented in this chapter. Another objective, whiteness of the filter output, will be presented in Chapter 8. Just as in the diagram of the notch filter based method (Figure 4-1), BPSK modulation and code-on-pulse spreading are assumed in Figure 7-1.

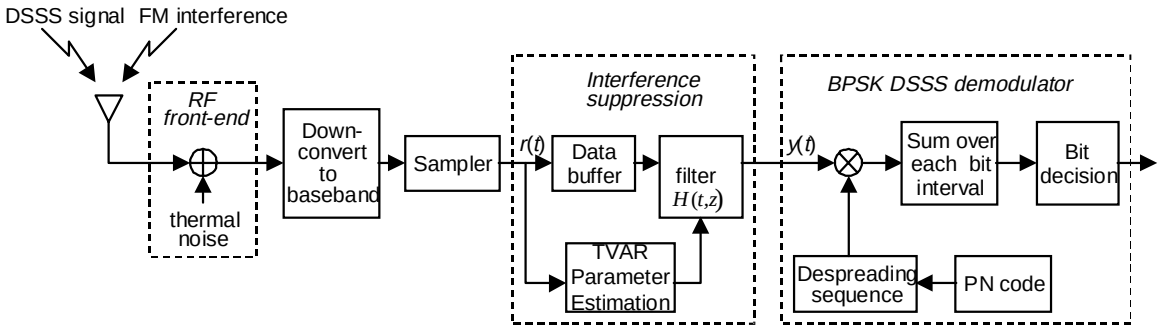

Figure 7-1. Block diagram of the DSSS receiver with TVAR based interference suppression.

7.3 FM Interference Suppression Based on TVAR-WF: Method and Example

We propose a time-varying interference suppression filter formulation that tailors the filter to fit the full time-varying spectral information about both the interference and the desired signal. Our formulation is aimed at minimizing the mean squared error of the output waveform. The TVAR model is used to identify the time-varying interference and to accordingly form the interference suppression filter based on the time-varying Wiener filter.

7.3.1 Method

At the receiver of a DSSS communications system, an interference suppression filter is applied before demodulation. We consider a received signal $r(t)$, where t refers to discrete time, composed of the DSSS signal $s(t)$, noise $w(t)$ and interference $i(t)$:

$$r(t) = s(t) + w(t) + i(t) \tag{7-1}$$

Here the noise $w(t)$ is assumed stationary and white. The DSSS signal $s(t)$ is also assumed stationary and white (non-Gaussian). In practice the DSSS signal may be "slightly colored", depending on the sampling rate (samples per chip) and the specific PN sequence used. The interference $i(t)$ could be from a broad range of time-varying sequences, such as a hostile jammer or an FM communication signal (for example, a cellular system overlapping CDMA and AMPS). The three components are assumed independent.

We feed $r(t)$ to a time-varying filter $H(t,z)$ to suppress $w(t)$, and denote the output as $y(t)$. The filter is aimed at minimizing the mean squared error

$$\min \mathrm{E}\left\{ \left| s(t)+w(t)-y(t) \right|^2 \right\} \tag{7-2}$$

This is a mean square estimation problem [19] with $s(t)+w(t)$ treated as the desired signal. For stationary processes, solving (7-2) leads to the Wiener filter [37]:

$$H_{stationary}(z)=\frac{P_s(z)+P_w(z)}{P_s(z)+P_w(z)+P_i(z)} \tag{7-3}$$

where $P_*(z)$ is the power spectral density function of the process denoted by the subscript. As in Chapter 3, to extend this Wiener filter to time-varying cases, we concatenate the optimal filters at each time instant t, and thus form the time-varying filter:

$$H(t,z)=\frac{P_s(z)+P_w(z)}{P_s(z)+P_w(z)+P_i(t,z)} \tag{7-4}$$

where $P_i(t,z)$ is the time-varying spectrum of the interference.

Let $s(t)$ and $w(t)$, both white, have spectra σ_s^2 and σ_w^2 respectively. Let $\sigma_d^2 = \sigma_s^2 + \sigma_w^2 = P_s(z) + P_w(z)$, so that the time-varying filter in (7-4) becomes

$$H(t,z) = \frac{\sigma_d^2}{\sigma_d^2 + P_i(t,z)} = \frac{1}{1 + P_i(t,z)/\sigma_d^2} \tag{7-5}$$

This is an IIR filter aimed to best recover the waveform in least mean square sense. The transfer function of this filter approximates unity at the frequencies where the interference spectrum is much weaker than the signal plus noise. Thus, unlike the time-varying notch filtering method, which distorts the signal and hence deteriorates system performance when the interference is absent or weak, this filter keeps the received signal intact if the interference is absent. The filter in (7-5) suppresses the interference according to its time-varying spectrum. It also applies to more complicated interference types, i.e. those which exhibit significant instantaneous bandwidth, as long as the received signal can be well approximated by a TVAR model.

To implement filter (7-5), we need to estimate $P_i(t,z)$, the time-varying power spectrum, or time-frequency distribution, of the interference. It is well known that a stationary narrow-band signal in white noise fits an ARMA model, and in case of moderate to high SNR, it can be approximated with an AR model. Extending to the time-varying cases, we approximately model the time-varying interference with a TVAR model.

As mentioned in Chapter 6, if we model the interference using the TVAR model, the power spectrum is expressed as:

$$P_i(t,z) = \frac{\sigma_i^2}{A(t,z)A^*(t,1/z^*)} \tag{7-6}$$

where $A(t,z)=\sum_{i=0}^{p} a_i(t)z^{-i}$ with $\{a_i(t)\}$ being TVAR coefficients ($a_0(t)\equiv 1$), and "*" denoting the complex conjugate operation. Substituting (7-6) in (7-5), the interference suppression filter is expressed as

$$H(t,z)=\frac{A(t,z)A^*(t,1/z^*)}{A(t,z)A^*(t,1/z^*)+\sigma_i^2/\sigma_d^2} \tag{7-7}$$

At each time instant *t*, we factor the denominator polynomial as follows

$$A(t,z)A^*(t,1/z^*)+\sigma_i^2/\sigma_d^2 = K(t)\,D(t,z)D^*(t,1/z^*) \tag{7-8}$$

where $D(t,z)$ is in the form of $D(t,z)=\sum_{i=0}^{p} d_i(t)z^{-i}$, with $d_0\equiv 1$, and has all its roots inside the unit circle. The filter becomes

$$H(t,z)=\frac{1}{K(t)}\cdot\left[\frac{A(t,z)}{D(t,z)}\right]\cdot\left[\frac{A^*(t,1/z^*)}{D^*(t,1/z^*)}\right] \tag{7-9}$$

The first set of brackets encloses the causal minimum-phase factor of the transfer function, and the second set of brackets encloses the anti-causal maximum-phase factor. The overall filter is zero-phase and non-causal. It can be realized with delay by first filtering a block of input *forward* with the causal part transfer function and then realizing the anti-causal part by filtering the previous result *backward*, as shown in Figure 7-2. The delay due to the non-causality is related to the processing power and the data block size. The data block size is likely on the order of hundreds of samples, and therefore on the order of a symbol or bit interval considering a few samples per chip and the number of chips per symbol commonly used. This delay is insignificant compared to the delay introduced by some other algorithms commonly used in a communication system, such as block coding, interleaving/scrambling, or Viterbi decoding.

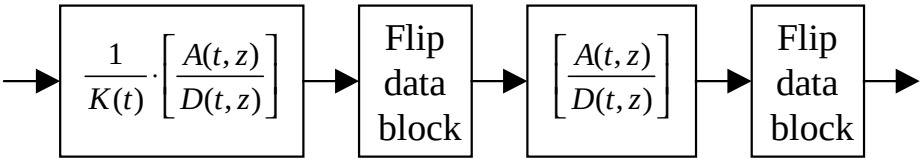

Figure 7-2. Implementation of the non-causal filter by filtering forward and then backward.

Half of the filter, $\left[\frac{A(t,z)}{D(t,z)}\right]$, is an IIR filter with zeros and poles guaranteed to fall inside the unit circle. It has p zeros and poles, where p is the autoregressive order. For interference at different power levels (different SIR levels), the zeros are always located at the interference frequencies, while the locations of the poles vary. At high SIR, the poles are close to the zeros, and therefore the magnitude response tends to be flat. At low SIR, the poles are far away from the zeros, and therefore deep notches are formed to reject the interference.

In the forward-and-backward implementation, a filter transient appears at both ends of the data block. Proper block overlapping can be introduced to cover most of the transient at both ends of the data block. This makes the size of the data block slightly larger.

7.3.2 Example

To illustrate how the proposed interference rejection filter is tailored to the received data, we plot the frequency response of an example of this filter in Figure 7-3, and compare it against the brute-force FIR notch filter (see Section 4.3.1 for details of the length-5 FIR notch filter). Here an FM interference with a constant frequency is

considered, and the exact frequency and autoregressive model parameters are assumed known and used in forming the filter in each case. The frequency response shown could be viewed as an "instantaneous frequency response" for the time-varying filter in a time-varying case. In Figure 7-3, we see that the proposed filter is close to the brute-force notch filter when the interference is very strong, i.e., at very low SIR. On the other hand, it approximates a flat unity response when the SIR is very high, where interference rejection is not needed.

7.4 Simulations of Interference Suppression Based on TVAR-WF

The effectiveness of the proposed interference suppression filter is illustrated by comparing it with notch filter based brute-force cancellation. Consider a single-user DSSS system with BPSK modulation and processing gain N=15 chips per bit. The spreading code is a randomly generated binary PN sequence. The noise in the received signal is an additive white Gaussian noise. It is assumed that the channel is free of fading and ISI (inter-symbol interference). The standard correlation de-spreading receiver is used, with or without an interference suppression filter. Without interference, the BER (bit error rate) of the system would be solely determined by SNR according to $P_e = Q(\sqrt{2E_b/N_0})$. Here E_b stands for the signal bit energy, N_0 is the one-sided noise power spectral density, and $Q(\cdot)$ is the standard Q function, defined as $Q(z) = \frac{1}{\sqrt{2\pi}} \int_z^\infty \exp(-\lambda^2/2) d\lambda$.

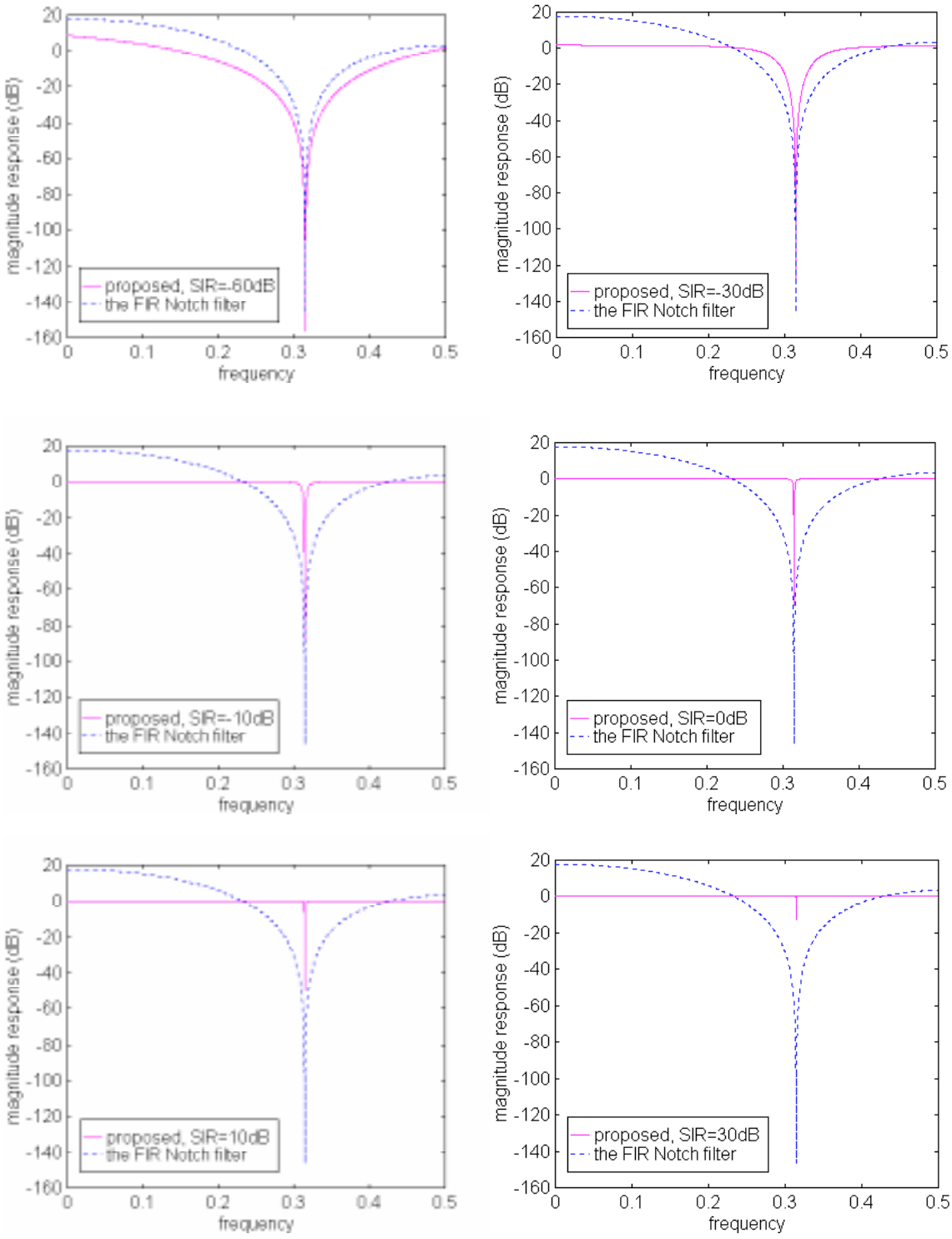

Figure 7-3. Magnitude responses of the proposed TVAR-WF filter (*solid*) vs. the brute force FIR notch filter (*dashed*), at SIR = –60dB (*top left*), –30dB, –10dB, 0dB, 10dB, and 30dB (*bottom right*).

7.4.1 Case 1: Fixed-Frequency and Known Parameters

Before looking at a more realistic case, we first examine the performance of the proposed TVAR based time-varying Wiener filter for a simple, yet important case. Here we consider an interference with fixed frequency over the data block in order to examine the advantage of the Wiener filter over the brute-force notch filter, without involving the time-varying characteristics of both kinds of filters.

In Figure 7-4, the proposed WF based interference suppression is compared with interference suppression using the length-5 FIR notch filter in terms of BER versus signal-to-interference ratio (SIR) for E_b/N_0 = 8dB. At each simulation trial, a new interference frequency is generated randomly, evenly distributed between 0 and 0.5Hz (normalized to unity sampling rate). Thus, the figure reflects the average performance of the filters at a random frequency. Here chip-rate sampling is used, i.e., 1 sample per chip. The exact frequency and model parameter information is used for both the proposed filter and the notch filter. For comparison, the simulated BER for the plain receiver without interference suppression ("no filtering") and the BER evaluated from the *Q* function for the interference-free case ("limit by SNR") are also shown in the figure.

For this case of fixed frequency with known parameters, the proposed Wiener filter outperforms the brute-force FIR notch filter for the entire range of SIR, and is especially advantageous when the SIR is not extremely low. The flatness of the BER versus SIR curve for the notch filter reflects the fact that the notch filter distorts the signal while deeply canceling the interference. The TVAR-WF yields desirable performance

over the entire range of SIR while the brute-force notch filter harms the system when the interference is weak.

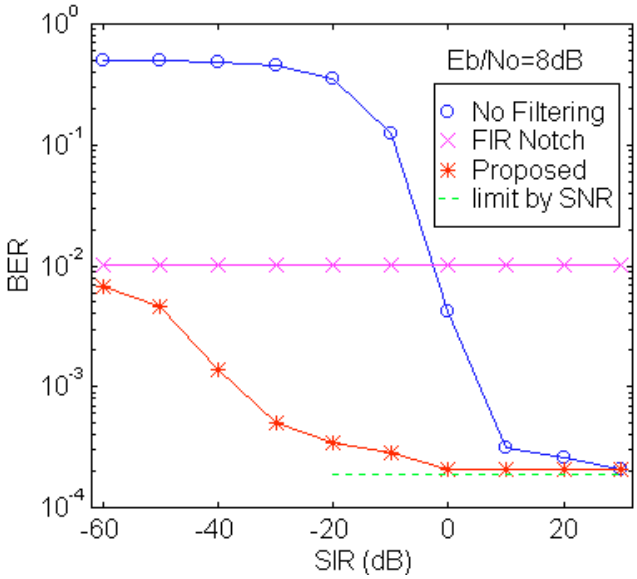

Figure 7-4. Comparing the proposed TVAR-WF with the FIR notch filter in terms of BER versus SIR for the DSSS scenario with fixed frequency and known parameters, E_b/N_0 = 8dB.

7.4.2 Case 2: Nonlinear FM Jammer Using Estimated Parameters

Now we examine a more practical case where the TVAR parameters are estimated from a block of data involving a nonlinear FM jammer. As in the examples in Chapter 4, a DSSS system using BPSK modulation and processing gain of 15 chips per bit is considered. The sampling rate is 8 samples per chip, or equivalently, 120 samples per bit. The data block is of length 136 samples. The 120 samples in the middle of the data block represent a bit, while the first 8 samples and the last 8 samples of the data block are part of the bits before and after. The bit decision is made based on each data block. The extra samples near the ends of the data block are included to pass the transients of the

backward-then-forward non-causal filter implementation shown in Figure 7-2. In this case, a nonlinear FM jammer is considered, with instantaneous frequency as shown in Figure 7-5, which is generated by the IF law

$$f(t) = 0.15 + 0.3\sin(\frac{\pi}{2} \cdot \frac{t}{127}),\ t = 0,1,\cdots,135 \tag{7-10}$$

In each simulation trial, the FM jammer is generated independently with a random initial phase, and a new random binary sequence is generated and used as the spreading code. Therefore, the simulation result is not dependent on the specific PN code or initial phase.

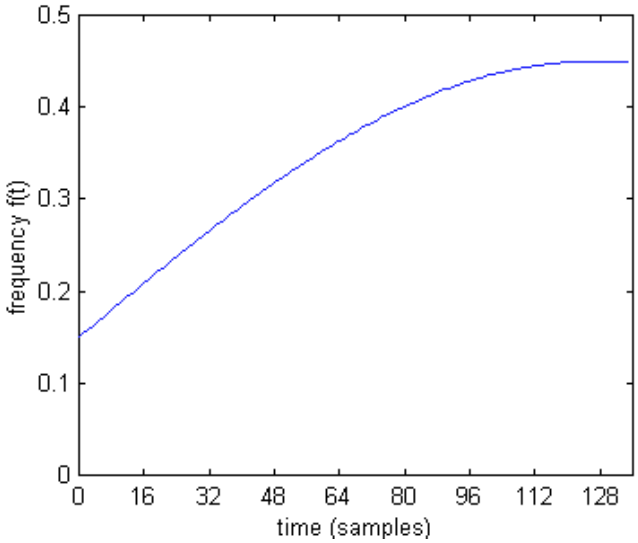

Figure 7-5. Instantaneous frequency law of the jammer inside the data block.

The simulated BER versus JSR (jammer-to-signal ratio) with fixed E_b/N_0 =10dB for the four types of receiver is given in Figure 7-6. The compared receivers include the plain decorrelating ("no filtering") receiver, the receiver with proposed TVAR-WF based interference rejection, and the receiver with brute-force length-5 FIR notch filter based interference rejection in two cases: using the exact (supposedly known) IF or using the

TVAR based IF estimate. We observe that the proposed TVAR-WF method provides the best performance over the entire range of JSR. This is because the proposed filter, by using the full spectral information, is capable to "adapt" according to the data, as shown in Figure 7-3. By contrast, the brute-force notch filtering method provides good performance improvements when the jammer is strong, but needs to be switched off when the jammer is not strong, below 10 dB JSR in this case. Even with known parameters, the notch filter does worse than no filtering at low JSR. We mentioned earlier in Chapter 3 the existence of an SNR threshold for IF estimation, below which the performance of IF estimation drops dramatically. This phenomenon materializes here for the TVAR-IF for JSR below 10dB. Note that estimating IF produces errors relative to the known IF which cause deterioration of the FIR notch filter approach below 10 dB JSR. However, estimating TVAR parameters and directly using that information for Wiener filter design seems to work well even at low JSR. In the latter case there is little deterioration over not filtering at all. This situation is very desirable, as there is no need to switch between different methods depending on JSR (which would need to be measured).

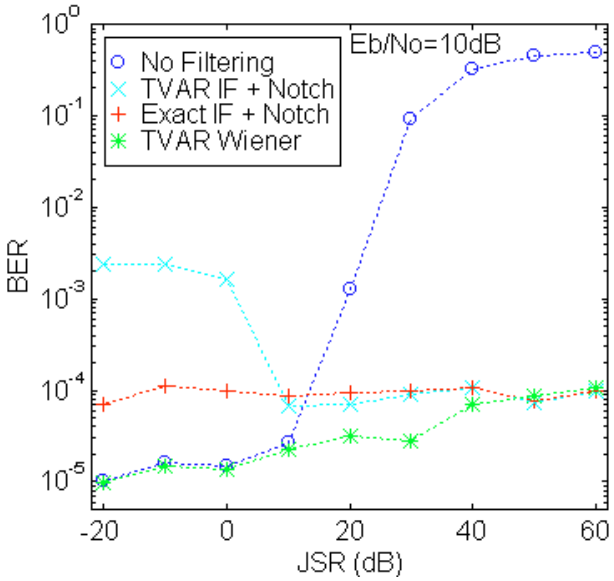

Figure 7-6. BER versus JSR for the proposed TVAR-WF compared with the notch filter method and the plain receiver without filtering for a case of non-linear FM jammer in DSSS, E_b/N_0 = 10dB.

7.5 Summary and Discussion

In the time-varying notch filter based interference cancellation approach, the filter is formed using the instantaneous frequency of the interference regardless of its power or other spectral information. Consequently, when the interference is moderate or weak, the notch filter may cancel more signal than interference, and hence yield deteriorating system performance. We developed a time-varying filter for interference cancellation in DSSS communications, which is tailored by the full time-varying spectral information to minimize the filter output error. The proposed method is a time-varying extension of the Wiener filter and is based on the TVAR model. The improved performance of the proposed method was evidenced through simulations.

Chapter 8

TVAR BASED TIME-VARYING WHITENING FILTER FOR SOFT-CANCELLATION OF FM INTERFERENCE IN DSSS

In this chapter, we propose another time-varying filter formulation for "soft-cancellation" of interference that uses full spectral information of the received data. The filter is aimed at flatness of the output spectrum and is referred to as a time-varying whitening filter. It uses the same information carried in the TVAR parameters as for the TVAR based Wiener filter studied in Chapters 6 and 7, and is formed as the TVAR model based time-varying linear prediction error (TVAR-LPE) filter. Since the term TVAR-WF is reserved for the TVAR based Wiener filter, we refer to the whitening filter as the TVAR-LPE filter for short.

8.1 Introduction

In the scenario of FM interference rejection in DSSS communications, the interference has a narrow instantaneous bandwidth, and therefore, has a highly colored

time-dependent spectrum. On the other hand, the desired signal has a relatively flat spectrum. This implies that if a filter is designed to whiten the received data, it must suppress the interference. We would also like to preserve the signal. This is the basic idea of interference rejection based on whitening filtering.

Since the spectrum of the FM interference is rapidly time-varying, the whitening filter should also be rapidly time-varying. The idea of time-varying whitening filtering based interference rejection is made realizable by TVAR modeling, similar to the cases of the TVAR-WF and the TVAR-KF. It is well known that in the stationary case the output of a linear prediction error (LPE) filter associated with an AR model is a white process if the input is an AR process and the order of the model is high enough, and the LPE filter output is then referred to as the innovation. The innovation, or LPE, is the component of the data that can not be represented by the AR model. Similarly, in our time-varying case, the FM interference can be approximated by a TVAR model with poles close to the unit circle (it does not have any zeros), while the desired signal, which is wideband and nearly white, does not fit that model. Therefore, in this scenario, the output of the TVAR based LPE filter approximates the desired signal.

The TVAR-LPE filter is an FIR filter with as transfer function the inverse of the transfer function of the TVAR model. The poles of the TVAR model become the zeros of the TVAR-LPE and those zeros annihilate the interference. For strong interference (high JSR), the TVAR poles, and consequently the TVAR-LPE zeros, are close to the unit circle and a deep notch is formed at the angle of each TVAR pole. For weak interference (low JSR), the estimated TVAR-LPE zeros are away from the unit circle and,

consequently, the notch at the angle of each TVAR pole is shallow. In this way, the filter provides soft-cancellation of the interference, similar to the TVAR-WF based filter.

8.2 FM Interference Suppression Based on TVAR Whitening Filter: Method and Example

8.2.1 Method

As shown in Figure 7-1, at the receiver of a DSSS communications system, an interference suppression filter is applied before demodulation. As in Chapter 7, we consider a received signal $r(t)$, where t refers to discrete time, composed of the DSSS signal $s(t)$, noise $w(t)$ and interference $i(t)$:

$$r(t) = s(t) + w(t) + i(t) \tag{8-1}$$

Here the noise $w(t)$ is assumed stationary and white. The DSSS signal $s(t)$ is also assumed stationary and white (non-Gaussian). In practice the DSSS signal may be "slightly colored", depending on the sampling rate (samples per chip) and the specific PN sequence used. The interference $i(t)$ could be a hostile FM jammer or an FM communication signal (for example, a cellular system overlapping CDMA and AMPS). The three components in (8-1) are assumed to be independent.

We feed $r(t)$ to a time-varying filter $H(t,z)$ to produce a white output. If we denote the output as $y(t)$, this means that we want the output $y(t)$ to have a flat time-dependent spectrum, i.e.

$$P_r(t,z)H(t,z)H^*(t,1/z^*) = \sigma_y^2 \tag{8-2}$$

where σ_y^2 is the variance of the whitening filter output and $P_r(t,z)$ is the time-dependent power spectrum of the received signal, which was used as the filter input.

As mentioned in Chapter 6, if we model the received signal using the TVAR model, the power spectrum is expressed as:

$$P_r(t,z) = \frac{\sigma^2}{A(t,z)A^*(t,1/z^*)} \tag{8-3}$$

where σ^2 is the variance of the excitation process and $A(t,z) = \sum_{i=0}^{p} a_i(t) z^{-i}$ with $\{ a_i(t) \}$ being TVAR coefficients. Substituting (8-3) into (8-2), we have

$$H(t,z)H^*(t,1/z^*) = \frac{\sigma_y^2}{\sigma^2} A(t,z)A^*(t,1/z^*) \tag{8-4}$$

This suggests that we take

$$H(t,z) = \frac{\sigma_y}{\sigma} A(t,z) \tag{8-5}$$

We can set $\sigma_y^2 = \sigma^2$ without affecting the output signal to noise ratio and, therefore, the resulting decision. Then the time-varying whitening filter is simply

$$H(t,z) = A(t,z) \tag{8-6}$$

This is also the time-varying linear prediction error (TVAR-LPE) filter.

Compared to the TVAR-WF filter, the TVAR-LPE requires less computational effort. Once the TVAR parameters are estimated, the TVAR-LPE filter is readily formed, unlike the TVAR-WF for which polynomial rooting/factorization is needed. Therefore, the TVAR-LPE method is more practical for cases of multiple-component interference where a higher autoregressive order is needed for the TVAR model. Another feature of the TVAR-LPE method is that it is a short FIR filter with the order equal to the order of

the TVAR model, which equals the number of interference components (for complex-valued data and filter) or two times that (for real-valued data and filter).

8.2.2 Example

To illustrate how the TVAR-LPE interference rejection filter is tailored to the received data, we evaluated a "snapshot" of its time-varying magnitude response and contrast it in Figure 8-1 against the brute-force notch filter. The frequency responses shown are instantaneous frequency responses when the IF is at 0.35Hz. It is taken at $t = 59$ in the nonlinear FM jammer case in Section 7.4.2, with the IF described by (7-10) and shown in Figure 7-5. Here the TVAR-LPE is formed using the TVAR parameters estimated from a data record while the exact frequency information is used to form the notch filter. The TVAR-LPE is implemented with TVAR order $p = 1$ and $q = 5$ after converting the real-valued data to analytic data, with the imaginary part generated via Hilbert transform filtering.

In Figure 8-1, we see that the magnitude response (in decibels) of the whitening filter, which is the inverse of the TVAR based spectral estimate of the data, yields a soft cancellation of the FM interference. That is, when the jammer is weak (lower JSR), the TVAR-LPE filter adapts to it and the notch becomes shallow or nearly flat when cancellation is not needed.

At higher interference levels, the TVAR-LPE filter yields an adequate notch depth, though it is not as deep as for the brute-force notch filter. The advantage of the TVAR-LPE is its relatively flat response outside the notch area compared to the notch filter. Consequently, the TVAR-LPE filter results in less signal distortion and could,

therefore, even at high JSR, yield lower BER than the brute-force FIR notch filter. At lower JSR, the frequency response of the TVAR-LPE becomes relatively flat, though not as flat as for the TVAR based Wiener filter shown in Figure 7-3.

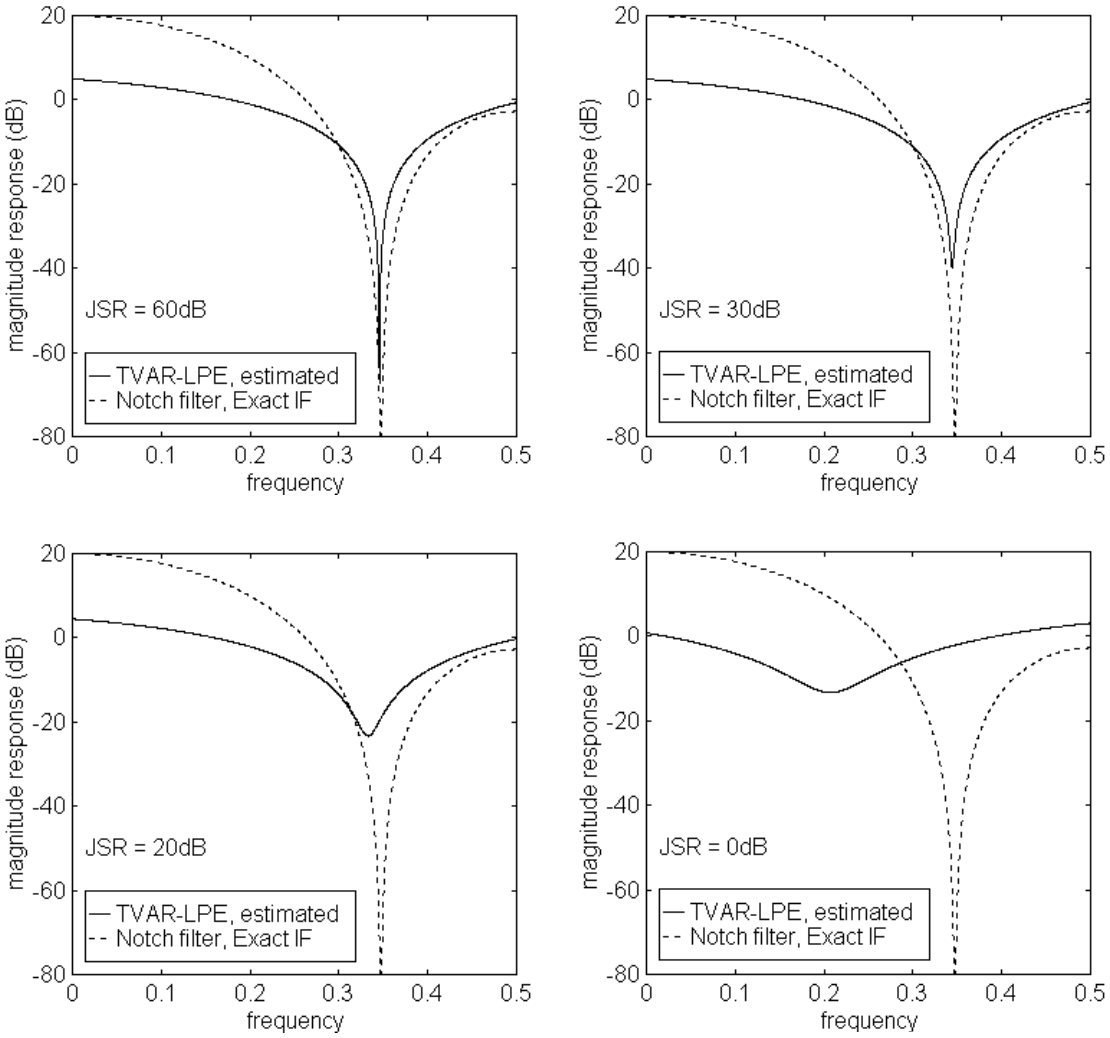

Figure 8-1. A snapshot of magnitude responses of the TVAR-LPE filter (*solid*) vs. the brute force FIR notch filter (*dashed*), at JSR = 60dB (*top left*), 30dB, 20dB, and 0dB (*bottom right*).

We see that the estimated TVAR parameters place the notch precisely at the interference frequency when the interference is strong. On the other hand, when the

interference is weak, the estimated TVAR parameters no longer represent the correct interference frequency (hence, at low JSR, the TVAR-IF estimate controlled notch filter may make the overall system performance worse than without any filtering, as shown in Figure 7-6). However, more importantly, in this case the TVAR estimate successfully captures the more important property of the jammer – the JSR level, which results in a relatively flat magnitude response for the TVAR-LPE filter. When the magnitude response is relatively flat, it does not matter much if the jammer frequency is captured precisely and, therefore, overall system performance is not harmed by the filter.

8.3 Simulations on TVAR-LPE and an Extensive Comparison

This section serves two purposes. The first purpose is to examine the performance of the proposed TVAR-LPE method, as done for our other methods in Chapters 4 and 7. Another purpose of this section is to provide a comparison for all the interference rejection methods we have considered through a common simulation case.

In each simulation trial, we generate a data record of 136 samples with 120 samples in the middle corresponding to a bit interval with 15 chips, sampled at 8 samples per chip. To provide a rather extensive comparison, we revisit all the linear and non-linear FM cases considered earlier in Chapters 4 and 7. These are scenarios of a fast-varying FM jammer that sweeps most of the DSSS bandwidth within a bit-interval, and, specifically, include the following, in order of increasingly higher non-linearity inside the data block:

1) Case 1, the linear FM case of Section 4.3.2. The jammer chirps linearly from 0.1Hz to about 0.4Hz according to

$$f(t) = 0.1 + 0.3t/127\,,\ t = 0,1,\cdots,135$$

2) Case 2, the non-linear FM case of Section 7.4.2. The jammer chirps from 0.15Hz to about 0.45Hz according to

$$f(t) = 0.15 + 0.3\sin(\frac{\pi}{2}\cdot\frac{t}{127}),\ t = 0,1,\cdots,135$$

3) Case 3, the non-monotonically non-linear FM case of Section 4.3.3. The jammer starts from 0.1Hz, increases to 0.4Hz, and then decreases to 0.1Hz, non-monotonically according to

$$f(t) = 0.1 + 0.3\sin(\pi t/127)\,,\ t = 0,1,\cdots,135$$

The FM laws inside the duration of a data block are shown in Figure 8-2 for the three cases. As mentioned earlier, the bit decision is based on the 120-sample bit duration $t = 8,1,\cdots 127$. The extra samples near the ends of the data block help to avoid the effects of the filter transient response on the bit decision.

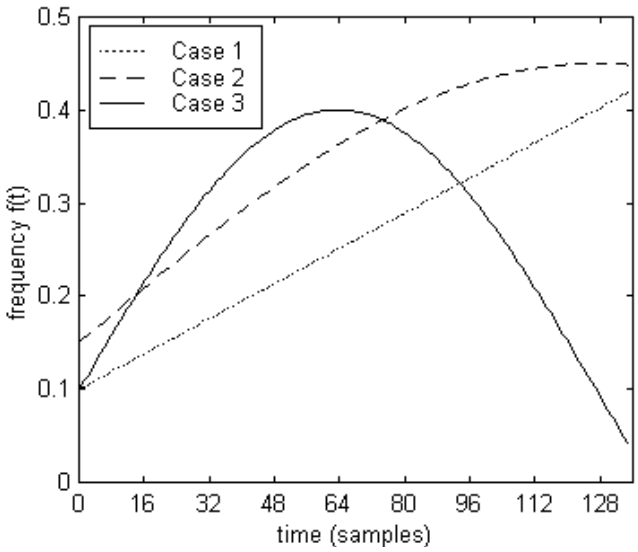

Figure 8-2. Jammer IF laws for the duration of a data block in the three cases of FM interference cancellation for DSSS communications.

BER versus JSR with fixed E_b/N_0 =10dB is simulated for the following methods of interference rejection:

1) the plain receiver without interference rejection filtering (*No-Filtering*),
2) the brute force length-5 time-varying FIR notch filter utilizing the exact (supposedly known) IF (*Exact IF + notch*)
3) the FIR notch filter using the WVD peak based IF estimates (*WVD-IF + notch*), where 512-point zero padding is used to calculate the WVD estimate,
4) the FIR notch filter using the TVAR based IF estimates proposed in Chapter 4 (*TVAR-IF + notch*),
5) FM interference rejection using the TVAR Wiener filter developed in Chapter 7 (*TVAR-WF*),
6) FM interference rejection using the TVAR based whitening filter developed in this chapter (*TVAR-LPE*).

All the above methods are implemented as explained individually before. Since we consider BPSK modulation, the data is generated as real-valued. The length-5 FIR notch filtering methods (with various IF estimates or known IF) also imply using real-valued data. The data is converted to analytic data via Hilbert transform filtering for the WVD calculation and for the TVAR-LPE method. In all the methods that involve a TVAR model, the time-varying coefficients are represented by the polynomial approximation with fixed order $q = 5$.

The simulation results are given in Figure 8-3. At low JSR, both our TVAR based soft-cancellation methods – the TVAR-LPE and the TVAR-WF – yield better performance than the notch filtering methods even if the exact IF is known. Unlike the

brute-force notch filtering methods, our TVAR based soft-cancellation filters do not harm the receiver when filtering is not needed.

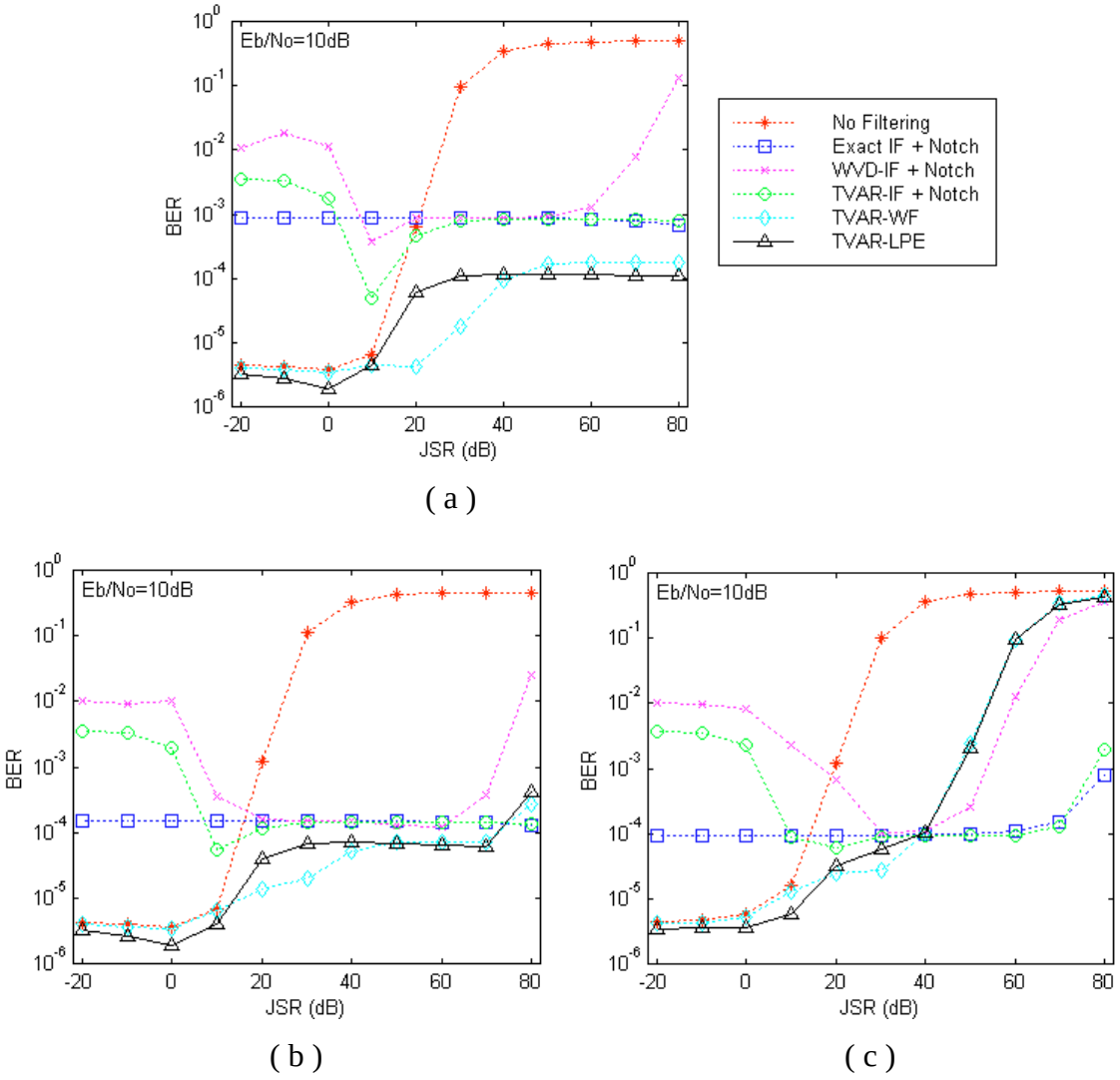

Figure 8-3. Performance comparison of TVAR-LPE with other methods for three different jammer scenarios, E_b/N_0 = 10dB and $q = 5$ for the TVAR models:
(a) case 1, linear FM, (b) case 2, moderately non-linear FM, (c) case 3, highly non-linear FM.

At high JSR, the TVAR based soft-cancellation methods provide consistent and advantageous performance improvement for the linear FM case. The BER resulting from the soft-cancellation methods is about an order of power less that resulting from the brute force notch filter. This is attributed to the relatively flat top and adequate notch depth associated with the soft-cancellation magnitude responses, as shown in Figure 8-1 and Figure 7-3.

For the non-linear cases, Figure 8-3 (b) and (c) show that the processing gain of the TVAR-WF and TVAR-LPE methods is limited, progressively more severely the more severely non-linear the jammer. This effect can be reduced by increasing the polynomial order (q) of the TVAR model. For better performance of the TVAR based soft-cancellation methods in case of highly non-linear FM jammers, a higher order q can be used at the cost of computational complexity. To demonstrate this effect, Figure 8-4 shows the increasing performance of the soft-cancellation methods at high JSR for increasing order q. Figure 8-3 (c) showed that with order $q = 5$, the filter suppresses the jammer by about 30dB. Figure 8-4 shows that with orders $q = 7$ and $q = 8$, the filter suppresses the jammer by about 50dB and 60dB respectively. We also observe that the TVAR-IF based notch filter is less sensitive to the order than the TVAR based soft-cancellation filters. This suggest that if the order q is not high enough, the JSR information captured by the model estimate is not accurate, and consequently, the resulted TVAR-LPE filter does not match the data well.

In conclusion, the TVAR-LPE whitening method, similar to the TVAR-WF method, provides improved performance over the notch filtering methods for the entire range of JSR. They both utilize the full spectral information and are capable of

"adapting" to the data. The brute force notch filtering methods improve the overall DSSS system performance when the jammer is strong, but deteriorate the system performance, even with the exact IF, when JSR is low. Similar to the TVAR-WF, the TVAR-LPE does not make the system worse than not filtering at all, regardless of JSR.

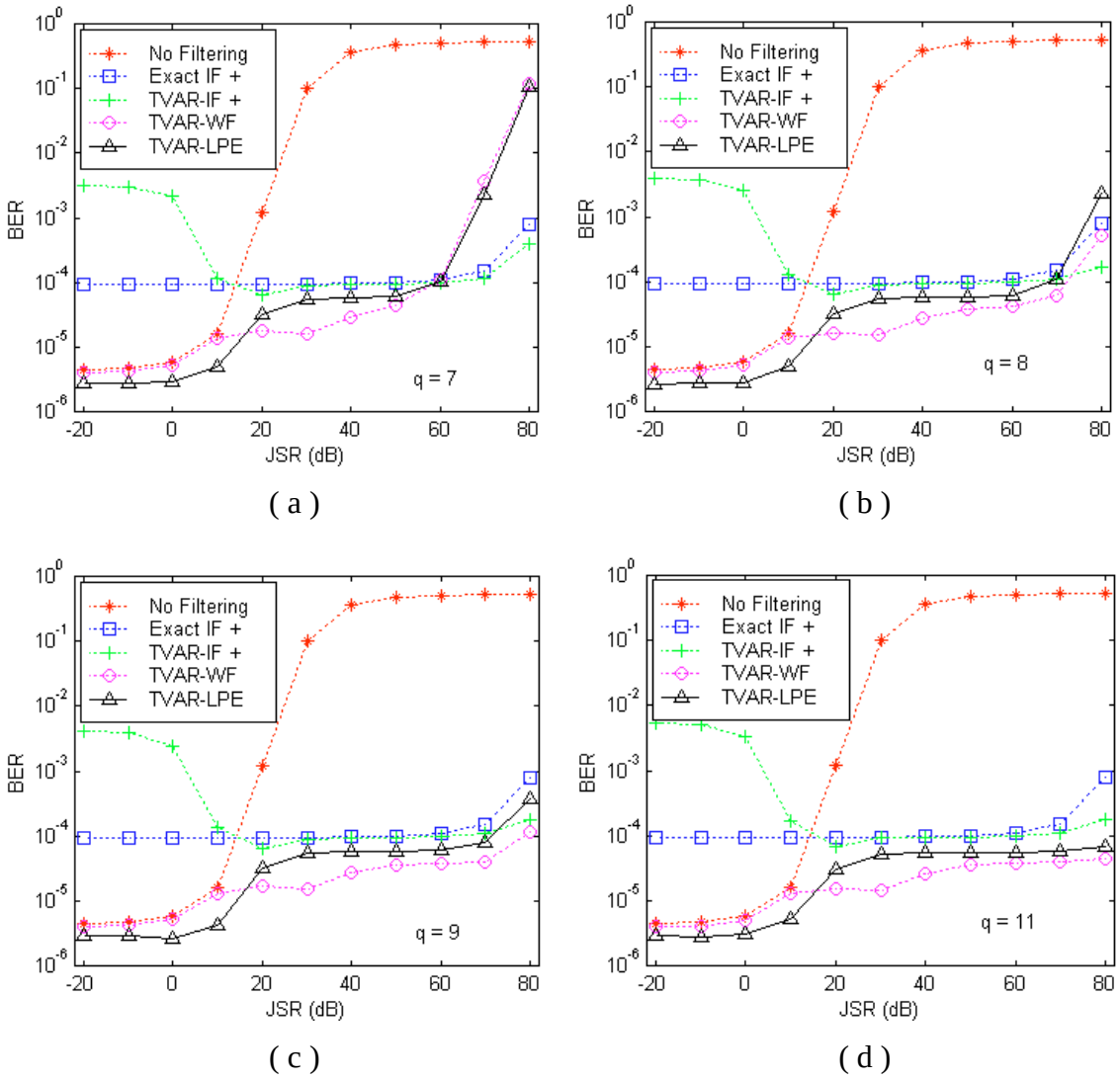

Figure 8-4. Effect of TVAR model basis function order on the performance of TVAR based methods at high JSR for a highly non-linear FM jammer (case 3), E_b/N_0 = 10dB:
(a) $q = 7$, (b) $q = 8$, (c), $q = 9$, (d) $q = 11$.

8.4 Summary and Discussion

We proposed a time-varying filter for interference cancellation in DSSS communications, which is a whitening filter based on TVAR modeling, named the TVAR based linear prediction error (TVAR-LPE) filter. The proposed TVAR-LPE is a time-varying extension of the AR model associated LPE filter in the stationary case. It performs similarly to the TVAR-WF developed in Chapter 7, but is much less complicated to implement than the TVAR-WF due to its short FIR structure and its direct formulation from TVAR parameters, without the need for spectral factorization. The TVAR-LPE and TVAR-WF methods both have distinct advantages in performance over the IF estimate controlled brute-force notch filter in the DSSS interference cancellation scenario.

Chapter 9

SUMMARY AND SUGGESTIONS FOR FUTURE WORK

9.1 Summary

This dissertation is devoted to TVAR model based time-varying signal processing and its applications to FM interference cancellation for DSSS communications. For slowly time-varying environments, the adaptive signal processing methods can be applied to track the variations. However, for the fast variation cases, an explicit description of the variation is necessary for time-varying signal processing. Unfortunately, in practical cases, such a description is rarely available. In this dissertation, we solve this problem using the TVAR model. With the TVAR model, such a description is estimated from the observed data record, and filtering is performed based on the identified TVAR model.

In the first part of the dissertation, Chapters 2 through 4, we studied TVAR based IF estimation. In Chapter 2, we revealed the advantageous properties of TVAR based IF estimation, which is expected to change the prevailing opinion about TVAR-IF that it is a poor method for IF estimation. We demonstrated that TVAR-IF estimation is especially advantageous for non-linear IF laws and short data records. Most IF estimation methods

deteriorate dramatically when the data SNR falls below some threshold. In Chapter 3, we proposed a time-varying Prony method to improve the performance of TVAR-IF estimation for low SNR cases. It is a time-varying extension of a simplified Prony method for frequency estimation in the stationary case. Then in Chapter 4, we applied the TVAR-IF estimates to time-varying notch filtering to reject FM jammers in DSSS communications. It was demonstrated that the TVAR based IF estimate controlled notch filter performs nearly the same as when using the exact IF, and much better than when the notch filter is controlled by the prevailing WVD-IF estimate.

The second part of the dissertation, Chapters 5 through 7, focuses on time-varying optimum filtering based on the TVAR model. A general framework for optimum filtering, covering the Kalman filter and the Wiener filter, is provided in Chapter 5 with emphasis on time-varying considerations. In Chapter 6, we developed the TVAR based Kalman filter and TVAR based Wiener filters, with the latter including the causal version and the ideal non-causal version. The TVAR-KF is directly derived from the Kalman filter and therefore is the optimal causal filter assuming there are no modeling and/or identification errors. By comparing against the TVAR-KF, we find the causal TVAR-WF to be nearly optimal. Also, due to its non-causality, the non-causal TVAR-WF significantly outperforms the causal optimal filter. In Chapter 7, we developed a method of soft-cancellation of FM interference in DSSS communications based on the non-causal TVAR-WF. The resulting filter is tailored to the full spectral information and is aimed at minimum signal distortion. Unlike the brute-force notch filter, the TVAR-WF does not harm the overall system performance (relative to not filtering at all) and yields desirable performance improvements at both high and low JSR.

In Chapter 8, we developed another method of soft-cancellation of FM jammers in DSSS communications based on the TVAR model. It is aimed at flatness of the output spectrum, and the resulting filter is the TVAR based linear prediction error (TVAR-LPE) filter. Similar to the TVAR-WF method, the TVAR-LPE yields the desired performance over the entire range of JSR. Unlike the TVAR-WF and TVAR-IF methods, the TVAR-LPE is formed from the TVAR parameters directly without any further calculation. Another advantage of the TVAR-LPE filter is its short FIR structure, which further simplifies implementation.

9.2 Suggestions for Future Work

The reported research was concentrated on developing TVAR based signal processing methods and applying them to reject FM interference in DSSS communications. Future research may develop along two major directions: theoretical research and application and implementation issues. In the theoretical realm, some performance analysis of the proposed methods may be helpful to better understand and apply the proposed methods. The questions to be answered include, for example, how theoretical analysis is feasible and how the WVD and WS based TVWF [21] relates to our TVAR-WF and if it would be useful in predicting limitations on the practical use of TVAR modeling. In terms of application and implementation aspects, one may evaluate the computational load required to implement each method for given scenarios and widen the realm of applications. Based on a complexity versus performance tradeoff, one may provide advice on selection of time-varying filter methods. One may also study system design issues for applications of the proposed methods. For example, the TVAR-WF and

TVAR-LPE methods are based on treating the DSSS signal as an approximately white signal. From this point of view, a small over-sampling ratio (samples per chip) is desired. Other aspects of system design may desire a larger over-sampling ratio. The question of how to choose the sampling rate or design a multi-rate system may become a practical issue in a real-world application.

We have focused on the application of the proposed TVAR based filtering methods to the problem of FM interference rejection in DSSS communications. One may apply the TVAR based methods to other engineering and research scenarios, such as in speech enhancement, seismic signal processing, radar/sonar signal processing, and biomedical and biophysical signal analysis and processing. In the communication field, one may apply the proposed methods to reject co-channel interference for FM communications or perform multiple-FM demodulation. One may also study the use of these TVAR based methods, or modifications thereof, to reject a frequency-hopping jammer in DSSS communications. It is further suggested that the TVAR-KF or a similar TVAR based Kalman smoother (with delay) be evaluated for the interference suppression problem.

Appendix A

Wigner-Ville Distribution (WVD) and WVD Peak Based IF Estimation

A-1 Wigner-Ville Distribution (WVD)

The Wigner-Ville Distribution (WVD) is defined for both continuous signals and limited-length discrete-time sequences. Since this dissertation concerns signal processing for a discrete-time record (block) only, we limit our discussion to such cases.

Let $x(t)$ be a discrete-time series of length *N*, with time-index $t = 0, 1, \ ..., N-1$. For simplicity of presentation, we assume that the length *N* of the data record is even. We define the "instantaneous correlation function" as:

$$c(t,m) = x(t+m)x^*(t-m) \tag{A-1}$$

where zero-values are assumed for $x(t)$ outside of the data record and m is the "half of lag" which takes integer values from $-\frac{N}{2} \le m < \frac{N}{2}$. Then the discrete Wigner-Ville Distribution (WVD) is defined as the discrete Fourier transform (DFT) of the $c(t,m)$ with respect to the lag $2m$ for each time instant $t = 0, 1, \ ..., N-1$, which is

$$W(t,k) = 2\sum_m c(t,m)e^{-j2\pi(2m)k/N} \tag{A-2}$$

where k is the discrete frequency. For unity sampling rate, which we have assumed, the corresponding continuous frequency is $f = \frac{k}{2N}$.

Note that, from t in $x(t)$ to $2m$ in $c(t,m)$, decimation by 2 is involved and, consequently, for each given time instant t, the WVD $W(t,k)$ corresponds to an aliased power spectrum of the signal. If the original data is real-valued, it is usually converted to the analytic signal, which has a single-sided spectrum. The output of the real-to-analytic transform has the original signal as its real part and the Hilbert transform of the real part as its imaginary part.

A-2 WVD Based IF Estimation (WVD-IF)

Assume that the signal $x(t)$ consists of only one signal component. Then the instantaneous frequency (IF) of the signal component can be estimated by searching for the frequency peak position of its WVD $W(t,k)$ for each time instant t. The estimate can be expressed in terms of an estimate of the continuous frequency $\hat{f}(t)$ as

$$\hat{f}(t) = \frac{1}{2N} \arg\max_k \{W(t,k)\} \tag{A-3a}$$

or in terms of an estimate of the discrete frequency index $\hat{k}(t)$:

$$\hat{k}(t) = \arg\max_k \{W(t,k)\} \tag{A-3b}$$

The IF estimate takes values from a set of discrete values with quantization interval $\frac{1}{2N}$. For short data records, the estimate is poor due to the frequency quantization. This effect can be reduced by padding zeros to the data $x(t)$ or, more efficiently, padding zeros to $c(t,m)$ along the m axis. The latter means increasing the number of points in the DFT contained in (A-2).

A-3 Example of WVD and WVD-IF

For a 32-point data record of a linear chirp signal in white noise at SNR=20dB, we compute its WVD and WVD-IF. The IF law is $f(t) = 0.1 + 0.01t, t = 0,1,\cdots,31$. The data is the same as that used in Section 2.2.2, as shown in Figure 2-1. We compute the WVD in two versions, without zero-padding, which uses a 32-point DFT and is denoted as WVD(32), and with zero-padding to 64-points, which uses a 64-point DFT and is denoted as WVD(64). The result is shown in Figure A-1 in the top and middle rows, with the left column for WVD(32) and the right column for WVD(64). The IF estimates resulting from the peak locations in the WVD estimates are shown below also. The finer frequency quantization interval associated with the WVD(64) IF estimates is observable in the increased smoothness of the latter. The WVD-IF is improved by zero-padding at the cost of computational effort. The IF estimates near the ends of the data record are less reliable than in the center. This is due to the fact that there are fewer data samples

available for computing the "instantaneous correlation function" $c(t,m)$ near the data ends. This is referred to as the end effects of the WVD based IF estimation.

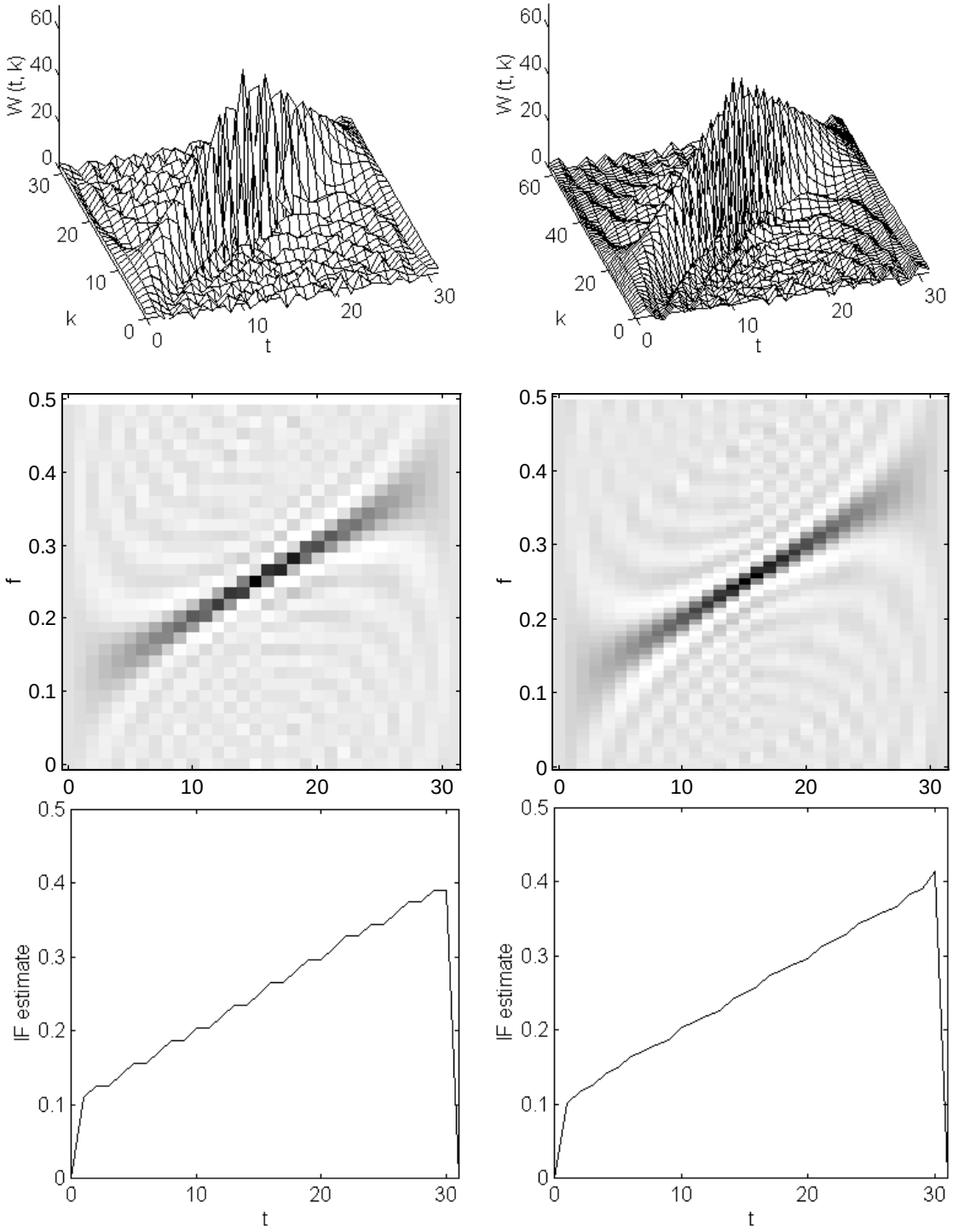

Figure A-1. Example of WVD (*top and middle*) and WVD-IF (*bottom*) based on WVD(32) (*left*) and WVD(64) (*right*), a linear FM signal in white nose at SNR=20dB.

Appendix B

Evolutionary Spectrum Theory and its Relation to this Work

B-1 Review of Priestley's Evolutionary Spectrum Theory [24]

Let $x(t)$ be a non-stationary time series that admits a representation of the form

$$x(t) = \int_{-\pi}^{\pi} \phi_t(\omega) dZ(\omega), \quad t = 0, \pm 1, \pm 2, ..., \tag{B-1}$$

where $Z(\omega)$ is an orthogonal process and $E[|\, dZ(\omega)\,|^2]$ plays the same role as the power spectrum in the Fourier analysis of stationary processes (where the kernel function family is taken as $\phi_t(\omega) = e^{j\omega t}$). Suppose that $\phi_t(\omega)$ can be expressed in the form of a jointly frequency- and amplitude-modulated (FM-AM) function

$$\phi_t(\omega) = A_t(\omega)\, e^{j\theta(\omega)t} \tag{B-2}$$

where the amplitude-modulating function $A_t(\omega)$ has its peak Fourier spectrum at zero frequency. When $\phi_t(\omega)$ is considered as a function of *t*, it is called an *oscillatory function* if it can be written in the form indicated in (B-2). If there exists a family of oscillatory functions $\{\phi_t(\omega)\}$ such that the process $\{x(t)\}$ can be expressed in the form (B-1), $\{x(t)\}$ is called an *oscillatory process*.

Further assuming that $\theta(\omega)$ in (B-2) is a single-valued function of ω, by transforming the variable in the integral in (B-1) from ω to $\theta(\omega)$ and adjusting the terms $A_t(\omega)$ and $Z(\omega)$, it is possible to write

$$x(t) = \int_{-\pi}^{\pi} A_t(\omega) e^{j\omega t}\, dZ(\omega), \quad t = 0, \pm 1, \pm 2, ..., \tag{B-3}$$

with

$$E[|\, dZ(\omega)\,|^2] = d\mu(\omega) \tag{B-4}$$

For a given family of oscillatory functions, $\{\phi_t(\omega)\} = \{A_t(\omega)\, e^{j\omega t}\}$, in terms of which an oscillatory process $\{x(t)\}$ can be expressed in the form (B-3), the *evolutionary power spectrum* $dH_t(\omega)$, at time *t*, of the oscillatory process $\{x(t)\}$ with respect to the specific family of oscillatory functions, is then defined by

$$dH_t(\omega) = |A_t(\omega)|^2 \, d\mu(\omega), \quad -\pi \le \omega \le \pi \tag{B-5}$$

For the special case when $\{x(t)\}$ is stationary, if the family of oscillatory functions $\{\phi_t(\omega)\} = \{A_t(\omega)\, e^{j\omega t}\}$ is chosen to be the family of complex exponential functions, the evolutionary power spectrum $dH_t(\omega)$ reduces to the standard Fourier power spectrum.

Priestley suggested a two-stage procedure for estimating the evolutionary spectrum from a data record. For frequency sample ω_0, the first step is to pass the data through a linear bandpass filter centered at ω_0, and, the second step is to estimate the time-varying power at ω_0 by averaging the squared value of the filter output over a sliding (short-time) temporal window. In other words, Priestley's evolutionary spectral estimation is based on a filter-bank (frequency-domain windowing) followed by short-time power estimation (time-domain windowing).

B-2 Relation of Priestley's Evolutionary Spectrum Theory to this Work

In this research, the data is modeled with a TVAR model, and time-varying characteristics are represented in the TVAR parameters. In many cases, such as time-varying filter design, we can use the model parameters themselves without estimating a two-dimensional evolutionary spectrum (also called a *time-frequency distribution* or *time-varying spectrum*). If needed, the time-varying spectrum estimation corresponding to the TVAR model can be evaluated in a straightforward manner from the TVAR parameters, as expressed in (6-18), in a fashion similar to parametric spectral estimation for stationary processes [30].

Since Priestley's evolutionary spectral estimation involves frequency-domain and time-domain windowing, it is not suitable for short data records and fast-varying signals. In contrast, our method models the entire data record or data block with the time-varying characteristics incorporated by the model. In other words, we capture time-varying information by model identification, rather than by short-time windowing. Consequently, the proposed work may be more suitable for short data records and fast-varying non-stationarity.

Although our method of capturing time-varying characteristics is distinct from that of Priestley's evolutionary spectrum estimation, our definition of the parametric *time-varying spectrum*, as expressed in (6-18), can be viewed as a special case under the umbrella of Priestley's evolutionary spectral theory, as explained next.

We model the data as the output of a linear time-varying system, $G(t, z)$, excited by a stationary white noise $e(t)$ with power σ_e^2, where

$$G(t,z) = \frac{1}{A(t,z)} = \frac{1}{\sum_{i=0}^{p} a_i(t) z^{-i}}, \quad a_0 \equiv 1 \tag{B-6}$$

We denote the impulse response of $G(t, z)$ as $g(t,\tau)$, representing the response at time t contributed by an impulse input at time $(t-\tau)$:

$$G(t,z) = \sum_{i=0}^{\infty} g(t,i) z^{-i} \tag{B-7}$$

Then, we can express the data $x(t)$ in terms of $g(t,\tau)$ and $e(t)$:

$$x(t) = \sum_{i=-\infty}^{t} g(t, t-i)\, e(i) \tag{B-8}$$

where $e(t)$ is stationary and white, and therefore can be expressed in terms of Fourier analysis. Following the notation of Priestley's evolutionary spectrum theory, we can write the Fourier analysis of $e(t)$:

$$e(t) = \int_{-\pi}^{\pi} e^{j\omega t} dZ(\omega) \tag{B-9}$$

where $Z(\omega)$ is a process satisfying

$$E[dZ(\omega_1) dZ^*(\omega_2)] = \delta(\omega_1 - \omega_1)\sigma_e^2 \frac{d\omega_1}{2\pi} \tag{B-10}$$

Substituting (B-9) into (B-8), we have an expression for the data in the form of (B-3):

$$x(t) = \int_{-\pi}^{\pi} G(t, e^{j\omega})\, e^{j\omega t} dZ(w) \tag{B-11}$$

The evolutionary spectrum defined in (B-5) is then,

$$dH_t(\omega) = |\, G(t, e^{j\omega})\,|^2 \; d\mu(\omega) \tag{B-12}$$

From (B-4) and (B-10), we have

$$d\mu(\omega) = \sigma_e^2 \frac{d\omega}{2\pi} \tag{B-13}$$

and from (B-6), we have

$$dH_t(\omega) = \frac{\sigma_e^2}{|A(t, e^{j\omega})|^2} \frac{d\omega}{2\pi} \tag{B-14}$$

This is equivalent to our time-varying spectrum (6-18) evaluated on the unit circle with $z = e^{j\omega}$.

BIBLIOGRAPHY

[1] G. F. Boudreaux-Bartels and T. W. Parks, "Time-varying filtering and signal estimation using Wigner Distribution synthesis techniques," *IEEE Trans. ASSP*, vol. ASSP-34, no. 3, pp. 442-451, June 1986.

[2] W. Kozek and F. Hlawatsch, "A comparative study of linear and nonlinear time-frequency filters," *Proc. IEEE Int. Symp. Time-Frequency Time-Scale Analysis*, Oct. 1992 (TFTS'92), Victoria, Canada, pp. 163-166.

[3] B. Boashash, "Time-frequency signal analysis," in *Advances in Spectrum Analysis and Array Processing*, vol. 1, S. Haykin Ed., Prentice Hall, New York, 1990.

[4] L. Cohen, "Time-frequency distributions," *Proc. IEEE*, vol. 77, pp. 941-981, 1989.

[5] W. Krattenthaler and F. Hlawatsch, "Time-frequency design and processing of signals via smoothed Wigner distributions," *IEEE Trans. Signal Processing*, vol. 41, no. 1, pp. 278-287, Jan. 1993.

[6] M. R. Portnoff, "Time-frequency representation of digital signals and systems based on short-time Fourier analysis," *IEEE Trans. ASSP*, vol. 28, no. 2, pp. 55-69, Feb. 1980.

[7] R. Bourdier, J. F. Allard, and K. Trumpf, "Effective frequency response and signal replica generation for filtering algorithms using multiplicative modifications of the STFT," *Signal Processing*, vol. 15, no. 2, pp. 193-201, Sept. 1988.

[8] I. Daubechies, "Time-frequency localization operators: A geometric phase space approach," *IEEE Trans. Information Theory*, vol. 34, no. 4, pp. 605-201, July 1988.

[9] S. Farkash and S. Raz, "Time-variant filtering via the Gabor expansion," *Signal Processing V: Theories and Applications*. Elsevier, 1990, pp. 509-512.

[10] I. Daubechies and T. Paul, "Time-frequency localization operators: A geometric phase space approach: II. The use of dilations," *Inverse Problems*, no. 4, pp.661-680, 1988.

[11] F. Hlawatsch and W. Kozek, "Time-frequency projection filters and time-frequency signal expansions," *IEEE Trans. Signal Processing*, vol. 42, no. 12, pp. 3321-3334, Dec. 1994.

[12] F. Hlawatsch, W. Kozek, and W. Krattenthaler, "Time-frequency subspaces and their application to time-varying filtering," *IEEE ICASSP'90*, pp. 1607-1610, Apr. 1990, Albuquerque, NM.

[13] F. Hlawatsch and W. Kozek, "Time-frequency analysis of linear signal spaces," *IEEE ICASSP'91*, pp. 2045-2048, May 1991, Toronto, Canada.

[14] R. G. Shenoy and T. W. Parks, "The Weyl correspondence and time-frequency analysis," *IEEE Trans. Signal Processing*, vol. 42, no. 2, pp. 318-332, Feb. 1994.

[15] W. Kozek, "Time frequency signal processing based on the Wigner-Weyl framework," *Signal Processing*, vol. 29, no. 1, pp. 77-92, Oct. 1992.

[16] B. A. Weisburn and T. W. Parks, "Design of time frequency strip filters," *Conference Record of the 29th Asilomar Conference on Signals, Systems and Computers*, pp. 930-934, Oct. 1995.

[17] B. A. Weisburn and R. G. Shenoy, "Time-frequency strip filters," *IEEE ICASSP'96*, pp. 1411-1414, Atlanta, GA, May 1996.

[18] M. A. Kutay, H. M. Ozaktas, L. Onural, and O. Arikan, "Optimal filtering in fractional Fourier domains," *IEEE ICASSP'95*, pp. 937-940, Detroit, MI, May 1995.

[19] H. L. Van Trees, *Detection, Estimation, and Modulation Theory, Part 1: Detection, Estimation, and Linear Modulation Theory*, John Wiley and Sons, Inc., New York, 1968.

[20] N. A. Abdrabbo and M. B. Priestley, "Filtering non-stationary signals," *Royal Statistical Society Journal*, Vol. 31, pp. 150-159, 1969.

[21] H. Kirchauer, F. Hlawatsch, and W. Kozek, "Time-frequency formulation and design of nonstationary Wiener filters," *IEEE ICASSP'95*, pp. 1549-1552, Detroit, MI, May 1995.

[22] A. A. Beex and M. Xie, "Time-varying filtering via multiresolution parametric spectral estimation," *IEEE ICASSP'95*, pp. 1565-1568, Detroit, MI, May 1995.

[23] H. A. Khan and L. F. Chaparro, "Non-stationary Wiener filtering based on evolutionary spectral theory," *IEEE ICASSP'97*, pp3677-3680, Munich, Germany, April 1997,

[24] M. B. Priestley, *Non-linear and non-stationary time-series analysis,* Academic Press, San Diego, CA, 1988.

[25] M. Xie and A. A. Beex, "Multiresolution parametric spectral estimation," *26th Southeastern Symposium on System Theory*, Athens, OH, pp. 432-436, March 1994.

[26] M. Xie, *Signal Decomposition for Nonstationary Processes*, Ph.D. dissertation, Virginia Polytechnic Institute and State University, Blacksburg, VA, 1995.

[27] P. Shan and A. A. Beex, "Time-varying Wiener filtering based on a time-varying AR model," *8th IEEE Digital Signal Processing Workshop*, Vol. 1, ppr. # 52, Aug. 1998, Bryce Canyon, Utah.

[28] M. G. Hall, A. V. Oppenheim, and A. S. Willsky, "Time-varying parametric modeling of speech," *Signal Processing*, vol. 5, no. 3, pp. 267-285, May 1983.

[29] Y. Grenier, "Time-dependent ARMA modeling of nonstationary signals," *IEEE Trans. ASSP*, vol. 31, no. 4, pp. 899-911, Aug. 1983.

[30] S. Kay, *Modern Spectral Estimation*, Prentice Hall, Englewood Cliffs, NJ, 1988.

[31] B. Boashash, "Estimating and interpreting the instantaneous frequency of a signal - part 2: algorithms and applications," *Proc. of IEEE*, vol. 80, no. 4, pp. 540-568, April 1992.

[32] F. Hlawatsch and G. F. Boudreaux-Bartels, "Linear and quadratic time-frequency signal representations," *IEEE Signal Processing Magazine*, vol. 9, no. 2, pp. 21-67, April 1992.

[33] P. Rao and F. J. Taylor, "Estimation of the instantaneous frequency using the discrete Wigner distribution," *Electronics Letters*, vol. 26, no. 4, pp. 246-248, Feb. 1990.

[34] P. Shan and A. A. Beex, "High-Resolution Instantaneous Frequency Estimation Based on Time-Varying AR Modeling," *IEEE-SP the 4th International Symposium on Time-Frequency and Time-Scale Analysis (TFTS'98*), pp. 109-122, Pittsburgh, PA, Oct. 1998.

[35] H. Cohen, G. F. Boudreaux-Bartels, and S. Kadambe, "Tracking of unknown non-stationary chirp signals using unsupervised clustering in the Wigner distribution space," *IEEE ICASSP'88*, pp. 2180-83, Seattle, WA, May 1988.

[36] K. C. Sharman and B. Friedlander, "Time-varying autoregressive modeling of a class of nonstationary signals," *Proc. ICASSP'84*, San Diego, CA, vol. 2, pp. 22.2.1-22.2.4, March 1984.

[37] C. W. Therrien, *Discrete Random Signals and Statistical Signal Processing*, Prentice Hall, Englewood Cliffs, NJ, 1992.

[38] S. Haykin, *Adaptive Filter Theory*, Prentice Hall, Upper Saddle River, NJ, 1996.

[39] L. Ljung, *System Identification: Theory for the User*, Chapter 5, Prentice Hall, Upper Saddle River, NJ, 1987.

[40] M. K. Tsatsanis and G. B. Giannakis, "Time-varying system identification and model validation using wavelets," *IEEE Trans. on Signal Processing*, vol. 41, no. 12, pp. 3512-23, Dec. 1993.

[41] T. S. Rao, "The fitting of nonstationary time-series models with time-dependent parameters," *J. Royal Statist. Soc. Series B*, vol. 32, no. 2, pp. 312-322, 1970.

[42] A. Duel-Hallen, J. Holtzman, and Z. Zvonar, "Multiuser detection for CDMA systems," *IEEE Personal Communications*, April 1995, pp.46-58.

[43] S. Moshavi, "Multi-user detection for DS-CDMA communications," *IEEE Communications Magazine*, Oct. 1996, pp.124-136.

[44] L. B. Milstein and R. A. Iltis, "Signal processing for interference rejection in spread spectrum communications," *IEEE ASSP Magazine*, April 1986, pp. 18-31.

[45] M. Medley, G. Saulnier, and P. Das, "Applications of the wavelet transform in spread spectrum communications," *Proc. SPIE, Wavelets Applications*, Orlando, FL, Apr. 1994, pp. 54-68.

[46] L. Milstein, "Interference suppression to aid acquisition in direct-sequence spread-spectrum communications," *IEEE Trans. Communications*, vol. 36, pp. 1200-1207, Nov. 1988.

[47] M. G. Amin, A. R. Lindsey, and C. Wang, "On the application of time-frequency distributions in the excision of pulse jamming in spread spectrum communication systems," *IEEE Workshop on SSAP*, pp. 152-155, Greece, June 1996.

[48] M. G. Amin, "Interference mitigation in spread spectrum communication systems using time-frequency distributions," *IEEE Trans. Signal Processing*, vol. 45, no. 1, pp.90-101, Jan. 1997.

[49] S. R. Lach, M. G. Amin, and A. R. Lindsey, "Broadband nonstationary interference excision for spread spectrum communications using time-frequency synthesis," *IEEE ICASSP'98*, pp. 3257-3260, Seattle, WA, May 1998.

[50] A. Bultan and A. N. Akansu, "A novel time-frequency exciser in spread spectrum communications for chirp-like interference," *IEEE ICASSP'98*, pp. 3265-3268, Seattle, WA, May 1998.

[51] A. Bultan, "A four-parameter atomic decomposition of chirplets," *IEEE ICASSP'97*, pp. 3625-3628, Munich, Germany, April 1997.

[52] S. Mallat and Z. Zhang, "Matching pursuits with time-frequency dictionaries," *IEEE Trans. Signal Processing*, vol. 41, pp. 3397-3415, Dec. 1993.

[53] R. Kumaresan, D. W. Tufts, and L. L. Scharf, "A Prony method for noisy data: choosing the signal components and selecting the order in exponential signal models," *Proceedings of IEEE*, vol. 72, no.2, pp. 230-233, February 1984.

[54] J. G. Proakis, *Digital Communications*, McGraw-Hill, New York, NY, 1995.

[55] L. W. Couch II, *Digital and Analog Communication Systems*, Macmillan Publishing Co., New York, NY, 1993.

[56] R. P. Hocking and L. L. Leslie, "Selection of the best subset in regression analysis," *Technometrics*, vol. 9, pp. 537-540, 1967.

[57] P. Shan and A. A. Beex, "FM interference suppression in spread spectrum communications using time-varying autoregressive modeling based instantaneous frequency estimation," *IEEE ICASSP'99*, vol. V, pp. 2559-62, Phoenix, AZ, Mar. 1999.

[58] S. R. Lach, A. R. Lindsey, and M. G. Amin, "A comparison between two time-frequency bilinear transforms for interference excisions in spread spectrum communications," *IEEE DSP Workshop'98*, ppr # 85, Bryce Canyon, UT, 1998.

[59] D. Wei, D. S. Harding, and A. C. Bovik, "Interference suppression in direct-sequence spread-spectrum communications using the discrete Gabor transform," *IEEE DSP Workshop'98*, ppr # 61, Bryce Canyon, UT, Aug. 1998.

[60] C. Wang and G. Amin, "Performance analysis of instantaneous frequency-based interference excision techniques in spread spectrum communications," *IEEE Trans. SP*, vol. 46, no. 1, pp. 70-82, Jan. 1998.

[61] L. Liporace, "Linear estimation of nonstationary signals," *J. Acoustics Soc. Amer.*, vol. 58, no. 6, pp. 1268-1295, Dec. 1975.

[62] D. C. Rife and R. R. Boorstyn, " Single tone parameter estimation from discrete-time observation," *IEEE Trans. Information Theory*, vol. 20, pp. 591-598, 1974.

[63] M. Morf, B. Dickinson, T. Kailath, and A. Vieira, "Efficient solution of covariance equations for linear prediction," *IEEE Trans. ASSP*, vol ASSP-25, no. 5, pp. 429-433, 1977.

[64] B. Friedlander, T. Kailath, M. Morf, and L. Ljung, "Extended Levinson and Chandrasekar equations for discrete-time linear estimation problems," *IEEE Trans. Automatic Control*, vol. AC-23, no. 4, pp. 653-659, 1978.

[65] A. A. Beex and P. Shan, "A time-varying Prony method for instantaneous frequency estimation at low SNR," *1999 IEEE International Symposium on Circuits and Systems*, vol. III, pp. 5-8, Orlando, FL, May 1999.

[66] C. Wang, M. G. Amin, and A. Lindsey, "Open loop adaptive filtering for interference exision in spread spectrum systems," *Conference Record of the 31st Asilomar Conf. on Signals, Systems & Computers*, pp. 520-524, Pacific Grove, CA, Nov. 1997.

[67] P. Shan and A. A. Beex, "Time-varying filtering using full spectral information for soft-cancellation of FM interference in spread spectrum communications," *Proceedings of the 2nd IEEE Workshop on Signal Processing Advances in Wireless Communications (SPAWC'99)*, pp.321-324, Annapolis, MD, May 1999.

[68] R. J. Wang, "The Determination of Optimum Gate Lengths for Time-Varying Wiener Filtering" *Geophysics*, vol. 34, no. 5, pp. 683-695, Oct. 1969.

[69] N. Wiener, *Extraction, Interpolation, and Smoothing of Stationary Time Series, with Engineering Applications*, MIT Press, Cambridge, MA, 1949.

[70] M. G. Amin, C. Wang, and A. R. Lindsey, "Optimum interference excision in spread spectrum communications using open-loop adaptive filters," *IEEE Trans. Signal Processing*, vol. 47, no. 7, pp. 1966-1976, July 1999.

Vita

Peijun Shan received the MS degree in Electrical Engineering in 1989 from Xidian University, formerly the Northwest Telecommunications Engineering Institute, Xi'an, China. Next he was employed as a research and development engineer by the same university where he worked on various projects. During that period, he was awarded two invention patents and published/presented about 20 papers. Later, he was employed by GE Medical Systems before he came to the U.S. for higher education. As a GRA (graduate research assistant) at Virginia Tech, he worked from 1996 to 1998 on EEG processing, analysis and visualization in the Center for Brain Research and Information Sciences Radford University, Radford, Virginia. He also instructed senior-level DSP Laboratory at Virginia Tech.

In his Ph.D. program, he concentrated on communications and signal processing and conducted research in the DSP Research Laboratory at Virginia Tech. His current research interests are in time-varying signal processing, interference cancellation and spread spectrum communications. In July 1999, he joined RF Micro Devices Inc., Greensboro, North Carolina, as a Senior Design Engineer working on communication baseband subsystem design. He is a member of IEEE Signal Processing Society and Communications Society.